

Development of a Shear Connection for a Portable Composite Bridge

by

Matthew George Bowser

A thesis

presented to the University of Waterloo

in fulfillment of the

thesis requirement for the degree of

Master of Applied Science

in

Civil Engineering

Waterloo, Ontario, Canada, 2010

©Matthew George Bowser 2010

I hereby declare that I am the sole author of this thesis. This is a true copy of this thesis, including any required final revisions, as accepted by my examiners.

I understand that my thesis may be made electronically available to the public.

ABSTRACT

Bridges consisting of steel plate girders and composite concrete deck slabs are common throughout North America. For a typical highway application, these composite bridges are constructed with a cast-in-place concrete deck; however, some composite bridge designs utilize precast concrete deck panels. For example, bridges built on temporary access roads which service resource industries throughout Western Canada often employ composite bridges that consist of steel plate girders and precast concrete deck panels. For spans between 18- to 36 metres, permanent bridges currently present the best economy; although, portable structures would be preferred on these temporary roads so that the bridge could be relocated after the road is decommissioned.

This study proposes a shear connection between steel plate girders and precast concrete deck panels, which allows fastening, and unfastening, of these two components enabling a portable composite bridge. In total, ten connection concepts were developed during this study and a multi-criteria assessment was performed to evaluate each concept respectively. Based on the outcome of this multi-criteria assessment, and subsequent sensitivity analysis, a preferred connection was established and a finite element model was developed for the analysis of composite bridge girders.

For the initial development of the finite element model, the test set up and experimental findings of a test program by other researchers was employed so that the finite element analysis results could be compared to those reported from a physical experiment. Following this initial finite element analysis, full scale composite bridge girders were modelled so that the influence of the proposed shear connection on the behaviour of a composite girder could be studied. The model was verified for its ability to capture the possible effects of flange buckling, web buckling, and lateral torsional buckling of the steel plate girder. It was then confirmed that these local responses do not influence the performance of the proposed portable composite bridge system.

A parametric study was also performed in which the effect of shear connection stiffness and spacing on the behaviour of the composite girder was investigated. This parametric study allowed the sensitivity of the proposed connection to variations in these two parameters to be assessed and also allowed preliminary study of the performance of composite girders with alternative shear connection designs.

ACKNOWLEDGEMENTS

At the University of Waterloo I would like to thank my supervisors Dr. Jeffrey West, P.Eng., and Dr. Scott Walbridge, P.Eng., for their contribution to this work by providing research advice, academic guidance, and engineering support; as well as Dr. Lei Xu, P.Eng., and Dr. Liping Fu., P.Eng., for their review of my thesis.

At The Surespan Group of Companies I would like to thank the following individuals: Nigel Bester, for enabling this applied research project and for always finding time to provide invaluable lessons on bridge fabrication and construction methods; Shawn Kelly, for repeatedly sharing with me his knowledge gained as a senior bridge construction superintendent; Mark Smith, for providing his economic perspectives of bridge construction alternatives; Steve Stacey, for specific comments regarding field installation of concrete anchors; Brad Gunnlaugson, for assisting with cost-estimates; and Morgan Trowland for providing engineering support.

Funding for this research was gratefully received from The Natural Science and Research Council of Canada in partnership with The Surespan Group of Companies.

To my beautiful wife for her friendship and support

TABLE OF CONTENTS

Author’s Declaration	ii
Abstract	iii
Acknowledgements.....	iv
Dedication	v
Table of Contents	vi
List of Figures	ix
List of Tables	xii
1 Introduction	1
1.1 Objectives.....	2
1.2 Thesis Outline.....	2
2 Literature Review	4
2.1 Modular Bridge Systems	4
2.1.1 Truss Bridges	4
2.1.2 Precast Concrete Composite Bridges.....	6
2.1.3 Modular Bridge Systems for Short Spans	8
2.2 Shear Connections	10
2.2.1 Connections by Adherence	10
2.2.2 Shear Resistance of a Polyurethane Interface	12
2.2.3 Post Installed Shear Connectors	13
2.2.4 Effects of Friction in Composite Bridges	15
2.2.5 Effects of Friction in Non-Composite Bridges	16
2.2.6 Slip Critical Connections.....	17
2.2.7 Embedded Ductile Connectors	17
2.3 Analytical Modelling of Composite Structures	18
2.3.1 FEA Model for Composite Plate Girders – Negative Bending	19
2.3.2 FEA Model of a Simple Span Composite Plate Girder.....	23
3 Connection Concepts.....	28
3.1 Threaded Concrete Inserts.....	28
3.1.1 Mechanical Splice.....	28
3.1.2 Post-Installed	29
3.1.3 Impression Cast.....	30
3.2 Through Bolts.....	31
3.2.1 Steel to Steel	31

3.2.2	Concrete to Steel.....	32
3.2.3	Impression Cast with Through Bolts	33
3.3	Headed Studs	33
3.3.1	Continuous Embed	34
3.3.2	Discrete Embed Bolted to Flange.....	34
3.3.3	Discrete Embed Bolted to Web.....	35
3.3.4	Panel End Connections.....	36
4	Multi-Criteria Assessment.....	39
4.1	Design Load and Bridge Geometry	39
4.2	Assessment Method	41
4.2.1	Performance.....	42
4.2.2	Function	43
4.2.3	Economy.....	44
4.3	Concept Evaluation	46
4.3.1	Threaded Concrete Insert	47
4.3.2	Post Installed Connection	48
4.3.3	Impression Cast Deck with Concrete Insert	48
4.3.4	Through Bolt with Steel to Steel Contact.....	50
4.3.5	Through Bolts with Concrete to Steel Contact.....	51
4.3.6	Impression Cast with Through Bolts	51
4.3.7	Continuous Embed with Ductile Shear Studs.....	52
4.3.8	Discrete Embed Bolted to Flange.....	53
4.3.9	Discrete Embed Bolted to Web.....	54
4.3.10	Panel End Connection	54
4.4	Concept Evaluation Results.....	55
4.5	Sensitivity Analysis	57
4.6	Concept Recommended for Further Development	60
5	Model Development	61
5.1	Finite Element Model.....	61
5.1.1	Input.....	61
5.1.2	Element Selection	64
5.1.3	Model Assembly.....	65
5.2	Model Validation.....	68
5.2.1	Finite Element Analysis	68
5.2.2	Mesh Refinement.....	71

5.2.3	Web Buckling	72
5.2.4	Interface Friction.....	74
6	Full-Scale Composite Bridge Girder Studies.....	75
6.1	Composite Girder with Shear Studs.....	75
6.1.1	General Specifications.....	76
6.1.2	Analysis	76
6.1.3	Composite Girder Design	77
6.1.4	FEA – Composite Girders with Shear Studs	78
6.2	Composite Girders with Panel End Connections	85
6.2.1	Connection Design Narrative	85
6.2.2	Connector Properties.....	86
6.2.3	Fatigue of Gusset Plates in Panel End Connection.....	88
6.2.4	FEA – Composite Girders with Panel End Connections.....	88
6.3	Model Verification	92
6.3.1	Local Buckling in Compression Flange of Girder.....	92
6.3.2	Lateral Torsional Buckling	96
6.3.3	Stiffened Plate Girder Web Buckling.....	103
6.4	Parametric Study.....	105
6.4.1	Connection Stiffness	105
6.4.2	Connection Spacing.....	108
7	Conclusions	111
7.1	Research Summary	111
7.2	Significant Findings	112
7.3	Recommendations	113
	Appendix A: BC MOF DRAWING for L165 Composite Deck Panel	114
	Appendix B: Connection Design Calculations	116
	Appendix C: Cost Analysis	130
	Appendix D: 36 m Composite Bridge Girder Design Summary.....	141
	Appendix E: Panel End Connection Calculations	145
	Appendix F: Lateral Torsional Buckling Calculations.....	152
	Bibliography	156

LIST OF FIGURES

Figure 2-1: Bailey Bridge Spanning Buttler Creek, Moosonee [Paul Lantz 2006]	5
Figure 2-2: The Mabey Compact 200 bridge system [Mabey Bridge Ltd. 2010]	6
Figure 2-3: Steel Composite Bridge with Precast Deck [Surespan 2006].....	7
Figure 2-4: Shear Connection for a Re-usable Composite Bridge [US Patent 5,826,290]	8
Figure 2-5: All-Steel Portable Bridge [Surespan Construction, 2004].....	9
Figure 2-6: M60A1 Armoured Vehicle Landing Bridge [Lance Cpl. Kevin Quihuis Jr., 2003]	9
Figure 2-7: Connection by Adherence [Thomann and Lebet 2008].....	10
Figure 2-8: Polyurethane Shear Interface.....	12
Figure 2-9: Post Installed Shear Connection [Kwon 2008]	14
Figure 2-10: Shear Force Diagram for a UDL and Single Point Load	15
Figure 2-11: Dywidag Ductile Connector® [Dywidag-Systems International 2009]	18
Figure 2-12: Test set-up used for Physical Testing and Model Calibration [Allison et al. 1982]	19
Figure 2-13: Stress-strain Curves for Steel and Concrete [Baskar et al. 2002]	20
Figure 2-14: Post-Analysis Geometry of Composite Plate Girder [Baskar et al. 2002]	21
Figure 2-15: Load Deflection Curves for Composite Plate Girder [Baskar et al. 2002].....	23
Figure 2-16: Cross Sections of Experimental Girders [Barth and Wu 2006]	24
Figure 2-17: Elevations of Experimental Girders [Barth and Wu 2006].....	24
Figure 2-18: Stress-Strain Plots used for Steel (left) and Concrete (Right) [Barth and Wu 2006]	25
Figure 2-19: Experimental and FEA Load Deflection Plots [Barth and Wu 2006].....	26
Figure 3-1: Mechanical Splice	28
Figure 3-2: Post-Installed Connection.....	30
Figure 3-3: Impression Cast with Concrete Insert.....	30
Figure 3-4: Through Bolt with Steel to Steel Contact	32
Figure 3-5: Through Bolt with Concrete to Steel Contact.....	32
Figure 3-6: Impression Cast with Through Bolts	33
Figure 3-7: Continuous Embed with Ductile Shear Connectors.....	34
Figure 3-8: Discrete Embed Bolted to Flange	35
Figure 3-9: Discrete Embed Bolted to Web	36
Figure 3-10: Precast Concrete Deck Panel and Steel Embed Assembly for Panel End Connections	37
Figure 3-11: Installation Sequence using Panel End Connections	38

Figure 4-1: BCFS L165 Logging Truck compared to a CL-625 Design Truck	39
Figure 4-2: General Arrangement and Cross Section of Design Bridge	40
Figure 4-3: Failure Mode of an Impression Cast Deck at the Ultimate Limit State	49
Figure 5-1: Geometric Details for Initial Model [Barth and Wu 2006]	62
Figure 5-2: Stress Strain Relationship for Concrete	63
Figure 5-3: Tri-linear Stress Strain Relationship for Structural Steel	64
Figure 5-4: Composite Girder Modelled with Shell Elements.....	65
Figure 5-5: Load-Slip Envelope for 15 Static Push-out Tests [Hanswille et at. 2007]	67
Figure 5-6: Load-Slip Curve for 19mm Diametre Shear Stud.....	67
Figure 5-7: Stress Distribution in a Composite Plate Girder at Ultimate Load	69
Figure 5-8: Comparison of FEA (Abaqus) and Experimental Load Displacement Results.....	70
Figure 5-9: Effect of Mesh Density on the Initial Finite Element Model.....	71
Figure 5-10: Imperfect Shape in Web to Trigger Local Buckling in a Plate Girder.....	72
Figure 6-1: Live Shear and Moment Envelopes for an L165 36 m Composite Plate Girder.....	77
Figure 6-2: Cross-Section for a 36m L165 Composite Bridge Girder	78
Figure 6-3: Truck Position Resulting in Maximum Moment	79
Figure 6-4: Analytical Load Displacement References for Evaluation of FEA Results.....	81
Figure 6-5: Effect of Partial Interaction on Girder Stiffness.....	82
Figure 6-6: Applied Moment and Mid-span Displacement – UDL and L165 Axle Load	83
Figure 6-7: Schematic View of a Composite Girder with Panel End Connections	85
Figure 6-8: Load Displacement Properties for a Panel End Connection	87
Figure 6-9: Shear Stud Connection Compared to Panel End Connection.....	90
Figure 6-10: Initial Imperfection in the Top Flange of the Plate Girder for Local Buckling	93
Figure 6-11: Local Buckling in Top Flange of Plate Girder	94
Figure 6-12: Local Displacement to Illustrate Local Buckling in Top Flange of Plate Girder.....	94
Figure 6-13: Critical Stress in a Steel Plate to Cause Local Buckling	95
Figure 6-14: Two Step Loading for Modelling Lateral Torsional Buckling	97
Figure 6-15: Lateral Torsional Buckling – Flexural Resistance Vs. Unsupported Length	98
Figure 6-16: Lateral Torsional Buckling – Comparison of FEA and Calculated Results.....	99
Figure 6-17: Transformed Section Analysis to Determine Moment in Plain Girder	101
Figure 6-18: Critical Un-Braced Length of a Plate Girder within a Composite System	102
Figure 6-19: Initial Imperfections that Cause Web Buckling in a Plate Girder.....	104

Figure 6-20: Web Buckling for Tension Field Action in a Composite Plate Girder.....	104
Figure 6-21: Results of Parametric Study for the Effect of Connector Stiffness.....	106
Figure 6-22: Results of Parametric Study for the Effect of Connector Spacing	109

LIST OF TABLES

Table 2-1: Comparison between Experimental and FEA Load Deflection Data.....	26
Table 4-1: Description of Connection Assessment Criteria	41
Table 4-2: Unit Costs for Economic Analysis*	46
Table 4-3: Assessment of shear connection concepts.....	56
Table 4-4: Sensitivity Analysis	59
Table 5-1: Material Properties for Initial Finite Element Model.....	62
Table 5-2: Abaqus Results compared to Experimental Findings by Mans	70
Table 5-3: Finite Element Analysis for Local Buckling.....	73
Table 5-4: Effect of Friction on the Contact Surface between Deck Slab and Plate Girder	74
Table 6-1: Axle Loads per Girder that Develop the Yield and Plastic Moments	80
Table 6-2: Connection Properties for Centre and Side Gusset Plates	87
Table 6-3: Service and Ultimate Limit States of a Composite Girder.....	91
Table 6-4: Critical Buckling Stresses in Top Flange of Non-Composite Plate Girder	96
Table 6-5: Comparison of Effect of Connection Stiffness on Mid-Span Girder Deflections	107

1 INTRODUCTION

Steel girder bridges with composite concrete decks are a common type of bridge throughout North America. The composite connection in these structures is facilitated by the use of ductile shear studs that are welded to the top flange of the girder and protrude into the cast-in-place concrete deck slab.

In Western Canada, a composite bridge system that utilizes steel plate girders with full-depth precast concrete deck panels is used in the resource industries and, in some cases, for rural highways. With this system, the ductile shear studs are concentrated in groups that are spaced at one metre on centre along the girder. Each group of shear studs corresponds with void 'pockets' in the precast concrete deck, and the composite connection is facilitated by placing non-shrink grout in each of the pockets. Since these bridges are typically installed in remote locations, precast concrete deck panels are preferred because of the difficulty in supplying ready-mixed concrete to the bridge site.

The current design for a composite bridge with full-depth precast concrete deck panels results in a permanent bridge structure. In the resource industry, roads are commonly built to provide temporary access during the extraction of a particular resource. On these temporary roads, portable bridges are preferred so that the bridge structure can be re-used after the road is de-commissioned. An all-steel portable box girder bridge is used for spans up to 18 metres; however, permanent structures are typically chosen for larger spans because an economic portable structure does not exist.

This research was initiated with an interest in developing a shear connection detail that can be used for a portable composite bridge. Several concepts were developed and, based on the results of a multi-criteria assessment, one of these concepts is recommended as a preferred connection for a portable composite bridge. To study the effect of incorporating this preferred connection in a composite girder, a detailed finite element analysis was performed.

In the following two sections of this Introduction, the objectives of this research study are summarized followed by a brief description of the contents for each chapter in this thesis.

1.1 Objectives

The general goal of this research was to develop a shear connection concept that could enable a portable composite bridge. The following objectives were established during this study, and are summarized in the order in which they appear in this thesis:

- Identify existing portable bridge products and review literature on research that could assist the development of a shear connection for a portable composite bridge;
- Propose several connection concepts that could be used to enable a portable composite bridge; evaluate each of the proposed connections for their performance, function, and economy; and complete a multi-criteria assessment of the proposed connection alternatives that identifies a preferred connection for a portable composite bridge;
- Develop a finite element model that accurately predicts the ultimate response of a composite girder; apply finite element analysis to model a composite girder with the proposed shear connection and a composite girder with a regular shear stud connection; and
- Study the performance of a composite girder with the proposed connection; and perform a parametric study to determine the sensitivity of the composite system to variations in the connection properties.

1.2 Thesis Outline

Following the Introduction, Chapter 2 presents a literature review, which contains three main sections. The literature review begins by summarizing existing modular bridge products that can be used as either permanent or portable structures; is followed by a summary of research on structural shear connections; and concludes with a detailed description of two studies performed in which general finite element analysis was employed to model composite plate girders.

Chapter 3 presents ten connection concepts that were proposed during this study. In this Chapter, a general detail for each connection is produced and the structural system for each concept is discussed. Based on their primary structural components, each of the ten connections is categorized into one of the following three general connection types: threaded concrete inserts; through bolts; or headed shear studs.

In the fourth Chapter, a multi-criteria assessment is performed. As part of this assessment, each of the ten connection concepts is evaluated based on their anticipated performance, function, and economy.

After completing the multi-criteria assessment, a sensitivity analysis is completed and a preferred connection concept is chosen.

Chapter 5 presents the development of the finite element model used, in this research, to analyze composite girders. The finite element model presented in this chapter is based on the material properties, and geometric layout, of a physical composite plate girder tested in a laboratory by other researchers. This chapter concludes with a comparison of the results from the finite element analysis in comparison to the physical tests.

In the sixth Chapter, the finite element model is applied for the analysis of full-scale composite bridge girders. First, a model for a composite plate girder with regular shear studs is completed to establish a benchmark for the comparison of a regular composite girder to one with the proposed shear connection. The finite element models for full-scale bridge girder studies are verified and a parametric study is performed to assess the sensitivity of the proposed composite system to specific properties of the connection.

In the final Chapter, important findings resulting from this research are summarized in a conclusion and recommendations are made for future developments of the proposed shear connection for a portable composite bridge as well as recommendations for future research.

2 LITERATURE REVIEW

The literature review presented in this chapter provides a brief background on the development of modular bridge systems, followed by a detailed review of current research and product developments associated with shear transfer in composite or multi-component structures. The literature review concludes with a summary of two analytical models developed to study the structural behaviour composite girders.

2.1 Modular Bridge Systems

Bridge structures that are constructed with pre-fabricated components are referred to as modular bridges. All of the individual components in a modular bridge are built in a controlled environment such as a steel fabrication plant or precast concrete yard and are shipped to site for assembly. Modular bridges can be built as either portable or permanent structures and are often chosen for temporary bridges installed in urban settings or for river crossings in remote areas where accessibility to the site is limited and ready-mixed concrete is unavailable.

Perhaps the most famous modular bridge is a portable truss structure which is often referred to as the Bailey bridge. Another modular bridge, used extensively in the resource industries throughout Western Canada, is a composite structure incorporating steel plate girders and precast concrete deck panels. Each of these two bridges is described in detail in the following two sections followed by a brief summary of other types of modular bridges.

2.1.1 Truss Bridges

The concept and design of the first mass produced modular bridge, known as the Bailey bridge, was developed by the British engineer Sir Donald Coleman Bailey during the Second World War. Capable of spanning clear distances of up to 60 metres and having an ability to support tanks and other heavy trucks, the Bailey bridge was chosen in 1941 as the official military bridge [Mabey Bridge 2010]. To enable ease of transport and installation, the bridge was designed so that any individual component could be handled by six soldiers. After the War ended, Bailey bridges found new applications as temporary structures in both rural and urban settings and in many instances these temporary Bailey bridges became permanent structures. In 1946 Sir Donald Coleman Bailey was knighted for his bridge design [Mabey Bridge 2010].

A typical Bailey bridge has a bridge deck that provides a single 3.659 metres (12 feet) wide lane. The wearing surface consists of either steel grating or heavy timber planks that are fastened to steel

stringers which run parallel to the bridge span. The stringers are supported every 1.524 metres (5 feet) by 5.183 metre (17 feet) long wide flange steel beams. These wide flange beams transfer the loads from the bridge deck to the steel pony trusses. The trusses on each side of the bridge are built with individual truss segments that are 3.048 metres (10 feet) long and 2.134 metres (7 feet) deep. These truss segments are pinned together to form a structure that suits the required span and specified loads. Depending on the structural demand, truss segments can be combined so that they are two or three segments wide and also two or three segments deep. The 45.7 metre (150 foot) long single span Bailey bridge in Figure 2-1 shows a 'double-double' configuration, meaning that each side of the bridge has a truss that is two panels wide and two panels deep.



Figure 2-1: Bailey Bridge Spanning Buttler Creek, Moosonee [Paul Lantz 2006]

While Bailey bridges are still available and used today, improved versions of the Bailey bridge are now available from the American producer Acrow Bridge, and the British producer Mabey Bridge. For example, Acrow Bridge [2010] states that their 700XS® Acrow Panel Bridging system utilizes structural panels composed of truss segments that are: 50% stronger in bending, 20% stronger in shear, and lighter, than the truss segments used in Bailey bridges, while Mabey Bridge [2010] states that their Mabey Compact 200 bridge system is the latest development of the original Bailey bridge.

Neither producer provides specific details as to how their systems are superior to the Bailey bridge; however, Acrow Bridge partially accredits their improvements to truss panels that are deeper and lighter than Bailey bridge panels and Mabey Bridge mentions that improved material properties and

fewer overall components are contributing factors to their improved design. A 3.048 metre (10 foot) section of The Mabey Compact 200 bridge system is presented, schematically, in Figure 2-2.

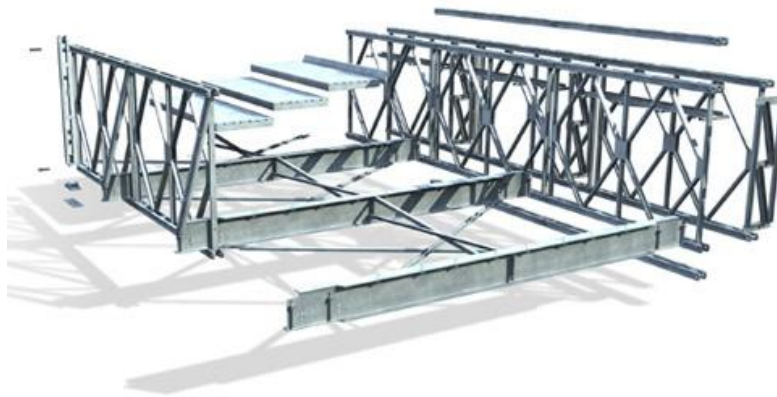


Figure 2-2: The Mabey Compact 200 bridge system [Mabey Bridge Ltd. 2010]

In general, the structural system of the Mabey Compact 200 bridge system is very similar to a Bailey bridge; although, one noticeable difference between the two bridges is that the Mabey Compact 200 bridge has a decking system that transfers vehicle loads directly to the steel wide flange beams without the need for longitudinal stringers.

Bailey bridges, and its successors, are extremely versatile structures that can be used for short or medium spans. For a general-use modular bridge system, this versatility is a marketable feature; however, bridges that are custom designed for a pre-defined span and specified load have the potential to present better economy than a modular truss bridge because they can be optimized for a specific application.

For example, in the resource industries throughout Western Canada the most popular modular bridge consists of steel plate girders and a composite precast concrete deck. These bridges typically span up to 36 metres and support logging trucks that are over two times heavier than a standard legal highway load. Modular truss bridges could be used as a comparable structure in this industry; however, the steel composite modular bridge system provides better economy and continues to be the preferred alternative.

2.1.2 Precast Concrete Composite Bridges

In Western Canada, a common bridge design used in the forest and resource industry for spans that exceed 18 metres is a composite structure consisting of steel plate girders and a precast concrete deck.

Since these bridges are often located in remote areas, the use of precast concrete not only simplifies on-site construction, but is also necessary because of the difficulty in supplying ready-mixed concrete to these job sites.



Figure 2-3: Steel Composite Bridge with Precast Deck [Surespan 2006]

To facilitate composite behaviour, shear studs are concentrated in groups that are located along the top flange of the plate girders (see Figure 2-3). Corrugated pipe is used to create voids, which are often referred to as ‘pockets’, in the precast deck panels that align with the grouped shear studs. Field placement of non-shrink grout between adjacent precast panels and in the corrugated steel pockets provides continuity between panels and enables a composite system.

Field grouting is required to make this system work; however, several benefits would be realized if this composite bridge design could be altered so that the placement of grout was rendered unnecessary. The primary benefits can be summarized as follows: a reduction in construction duration and cost would be realized because placing grout is a labour intensive task; the bridge would provide the capacity of its full design load immediately following construction; and bridge erection could be completed in sub-zero temperatures without the need for heating and hoarding.

To enable a reusable composite bridge, a connection enabling a removable precast concrete deck was invented by George D. Kokonis (see Figure 2-4) and patented by West Bridge Corporation in both Canada [Canadian Patent 2,202,193] and the United States [U.S. Patent 5,826,290]. With the exception of the removable shear connection, the structural system of this reusable composite bridge is the same as the standard composite bridge design described in the previous paragraphs.

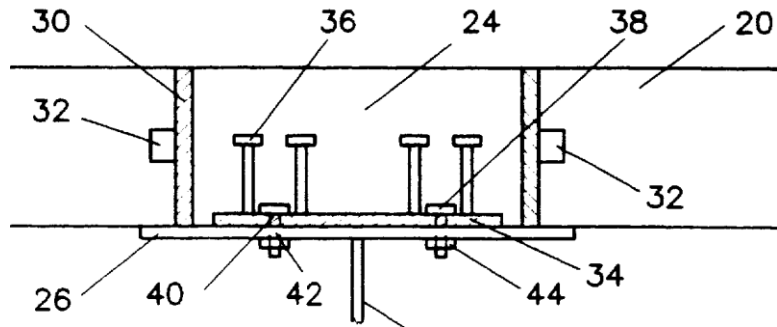


Figure 2-4: Shear Connection for a Re-usable Composite Bridge [US Patent 5,826,290]

Instead of welding the shear studs directly to the top flange of the steel plate girders, Kokonis' connection is made possible by welding shear studs (36) to steel plates (34) that are then bolted (38) to the top flange (26) of a plate girder. Another feature of this invention is the use of a smooth wall steel pipe (30) in place of the corrugated pipe to form the grout pockets in the precast concrete deck panel (20). After the deck panels are unbolted and removed from the bridge the smooth inside wall of the grout pocket is intended to allow the cured grout (24) along with shear studs and the steel plate to be removed like a plug from the precast concrete deck panel. After removal, the plug of cured grout and shear studs is discarded. A new set of shear studs and steel plates is required for reuse of the bridge.

This patent also includes several variations of the ideas described above; however, common to each of the variations is the requirement for holes to extend through the precast concrete deck panels to facilitate a method of fastening the deck directly to the top plate of the steel girder.

This patented system enables reuse of the primary bridge components but does not enable a fully portable composite bridge because critical components of the bridge are discarded after each use. Another disadvantage is its dependence on field grouting to enable composite behaviour and continuity of the deck. The main purpose of this thesis is to develop a shear connection system that is not limited by these disadvantages.

2.1.3 Modular Bridge Systems for Short Spans

Several modular bridge types exist for short spans of up to 18 metres. Permanent short span modular bridges have been made with precast concrete box girders. Each girder is placed directly parallel to one another and the number of girders is based on the desired lane width. Steel embed plates are installed in the box girders so that the concrete girders can be joined with a welded shear connection.

A common temporary structure, referred to as an all-steel portable, is produced for 12, 15, and 18 metre spans which consists of two 2.4 metre wide low profile steel box girders that are placed parallel to form a 4.8 metre wide bridge. Figure 2-5 shows the installation of an all-steel portable bridge.



Figure 2-5: All-Steel Portable Bridge [Surespan Construction, 2004]

Abutments for all-steel portable bridges are typically chosen to suit locally available materials. If the all-steel portable is being used as a remote logging bridge then heavy log sills may act as the abutment; alternatively, precast concrete lock blocks are often used for urban applications.

A common short span modular bridge used by the United States, and other countries, for rapid deployment in military applications is shown in Figure 2-6.

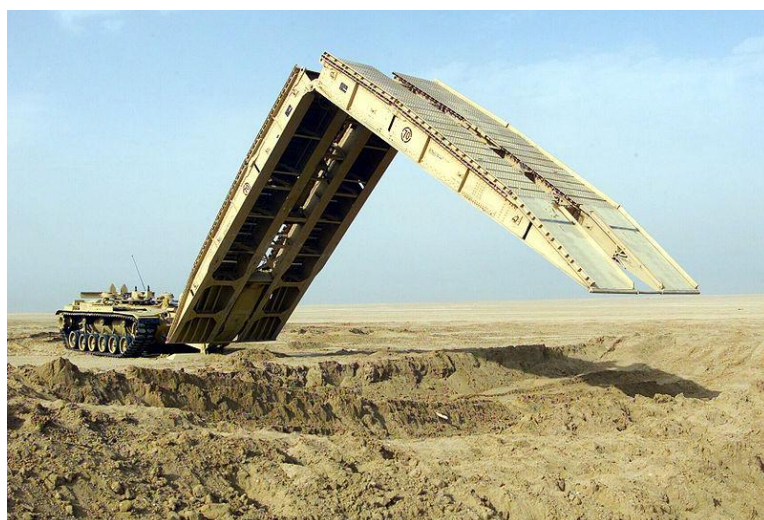


Figure 2-6: M60A1 Armoured Vehicle Landing Bridge [Lance Cpl. Kevin Quihuis Jr., 2003]

The M60A1 Armoured Vehicle Landing Bridge spans 18 metres (60 feet), and consists of two steel sections with a “hinge” at mid-span. In Sweden, a similar military bridge has been developed by Höglund and Nilsson [2006] using aluminum as the primary structural material in place of steel. These military bridges are designed so that they attach to an armoured tank for transportation. During installation, the tank also acts as the counter weight and replaces the need for a crane or excavator that is otherwise used for short span bridge installations.

2.2 Shear Connections

For the purpose of this study, an ideal shear connection for portable bridge applications is one that has the following three characteristics; facilitates fastening and unfastening of the precast element to the structural steel, does not require field grouting, and has the ability to develop a full composite section. No existing connection details or concepts were found to have all three of these qualities; therefore, products and research that have one or more of these ideal characteristics are presented in the following sections.

2.2.1 Connections by Adherence

Connections by adherence are a longitudinal shear connection where friction by adhesion is used to transfer stress between two materials to facilitate composite behaviour [Thomann and Lebet 2008]. These connections are being studied to enable rapid erection of composite bridges consisting of steel girders and precast concrete decks. The structural components in a proposed configuration for a connection by adherence are presented in Figure 2-7.

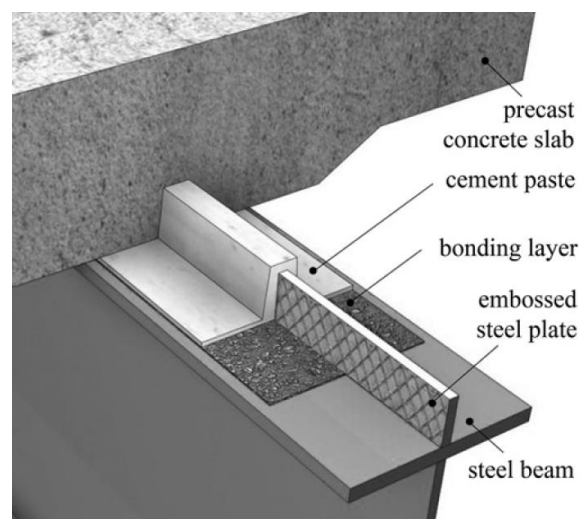


Figure 2-7: Connection by Adherence [Thomann and Lebet 2008]

The connection consists of a longitudinal embossed steel plate that is welded perpendicular to the top of the upper flange of a steel beam. During casting of the concrete deck, a deep longitudinal groove is set into the underside of the deck to correspond with the location of the embossed steel plate. The groove is large enough to facilitate the injection of a cement paste after bridge erection. Prior to installation of the precast deck the surfaces of the panels that will come in contact with the girder top flange are roughened, with an amplitude of at least a 6 mm, to enhance the bond. The reference suggests the use of a surface applied chemical retarder as an option for roughening the surface. After placing the deck panels on the girders, a cement paste is injected into the void between the precast panels and the embossed steel plate. Composite action is achieved after curing of the cement paste.

Direct shear push tests of several variations of this connection type have been completed by Dauner [2005] and Thomann [2005]. The two variations of the adherence connection tested were labelled as 'Perfobond' and 'adherence'. For comparison, push tests were also completed on a traditional shear connection consisting of headed studs.

With the Perfobond connection, a continuous series of holes were punched in the steel plate. Since the concrete deck is precast, placing transverse reinforcement through these holes is not possible. The Perfobond connection had similar stiffness but a lower ultimate shear strength when compared to the traditional connection provided by headed shear studs while the adherence connection showed significantly higher readings for both shear strength and stiffness when compared to the shear stud connection; however, the adherence connection lacked ductility.

Following the completion of the push tests, a mechanical model for connections by adherence was developed. The mechanical model was developed to determine if the limited ductility of the adherence connection could present a problem in composite beams; and to determine how the geometry of the steel-concrete interfaces affects the performance of the connection with particular attention to the influence of normal stress on shear resistance.

Despite the low ductility, Thomann and Lebet [2008] showed that composite beams with adherence connections provide full plastic flexural resistance in both positive and negative bending. They also determined that the optimum ratio for the surface area of the embossed steel plate to the combined area of the embossed steel plate and top flange of the steel girder should be between 0.35-0.40. Recommendations for minimum surface roughness were also established using this model.

2.2.2 Shear Resistance of a Polyurethane Interface

Ramsay [2007] conducted a series of tests to investigate the suitability of a polyurethane interface to bond full depth precast concrete deck panels to steel girders. Although Ramsay did not refer to the polyurethane interface as a ‘connection by adherence’ the principle mechanics of this connection are similar to the connection researched by Thomann and Lebet [2008].

Ramsay considered four different joint configurations. Differences between each configuration were made by altering the soffit of the precast concrete deck panels. Two of the configurations incorporated a direct bond between the concrete deck and the steel girder utilizing mechanical interlock. This was achieved either by casting shear keys in the concrete deck or by exposing the concrete aggregate to roughen the soffit. The two remaining configurations consisted of metal plates with shear studs that were cast in the underside of the precast panels (see Figure 2-8).

Two variations of steel plates were considered; one with continuous steel plates spanning each precast panel and aligned with the steel girders, the other with several rectangular steel plates embedded along each panel in line and aligned with the girders. The continuous steel plates were cast so that the underside of the steel plate was flush with the soffit of the concrete deck as shown in Figure 2-8; alternatively, test specimens with several rectangular steel plates constructed with the steel plates protruding below the concrete deck underside, enabling mechanical interlock.

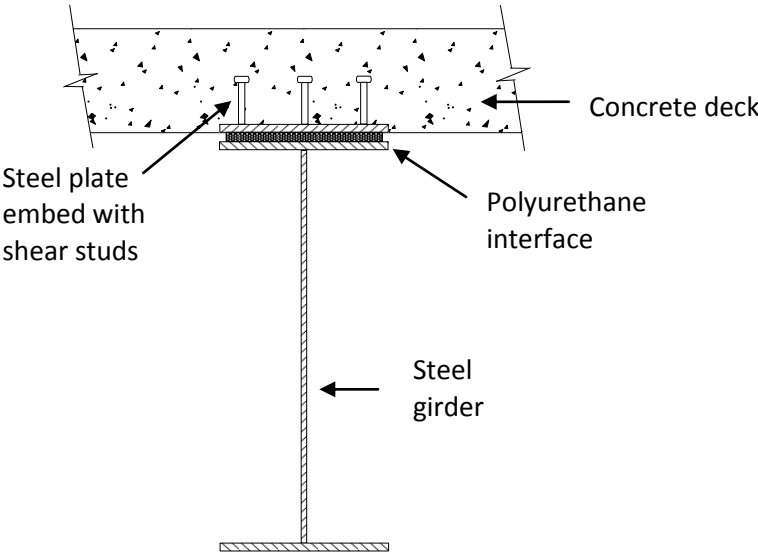


Figure 2-8: Polyurethane Shear Interface

During construction of the test specimen, a wooden frame was installed around the perimeter of the girder specimen's upper flange. This frame served as a spacer that maintained the gap between the precast concrete and the girder as well as a form for the polyurethane. Ramsay [2007] reports that the polyurethane was injected into this void; although, details of this process were not provided.

Push tests performed by Ramsay showed cohesive failures of the polyurethane at low stress levels. The failure stress of the polyurethane was too low to warrant comments regarding favourable soffit configurations. Several observations were made which led to hypothesis for the poor polyurethane performance but no definitive explanation was found. Ramsay notes that published test data [Si Larbi et al., 2006] suggests polyurethanes should be able to provide a bond that would facilitate a full composite connection between high strength concrete and structural steel. Ramsay recommended addressing the inadequate bonding characteristics of the polyurethane prior in future testing.

Immediately following the completion of Ramsay's tests, a program was launched by Cheung [2008] to correct the poor behaviour of the polyurethane. Cheung tested six formulations of polyurethane using a scaled down version of the push test. During this test period, a formulation was found that provides adequate strength and stiffness for use in composite bridges with full depth precast concrete decks. Cheung states that although the polyurethane formulation showed promising results, further testing should be conducted on specimens of a larger scale and in conditions representative of those encountered in the field.

2.2.3 Post Installed Shear Connectors

Work conducted by Kwon et al. [2008] demonstrated that shear connectors can be installed in existing non-composite bridges to provide partial composite behaviour between the concrete deck and steel girder superstructure. Several different 'post installed' shear connections were tested in this reference, with a preferred alternative illustrated in Figure 2-9.

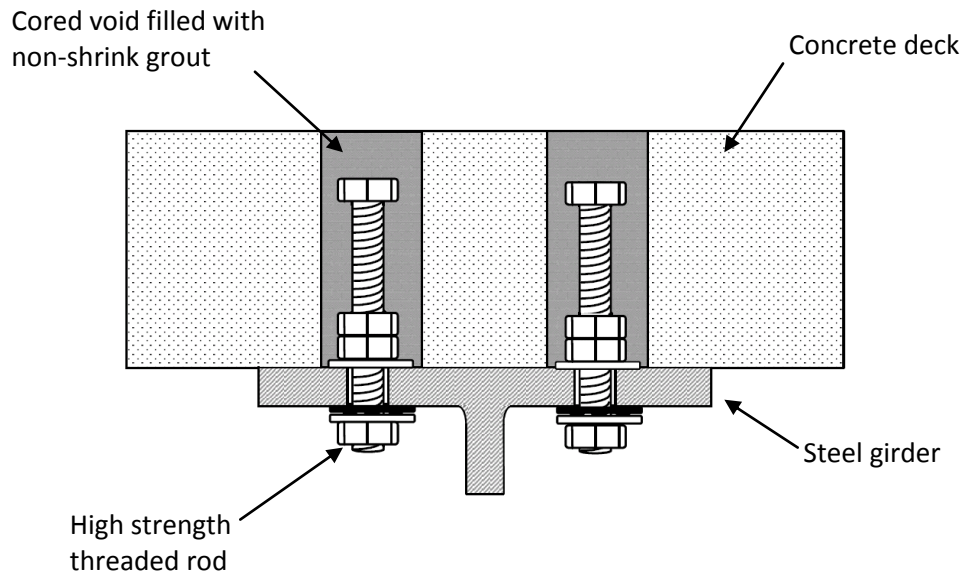


Figure 2-9: Post Installed Shear Connection [Kwon 2008]

The connector proposed by Kwon et al. consists of a bolted connection between the steel flange and concrete. This connection is installed by coring the concrete deck then drilling through the steel flange. A high strength threaded rod is then bolted to the steel flange with its shaft extending into the cored void in the concrete deck. A nut is placed on the free end of the threaded rod so that the rod acts as a headed assembly. Composite behaviour is achieved by placing non-shrink grout in the void between the cored concrete deck and the threaded rod. This research showed that an increase in flexural strength of about 40- to 50-percent in locations of positive moment could be achieved with a partial shear connection facilitated by approximately 30- to 50-percent of the connectors that would be required for a full shear connection.

Although the application is different, this post installed shear connection shares similarities with the connection utilized in Kokonis' [U.S. Patent 5,826,290] patented reusable composite bridge. Both connections utilize: holes through the full depth of the concrete deck, bolted connections between concrete decks and the steel girders, and field placement of grout to enable the bond between the fastening assembly and the concrete deck.

2.2.4 Effects of Friction in Composite Bridges

It is not common for engineers to consider the effects of friction when designing shear connections for composite girders; however, some research has been completed in an effort to quantify the contribution that friction makes to transfer shear stress in composite bridges.

Oehlers et al. [2000] proposed that longitudinal shear forces transferred by friction reduce the maximum stress in shear connectors resulting in a prolonged fatigue life for headed shear studs. Their study focused on determining the level of shear force transferred by friction, so that actual stress levels in the mechanical shear connectors could be quantified. It was found that friction acts to reduce stress in shear studs located near the supports of a simply supported composite beam; however, stress levels in studs located along the middle section of the beam actually increased.

To understand this phenomenon, consider a simply supported composite beam subjected to a moving point load that travels from the left end of the beam to the right. At each load position, the normal stress in the vicinity directly below the point load will be large, enabling a friction based resistance to longitudinal shear stress at the concrete/steel interface. Initially, as the point load begins to travel across the beam, the transition point between positive and negative shear will be to the right of the point load as illustrated in the instance presented Figure 2-10.

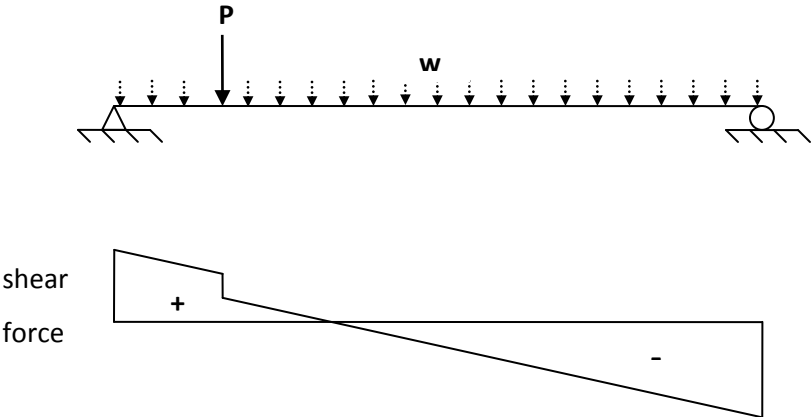


Figure 2-10: Shear Force Diagram for a UDL and Single Point Load

The shear force diagram illustrated in Figure 2-10 represents vertical shears; however, since the diagram is qualitative, and since longitudinal shear stress is proportional to vertical shear stress, this diagram is also representative of the longitudinal shear stress in a fully composite girder at the steel/concrete interface. If the effects of friction at this shear interface are ignored, then the full magnitude of the interface shear will be resisted by the shear studs; however, the influence of friction has an effect on the stress experienced by the shear studs.

Continuing with the illustrative example in Figure 2-10, Oehlers et al. [2000] observed that the interface friction reduces the maximum stress in shear studs located left of the point load P , where the design stress is largest; and increases the maximum stress in studs to the right of the point load. Despite the unexpected results of increased stress in studs located in the middle section of the bridge span, the findings of this study showed that decreased stress in studs at both ends of the bridge resulted in a net benefit to the overall fatigue life of shear studs in single span composite bridges.

This study resulted in the development of an analysis procedure, which may be applied for the assessment of fatigue life in existing structures. It is noted that consideration of even a small amount of stress reduction in shear studs due to friction can result in a substantial increase to the remaining fatigue life.

2.2.5 Effects of Friction in Non-Composite Bridges

Additional work completed by Seracino and Oehlers [2002] led to the development of a method for determining the level of composite action achieved by friction between concrete and steel in non-composite single span slab on girder bridges. This study demonstrates that friction enables partial interaction between the concrete and steel in these bridges. Based on previous work by Bakht and Jaeger [1992], it was known prior to the outset of this study that interaction caused by friction provides only a minute increase in flexural capacity. Therefore, the focus of this study was to provide an approach that could be used to quantify the benefit to fatigue life of non-composite bridge beams.

The outcome of this work by Seracino and Oehlers [2002] was the development of a mathematical assessment tool referred to as the Non-Composite Mixed Analysis Fatigue Approach, which can be used by engineers to assess the remaining strength or endurance of existing non-composite bridges that are near the end of their design life.

2.2.6 Slip Critical Connections

Slip critical connections are commonly used in bridge construction to facilitate field connections of structural steel. With this type of connection, friction between adjoining members enables the transfer of shear stress. The normal force needed to generate friction is produced by applying a pre-tension to the bolts during installation. For bolts used in slip critical connections a minimum pre-tension equal to 70 percent of the bolts tensile strength is required. A field study performed by Kulak and Birkemoe [1992] confirmed the development of this pre-tension in bolted connections tested in steel buildings and bridges.

During this field study, pre-tension was recorded with a device that uses ultrasound to measure the lengths of the installed bolts. The measured bolts were then released and a second measurement was taken so that the original elongation could be calculated and used to back calculate the pre-tension. An advantage of this method is that all testing took place after the installation of the bolts, which meant that the iron workers were not aware that their connections would be tested. A total of 232 bolts of various sizes and grades were tested throughout Western Canada, Eastern Canada, and Eastern United States. A summary of the test results for all of the bolts in this study showed that on average, bolt pre-tensions exceeded the specified minimums by 15%; however, grade A325 bolts that were installed in bridges located in Western Canada exceeded, on average, specified minimum pre-tensions by 27%. The Canadian Institute of Steel Construction [2007] also makes reference in their commentary to a minimum pre-tension equal to 70 percent of the bolts tensile strength for slip critical connections.

While the design of slip critical connections for fastening steel to steel is well established, no record exists of slip critical connections used to fasten steel to concrete. Information that could be useful for predicting the potential of slip critical connections between steel and concrete includes tests that were conducted by Rabbat et al. [1985] that quantified friction coefficients of concrete to steel. Rabbat found that the coefficient of friction decreased as the normal force increased. Measured coefficients ranged from 0.57 to 0.70.

2.2.7 Embedded Ductile Connectors

Embedded ductile connectors are threaded inserts designed to be cast into concrete to enable bolted connections between pre-cast concrete members as illustrated in Figure 2-11. Two manufacturers of these inserts are Dywidag International Systems and Dayton Superior.

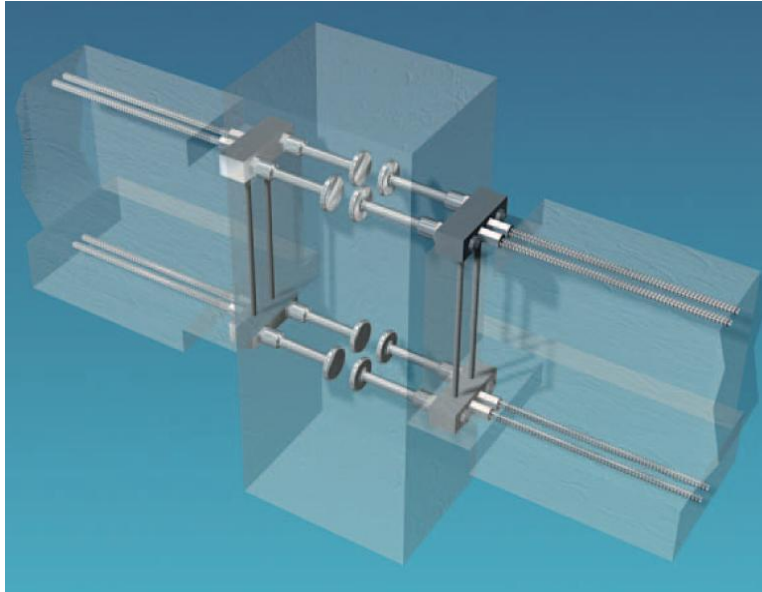


Figure 2-11: Dywidag Ductile Connector® [Dywidag-Systems International 2009]

The patented Dywidag Ductile Connector® enables moment resisting bolted connections between elements of precast concrete. Each Dywidag Ductile Connector facilitates a 38 mm diameter A490 bolt, has a yield strength of 1,254 kN in 35 MPa concrete, and requires an embedment depth of 375 mm. The first application for the Dywidag Ductile Connector was a three storey parking garage in Southern California [Dywidag-Systems International 2009]. With the exception of the foundation, this entire parking garage was constructed with precast concrete.

Dayton Superior's F-54 Ductile Embedded Insert is available in five different sizes that accommodate bolts ranging from 16 mm to 32 mm in diameter. The intent of this connector is to facilitate connections between concrete and other building components such as structural steel and overhead hangers for piping or ductwork. The largest F-54 Ductile Embedded Insert has an un-factored tensile resistance of approximately 442 kN and requires an embedment depth of 375 mm.

2.3 Analytical Modelling of Composite Structures

Finite element analysis to model complex structural systems, including composite bridges, provides a powerful analytical tool for research and design. Two independent researchers recently developed finite element models of composite girders to study their post buckling behaviour and non-linear response to ultimate loads. These two studies are summarized herein.

2.3.1 FEA Model for Composite Plate Girders – Negative Bending

Using Abaqus [2002], a general purpose finite element software, Baskar et al. [2002] developed a model that can be used to perform non-linear analysis of composite plate girders subjected to negative bending and shear loads. Baskar et al. observed that Bernoulli beam elements are not suitable for completing non-linear analysis of composite plate girders because of the occurrence of local buckling and plastic deformation. Based on this observation, Baskar et al. developed a model specifically for the analysis of composite plate girders with thin stiffened webs.

The flexural response of a plate girder is influenced by the magnitude of its applied load. When insignificant loads are applied the girder responds as a regular beam. As the applied load increases, the compression forces in the web eventually cause the web to experience local buckling between vertical stiffeners, resulting in the development of tension field action. Finally, at the ultimate limit state, a plastic response is realized due to yielding of the flange plates. To enable a non-linear analysis, modelling each of these responses is necessary.

Baskar et al. considered several different combinations of elements and material types to find a combination that accurately modelled the post-buckling and plastic response of the girder. To calibrate the finite element model, results of an experimental investigation completed by Allison et al. [1982] that involved physical testing, to failure, of five composite and one non-composite plate girders were employed. The Allison et al. test set up is illustrated in Figure 2-12.

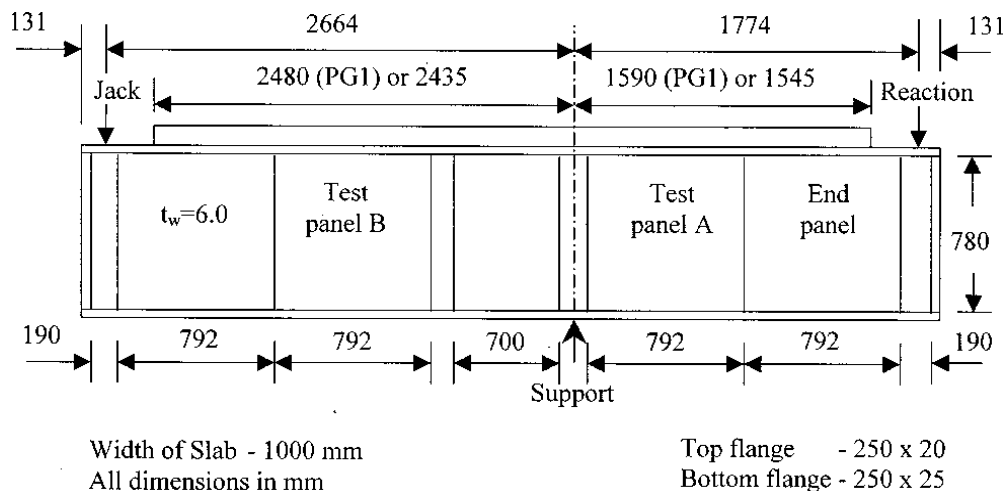


Figure 2-12: Test set-up used for Physical Testing and Model Calibration [Allison et al. 1982]

In the experiments by Allison et al., six girders were tested so that the effect of changing particular variables could be studied. One of the six girders was a control specimen. In general, the fabrication of

the remaining five girders varied from the control specimen as follows; the concrete strength was doubled, the number of shear studs was reduced by a factor of three, the thickness of the slab was doubled, the slab was removed, and a propped construction sequence was introduced.

Key components of the finite element model [Baskar et al. 2002] are presented below including descriptions of materials and a summary of the element types and constraints considered. Included are recommendations for specific types of elements that accurately model the composite section.

The structural steel was defined as an elastic-perfectly plastic material in both tension and compression. Young's modulus, E , was assigned a value of 207 kN/mm². Specific steel strengths were assigned to the top flange, web, and bottom flange plates, corresponding with the results of coupon tests. The assumed stress-strain curves for steel and concrete are presented in Figure 2-13.

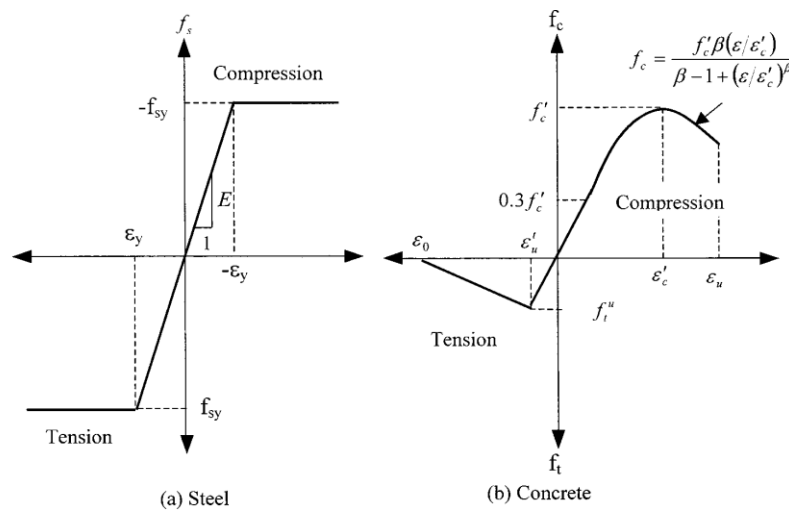


Figure 2-13: Stress-strain Curves for Steel and Concrete [Baskar et al. 2002]

Concrete in compression is modelled as a linear-elastic material up to a value of $0.3 \cdot f'_c$, where f'_c is the cylinder compressive strength in MPa. For stresses that exceed $0.3 \cdot f'_c$ the stress-strain curve takes on the following parabolic form suggested by Carreira and Chu [1985]:

$$f_c = \frac{f'_c \beta \left(\frac{\epsilon}{\epsilon'_c}\right)}{\beta - 1 + \left(\frac{\epsilon}{\epsilon'_c}\right)^\beta} \quad [2-1]$$

where ϵ is the strain in the concrete up to a maximum value of ϵ_u , ϵ'_c is the strain associated with the maximum concrete stress, and:

$$\beta = \left[\frac{f'_c}{32.4} \right]^3 + 1.55 \quad [2-2]$$

where units of MPa are used for f'_c . Baskar uses a strain of 0.002 (ϵ'_c) corresponding to the maximum compressive load and a crushing strain of 0.003 (ϵ_u). Concrete in tension is defined as a linear-elastic material up until cracking. A “tension stiffening” option in Abaqus was used to define the post-failure response of the concrete in tension. Reinforcement in the concrete slab is specified using the rebar option. The reinforcement is incorporated into the model as a one-dimensional strain element.

Two approaches were considered for modelling the shear connection between the concrete slab and the top flange of the plate girder. A surface interaction technique was considered first. With this method, a specific interaction between the concrete deck and steel plate is used to eliminate a requirement to specify common nodes between the two materials. The properties of the shear studs are used to define a bilinear stress-strain interaction between the concrete and steel in the longitudinal direction enabling excessive strain, which would be representative of a plastic shear connection. For vertical separation between the concrete deck and the top flange, the surface behaviour option is used with a tensile capacity representative of the pull-out resistance provided by the shear studs. It is noted that local effects of bond for the studs are not considered explicitly in the model. This interaction technique was found to simulate the composite girders well up to the ultimate load; however, once the ultimate load was exceeded, simulations with a model using the interaction technique were terminated. Although the surface interaction allows differential strains, severe and sudden discontinuities are realized in the post buckling stress range as the plate girder experiences excessive deflections. These excessive deflections, as illustrated in Figure 2-14 are the reason for the termination of analysis.

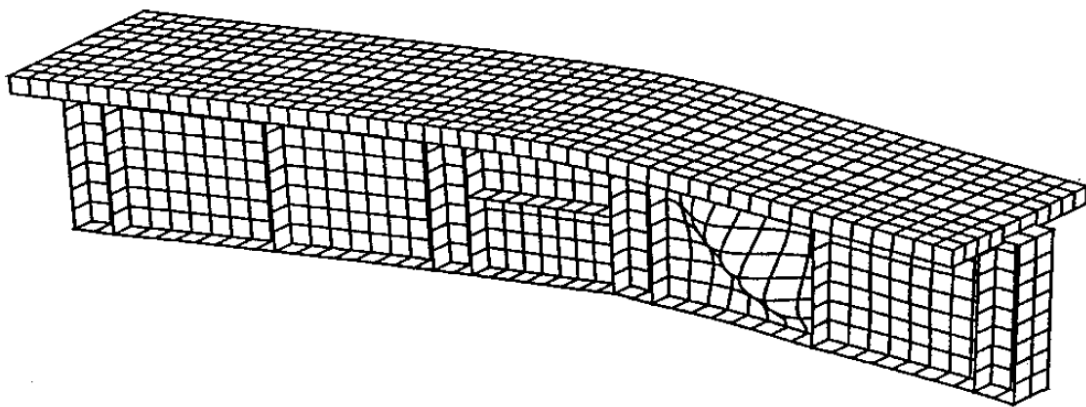


Figure 2-14: Post-Analysis Geometry of Composite Plate Girder [Baskar et al. 2002]

The second approach was found to be successful in analyzing the composite girder in the post-buckling range. This method involved replacing the interaction restraints with general beam elements used to represent the shear studs. Using these beam elements, the concrete slab was connected to the top flange of the girder.

Baskar et al. [2002] reports that an initial sinusoidal imperfection was introduced in the web of the girder with a maximum displacement equal to one thousandth of the web panel length. It was not reported whether this imperfection was introduced as single or double curvature; however, this initial imperfection successfully initiated the expected post-buckling response. The final buckled shape of the web panel exhibited double curvature.

For the plate girder, eight-noded doubly-curved shell elements were assigned to the bottom flange, web, and top flange. Initially, 20-node brick elements were used for modelling the concrete slab; however, it was found that these brick elements were not able to model the composite girder through to post-buckling failure. Since the girders were tested in negative bending, tensile loads were introduced in the concrete deck. These tensile loads, combined with rotation of the slab due to deflection of the composite system, caused local cracking in the concrete, which resulted in the termination of analysis. The best over-all, and post-buckling, response was realized when thick shell elements were used to model the concrete deck; consequently, thick shell elements are recommended by Baskar et al. for modelling the concrete deck in a composite girder.

Since strain measurements were not available from the Allison et al. experiments, the finite element models were compared to load deflection plots. The experimental and analytical results are presented in Figure 2-15 for the beam with the reduced number of shear studs.

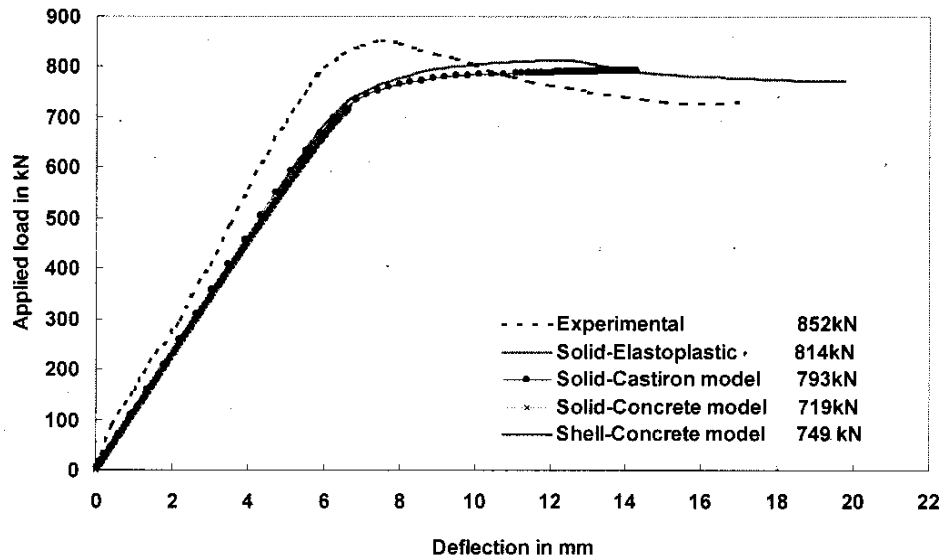


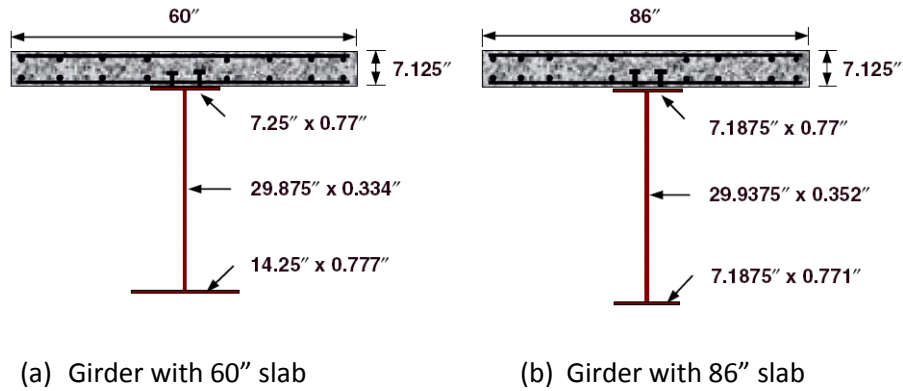
Figure 2-15: Load Deflection Curves for Composite Plate Girder [Baskar et al. 2002]

The post-buckling response is captured and the experimental results show a maximum load of 852 kN, while the model that uses thick shell elements for the concrete deck predicts a maximum capacity of 749 kN. This predicted ultimate load is equal to 88% of the actual load. The other trends in Figure 2-15 represent the models which employed brick elements for modelling the concrete deck.

2.3.2 FEA Model of a Simple Span Composite Plate Girder

The general purpose finite element software package, Abaqus, was also used by Barth and Wu [2006] to develop models for the non-linear analysis of composite plate girders. Simply-supported and continuous bridge girders were studied. This review focuses entirely on the simply-supported composite girder models. The material properties and element selection used in the models are described in detail with specific reference to element types and model functions in Abaqus [2002].

Experimental results from two composite stiffened plate girders tested to failure by Mans et al. [2001] were used to calibrate the model. The girders were simply supported at each end and loaded with a single load at their mid-span. Restraint was provided so that lateral-torsional buckling would not occur. The cross-section geometry of these two specimens is presented in Figure 2-16.



note: 1 inch = 25.4 mm

Figure 2-16: Cross Sections of Experimental Girders [Barth and Wu 2006]

Shear studs in each girder were 114 mm long and had a 19 mm diameter. In total, the girder with a 60 inch wide concrete slab employed eighty pairs of shear studs while the girder with an 2,184 mm slab employed 60 pairs. Information on the spacing of the shear studs was not provided. Figure 2-17 presents elevations for each of the two girders.

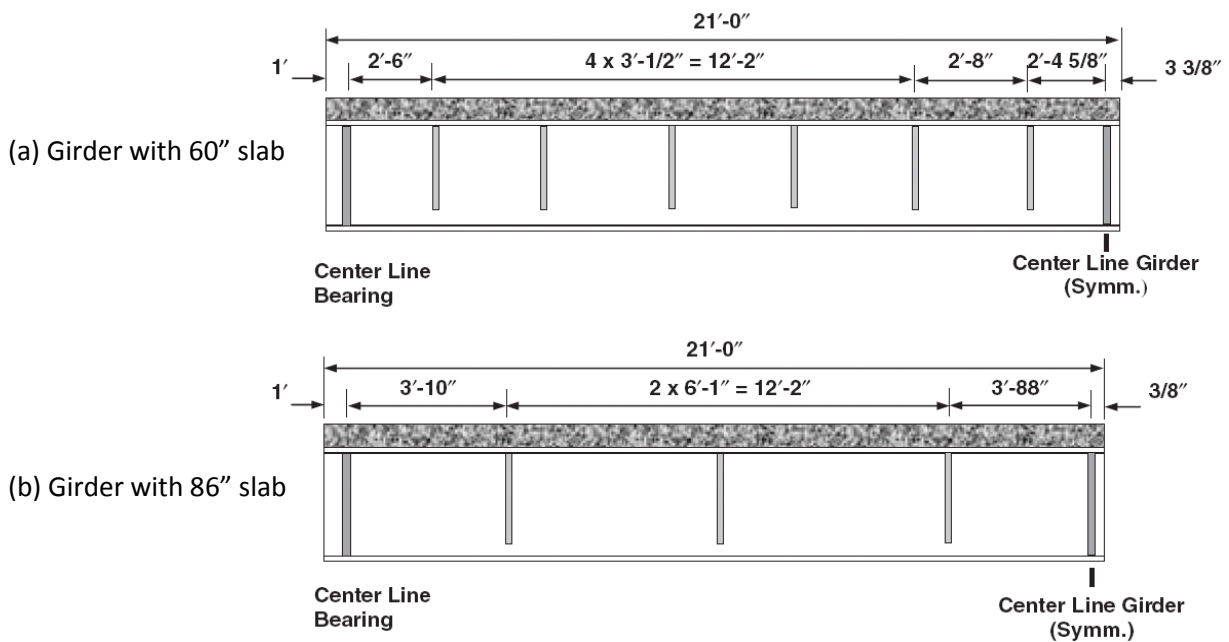
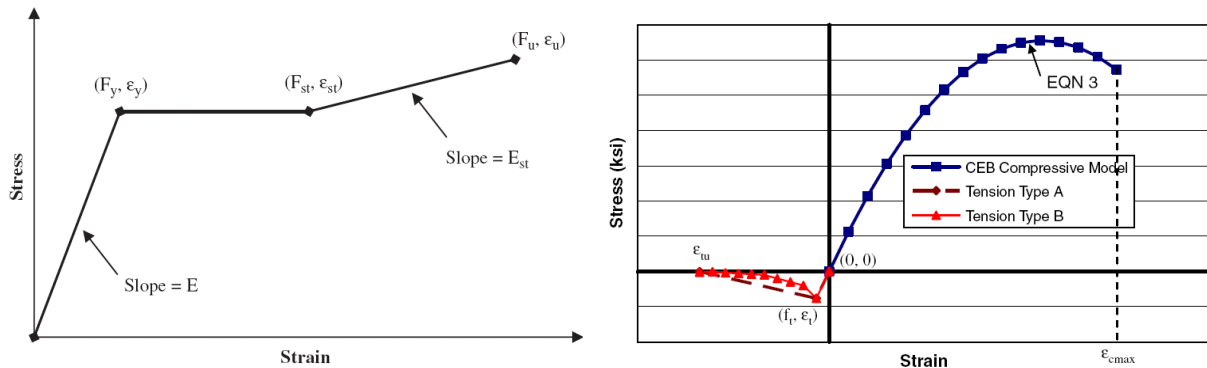


Figure 2-17: Elevations of Experimental Girders [Barth and Wu 2006]

Each of the two girders had a clear span of 12,192 mm and a total length of 12,497 mm. Stiffeners in each of the girders exceeded the code requirements to ensure that shear failures would not occur.

Material properties are summarized in the reference, but are not presented herein. Figure 2-18 presents the stress-strain relationships employed by this model for structural steel and concrete.



note: 1 ksi = 6.89 MPa

Figure 2-18: Stress-Strain Plots used for Steel (left) and Concrete (Right) [Barth and Wu 2006]

To model the structural steel, a tri-linear stress-strain relationship was chosen for both compressive and tensile stresses to account for the elastic, plastic, and strain-hardened material behaviour. For the reinforcing steel, a similar stress-strain relationship is defined in the reference. To represent the compressive concrete behaviour, the Comite Europeen Du Beton (CEB) model was chosen:

$$f_c = \frac{f'_c \beta \left(\frac{\epsilon}{\epsilon'_c}\right)}{\beta - 1 + \left(\frac{\epsilon}{\epsilon'_c}\right)^\beta} \quad [2-3]$$

where: $a = 6193.6 \cdot (0.85 \cdot f'_c + 1.015)^{-0.953}$;

$$b = 8074.1 \cdot (0.85 \cdot f'_c + 1.450)^{-1.085} - 850$$

With the CEB model, the entire response in the compressive range is a function of the cylinder compressive strength, f'_c , measured in Imperial units. The value of concrete crushing strain was chosen to be 0.003. Two models are considered for concrete in tension. Both assume a linear elastic response of the concrete up to its cracking stress. Beyond this point, one model assumes a linear post-cracking softening of the concrete; the other model, which is more representative of the actual response of concrete, uses a parabolic curve. Both tensile models assume a maximum tensile strain in the concrete at which the section can no longer sustain load.

To model the flanges, web, stiffeners, and slab, a four node general-purpose shell element with reduced integration points (SR4) was used. Reinforcing bars are modelled using one-dimensional strain elements that are superimposed onto the web shell elements. To develop composite action between the concrete deck and steel girder, a beam type multi-point constraint, referred to in Abaqus as a MPC beam, is introduced ensuring nodal compatibility between the concrete slab and girder top flange. Input parameters for the shear connection, modelled with the MPC beam, were not provided.

From the Mans et al. [2001] experiments, load-deflection results recorded at mid-span for each of the two girders were compared to the predicted responses based on the Finite Element Analysis. Figure 2-19 presents these findings.

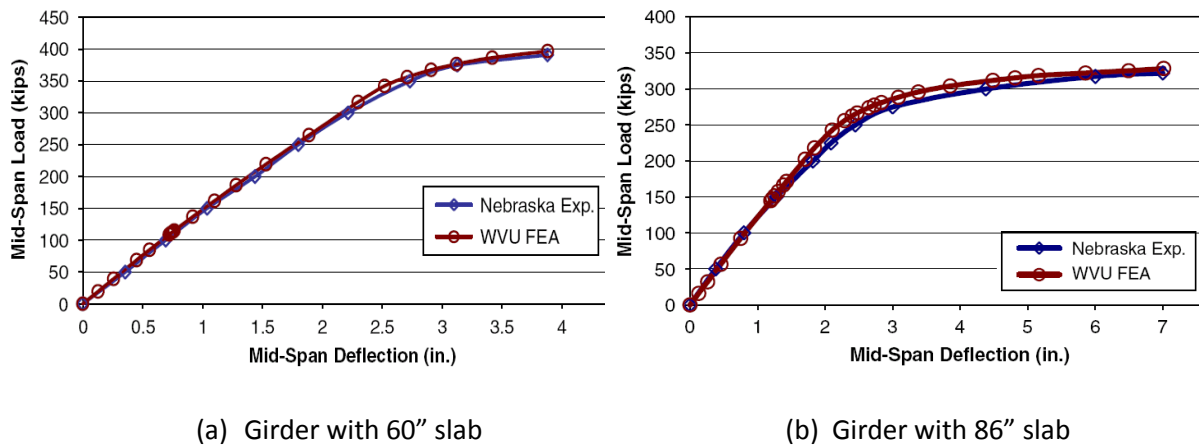


Figure 2-19: Experimental and FEA Load Deflection Plots [Barth and Wu 2006]

The FEA model successfully modelled the non-linear response of both girders through to failure. As illustrated in Figure 2-19, excellent correlation between the experimental and FEA results were observed. Table 2-1 provides a quantitative comparison for the ultimate loads and maximum deflections.

Table 2-1: Comparison between Experimental and FEA Load Deflection Data

	Girder with 60 inch slab		Girder with 86 inch slab	
	Ultimate Load	Max. Deflection	Ultimate Load	Max. Deflection
Experiment	392 kips (1,744 kN)	3.88 in (98.5 mm)	322 (1,432 kN)	7.00 (177.8 mm)
FEA	399 kips (1,775 kN)	3.88 in (98.5 mm)	328 (1,459 kN)	7.01 (178.1 mm)

The mid-span deflections measured experimentally are the same, within a tolerance of 0.01 inch (0.3 mm), as the results based on finite element analysis. The ultimate loads predicted by finite element analysis over-estimated the ultimate capacity of each girder by 1.8% and 1.9% respectively. While an over-estimation of capacity is not desired in structural modelling, an agreement between analytical results and physical tests of less than two percent is well within acceptable tolerance of predicted and actual material properties. Thus, it can be concluded that for simply-supported composite plate girders, the model developed by Barth and Wu provided excellent analytical results.

3 CONNECTION CONCEPTS

This chapter introduces the connection concepts considered during this research. In total, there are ten concepts grouped into three categories referred to as threaded concrete inserts, through bolts, and headed studs. Each connection is presented with a figure and a general description of the concept. Chapter 4 contains detailed discussions regarding the performance, function, and economy of a precast-steel composite bridge incorporating each concept respectively.

3.1 Threaded Concrete Inserts

Three of the concepts examined herein incorporate some form of a threaded concrete insert. Common to each of these connections is the ability to fasten the precast panel to the girder with either bolts or mechanical post-installed anchors. The connection developed with each type of threaded concrete insert is considered to be slip-critical. The structural performance and design considerations associated with threaded concrete insert connections are presented in Chapter 4.

3.1.1 Mechanical Splice

A mechanical splice consists of a bolted connection of the precast concrete panel to the top plate of the steel girder. In Figure 3-1 a rebar coupler is shown which connects the bolts to the internal reinforcing. Initially, shear force would be transferred by friction between the concrete deck and steel girder. If friction is overcome, then bearing of the bolt on the top flange would enable additional shear transfer at the ultimate limit state.

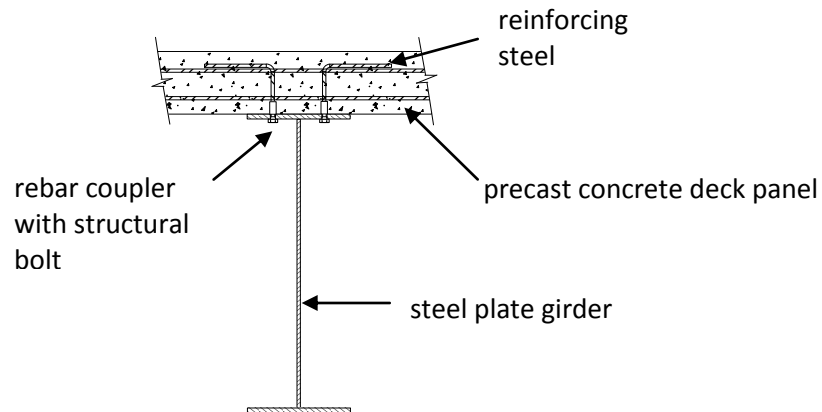


Figure 3-1: Mechanical Splice

The following process could be followed during fabrication and installation of a composite bridge with a mechanical splice shear connection. The steel supplier would pre-drill the bolt holes in the top flange of the plate girder then send this top flange plate directly to the precast plant so that the deck panels could

be match cast directly on this top flange. Prior to placing concrete, the rebar couplers would be installed using dowels so that they line up with the bolt holes. While placing concrete, unexpected movements of the concrete inserts (i.e. rebar and couplers) may occur. This could be avoided by bolting each of the inserts to the top plate; however, such a task maybe impractical and costly. If minor (i.e. up to 6mm) movements of a particular insert occur it may be possible to ream the corresponding hole on the top flange of the girder; however, if reaming can not correct the misalignment then facilitating that particular connection may not be feasible. An allowance for non-performing connections resulting from misalignment may be required.

After stripping the forms and removing the deck panels, the top flange would then be sent to the steel fabricator so that the plate girders could be produced. Match casting the deck panels directly onto the top flange of the girder will promote longitudinal alignment of the bolts during bridge installation, but the fabrication of cross bracing, which sets the distance between girders, would have to be controlled to ensure that lateral alignment of the connection is achieved. When connecting the steel and precast elements in the field, the bolts would have to be installed and impacted overhead, from the underside of the bridge. This step would be labour intensive, which is a potential drawback of this concept. Impacting the bolts successively as the deck panels are placed would reduce the distance in which iron workers would have to pack bolts and the pneumatic impact gun along the underside of the bridge.

3.1.2 Post-Installed

In contrast to the mechanical splice, this fastening system would be installed after placement of the precast deck panels. Holes in the top flange of the girder would be drilled by the steel supplier or fabricator. These holes would then act as guides for field drilling into the soffit of the precast deck panels. Field drilling ensures perfect alignment of the connection between the steel girder and concrete deck. Reinforcing steel in the precast panels would have to be placed precisely prior to deck casting to ensure that it does not conflict with the locations of each anchor. This concept is illustrated in Figure 3-2.

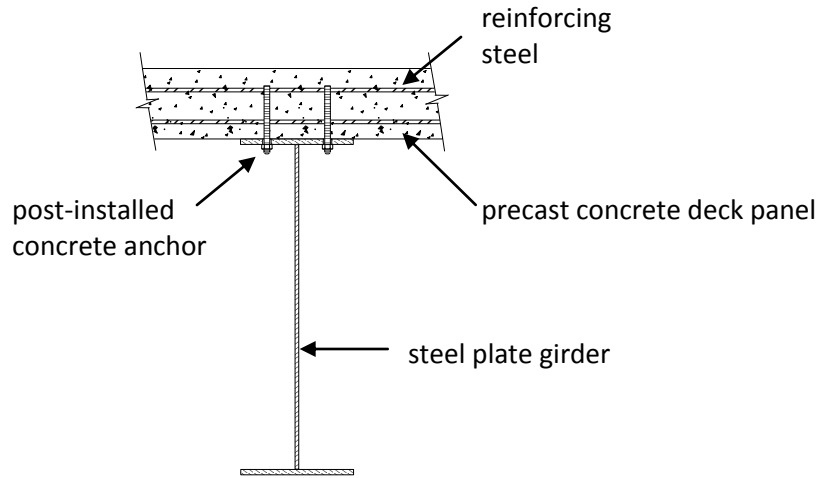


Figure 3-2: Post-Installed Connection

Working from the underside of the bridge to field drill overhead into the soffit of the deck panels would be a difficult and undesirable task; however, this approach eliminates the problem of insert movement during concrete casting, which may occur in the case of the mechanical splice concept. Similar to the mechanical splice concept, drilling and fastening each deck panel successively during deck installation would be beneficial.

3.1.3 Impression Cast

The difference between this concept and the previous two concepts is the presence of steel tabs on the top plate of the girder as illustrated in Figure 3-3. These steel tabs match impressions on the underside of the precast panel and resist slip between the steel girder and precast concrete deck by bearing against the concrete.

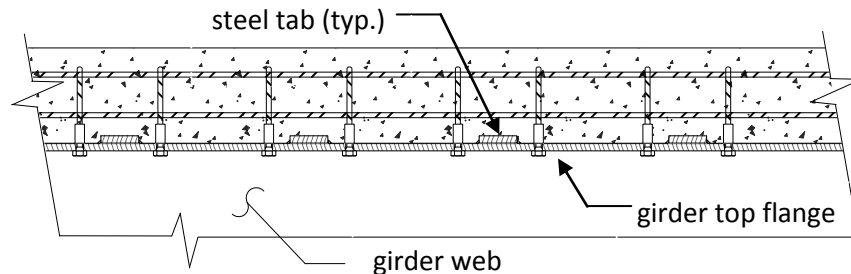


Figure 3-3: Impression Cast with Concrete Insert

The fabrication and installation required for a bridge using an impression cast deck and concrete inserts would be similar to the sequence proposed for the mechanical splice concept described in Section 3.1.1 (i.e. the top flange plate would have to be sent to the precast plant for match casting). The primary

difference would be the requirement for the steel fabricator to attach steel tabs on the top flange of the plate girder prior to placing concrete for the deck panels.

Three possibilities are suggested for fastening the steel tabs to the top flange of the girder; welding, bolting, and gluing. Welding the tabs to the girders top flange leads to a simple fabrication process and a strong connection; however, the welds between the tabs and the girder would be fatigue sensitive. Bolting the tabs to the girder would eliminate the connections sensitivity to fatigue but the size of the steel tab would likely have to be increased to facilitate the number of bolts required to provide the same capacity as a welded connection. Gluing the steel tabs to the girder may prove to be an alternative but there is little research, or applied practice, to date for heavy duty structural connections of this type.

Regardless of the fastening method chosen for the steel tabs, during installation of the bridge, a concern would be the durability of the corners of the impressions cast in the soffit of the deck panels. If the corners are chipped during installation, pieces of aggregate could prevent a snug fit between the steel and concrete and the connection would be compromised.

Another possibility for improvement of shear transfer between the soffit of the precast panels and the top flange of the steel plate girders is to use a friction enhancing interface. One way to increase friction is to roughen the soffit of the deck panel and make use of a bonding agent between the panel and the girder similar to laboratory specimens by [Thomann and Lebet, 2008] described in Section 2.2.1. Increasing the coefficient of friction between the deck panels and the girders would reduce the number of bolts that would be needed to facilitate the connection. Detailed consideration of a friction enhancing surface was not included in this study.

3.2 Through Bolts

The following three concepts utilize a bolted connection where the bolt is accessible from both the top surface of the bridge deck and the underside of the girder's top flange.

3.2.1 Steel to Steel

This particular concept employs shear transfer resulting from friction between two members of a bolted steel-to-steel connection. One possible way of achieving this is illustrated in Figure 3-4.

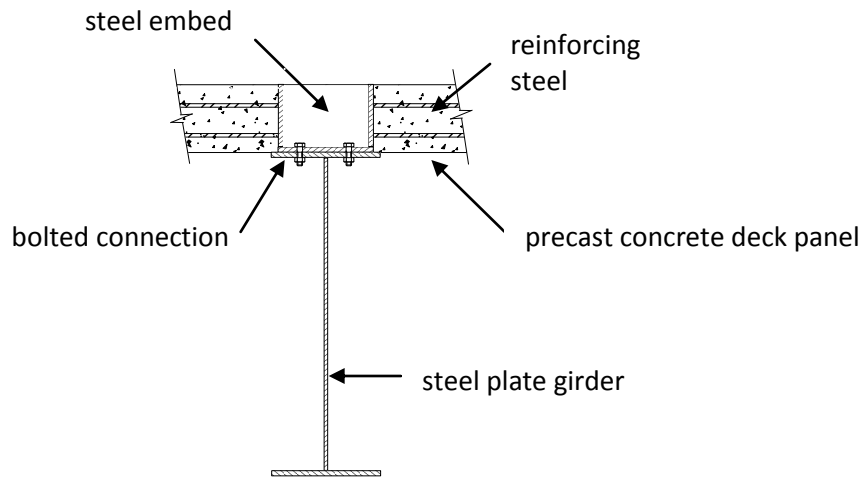


Figure 3-4: Through Bolt with Steel to Steel Contact

With this concept the steel fabricator would produce the steel embeds that bolt to the plate girder and send these embeds to the precast supplier. The longitudinal spacing of these embeds would be critical to ensure alignment of the bolt holes during installation. To allow a small amount of geometric tolerance, holes in the top flange of the girder would be slotted in the longitudinal direction and holes in the bottom plate of the embed would be slotted in the transverse direction. Working from the underside of the bridge would be required to plug bolts into the holes and to secure the head of the bolt while impacting of the nut is completed from the bridge deck. A cover for the connection would also be required.

3.2.2 Concrete to Steel

While similar to the previous concept, this idea differs because the underside of the concrete deck bears directly on the top flange of the steel girder.

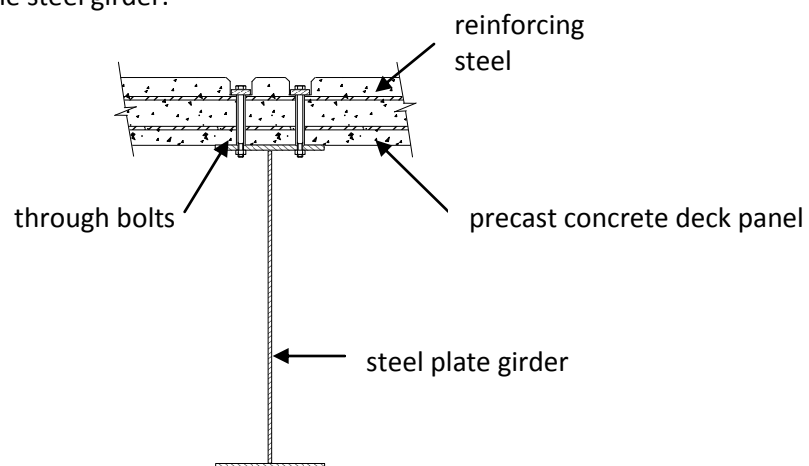


Figure 3-5: Through Bolt with Concrete to Steel Contact

Fabrication of a bridge using through bolts to fasten the precast deck to the steel plate girder would be similar to the process outlined in Section 3.1.1, but block-outs would have to be lined up with the bolt holes as opposed to threaded concrete inserts. Casting a deck with these block-outs would present additional work for the precast fabricator. Similar concerns regarding movement of the block outs during casting would also present difficulties.

To solve potential alignment problems, an alternative fabrication sequence could include drilling the holes in the top flange of the girder to line up with the block-outs cast into the deck panels. After casting the deck panels, a detailed as-built survey of the block-out locations could be sent to the steel fabricator for layout of the holes in the top flange. Risk of misalignment would accompany this alternative as its success would be dependant on the accuracy of the as-built survey and precise reproduction of this layout on the top flange of the plate girder.

3.2.3 Impression Cast with Through Bolts

This concept is a combination of a through bolted connection with an impression cast deck. Figure 3-6 illustrates how this might be accomplished. By introducing impressions on the underside of the precast concrete deck the shear transfer would be significantly improved in comparison to the previous concept.

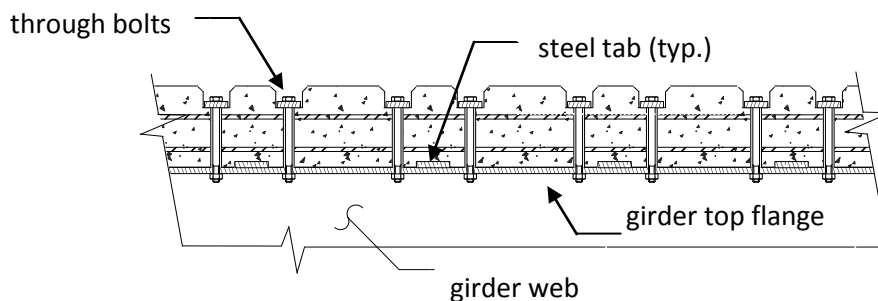


Figure 3-6: Impression Cast with Through Bolts

An impression cast deck with through bolts would combine the fabrication and installation challenges discussed in Sections 3.1.3 and 3.2.2.

3.3 Headed Studs

Each of the following four concepts utilizes ductile headed shear studs in some way. Similar to a permanent simple span composite bridge, ductility provided by the use of shear studs in a portable composite bridge system would allow plastic deformation of shear studs in areas of peak shear stress (i.e. near the supports) which would promote uniform transfer of shear stress along the bridge span.

Ductility provided by the use of shear studs would distribute the shear flow along the length of the bridge which would decrease the demand on connections in locations near peak shear stress.

3.3.1 Continuous Embed

This concept combines a ductile shear stud with a bolted connection. A longitudinal steel embed with shear studs attached would be cast into the underside of the precast deck. This steel embed would then be bolted to the top flange of the plate girder as shown in Figure 3-7.

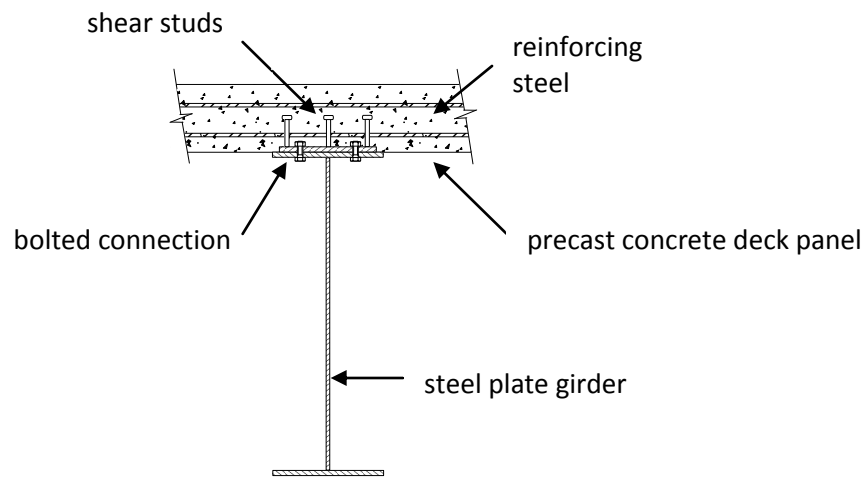


Figure 3-7: Continuous Embed with Ductile Shear Connectors

The continuous embed with ductile shear studs would be produced by the steel fabricator and then sent to the precast manufacturer. Each embed would be continuous along the entire length of each deck panel. Bolt holes in the top flange of the girder could be slotted in the transverse direction to provide geometric tolerance. A dry fit of the embeds would be completed by the steel fabricator, then the sequence of each embed would be marked for the precast manufacturer. Nuts would have to be welded onto the steel embed and a cap would cover each nut prior to placing concrete to allow for protrusion of the bolt during installation. One disadvantage of this approach is that when installing the deck panels, if a nut strips during impacting of the bolt, it is highly unlikely that the nut would be able to be replaced without creating further damage to the deck panel.

3.3.2 Discrete Embed Bolted to Flange

This concept utilizes steel tabs welded to the top flange of the girder at discrete locations. A steel plate containing an inner void and shear studs welded around its perimeter is cast into the deck panels to align with the locations of corresponding steel tabs. The inner void of the steel embed plate would be

made larger than the steel tab to provide geometric tolerance in two directions. After installation, the void space would need to be filled with a high strength grout or epoxy, to facilitate transfer of shear force to the steel tab. The steel embed would also contain threaded inserts or nuts so that the precast panels can be bolted to the steel plate girder after installation. These bolts are needed to prevent separation between the deck and the girder and are not intended to transfer lateral load.

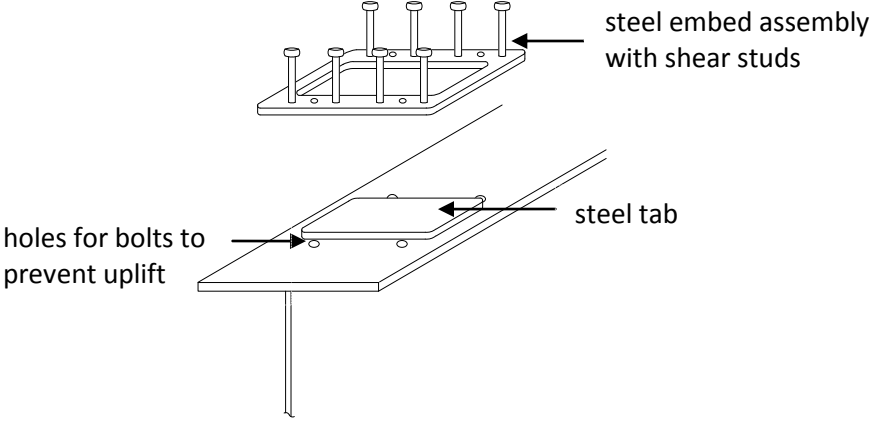


Figure 3-8: Discrete Embed Bolted to Flange

To allow the geometric tolerance required to make these discrete embeds feasible, a filler material (i.e. grout) is required to fill the void between the perimeter of the steel tab to the inside edge of the embed. If this void is not entirely filled, the design strength of the connection may be compromised. Ports would be required either on the soffit of the top flange of the girder or through the precast concrete deck to facilitate placement of this filler. Clearly, the placement of this filler would be a difficult step and ensuring that the void is filled would present significant challenges.

3.3.3 Discrete Embed Bolted to Web

This connection is facilitated by transferring shear and uplift forces from the precast panels directly to the web of the steel plate girder. Figure 3-9 shows how this could be accomplished.

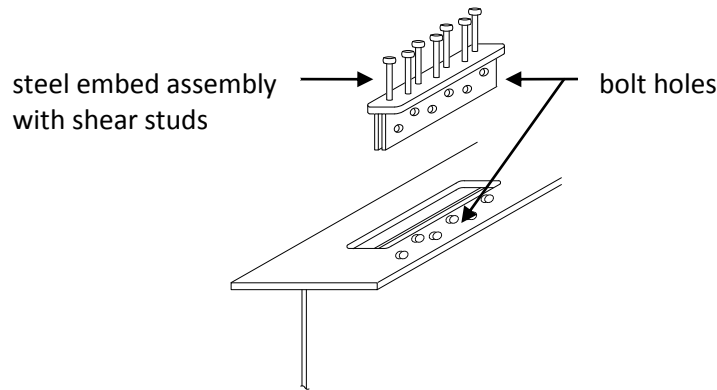


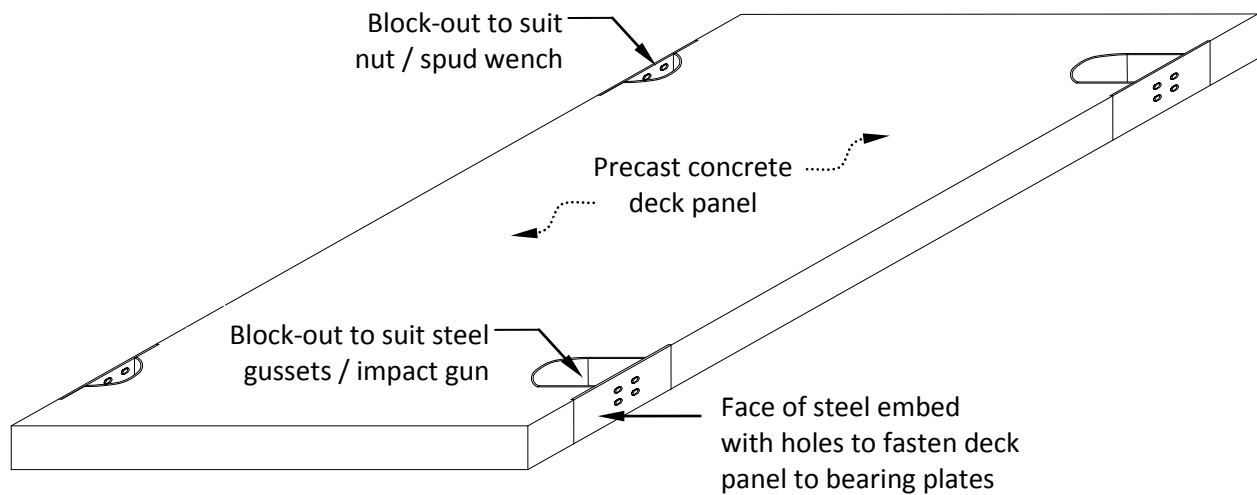
Figure 3-9: Discrete Embed Bolted to Web

The steel supplier would cut the holes in the top flange plate and include these cut outs with the steel shipped to the fabricator. Depending on the fabricator, better economy may be presented by having the fabricator cut these holes. The steel fabricator would then produce the plate girder complete with the steel embed. To facilitate geometric tolerance, holes in the web of the girder would be slotted vertical and holes in the flanges of the embed would be slotted longitudinally. For reasons of constructability, rather than sending the embed to the precast manufacturer, the steel fabricator would bolt the embeds to the girders. Grout pockets in the precast deck panels would be used for the first installation of the bridge. Removal and re-use of the bridge would be facilitated by the bolted connection of the embed to the web of the plate girder.

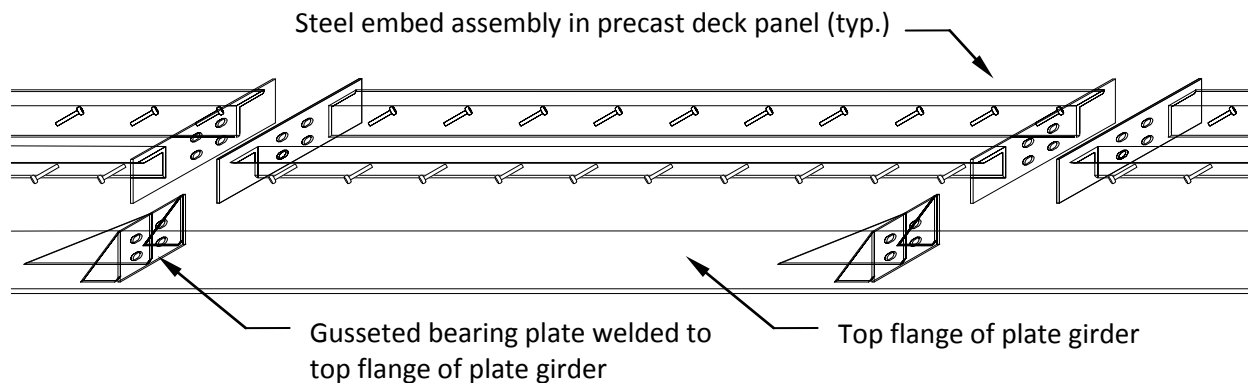
In addition to the difficulties associated with working from the underside of the bridge, there are other reasons why it may prove to be difficult to re-use a composite bridge with this type of connection. For example, even after removing the bolts from the connection it may be difficult to lift the panels from the plate girders, and even if the panels are removed with minimal effort it may be challenging to transport these panels without damaging the connection plates that would be extending from the underside of the deck. Fitting the panels back into place may also prove to be difficult.

3.3.4 Panel End Connections

The final concept examined herein uses ductile shear studs fastened to steel angle to transfer load from the concrete deck to steel bearing plates at each panel end. Gusseted steel plates that are welded to the top flange provide a point of connection for the deck panels. This connection is unlike any of the previous concepts in that fastening the deck panels to the girders can be performed entirely from the surface of the bridge deck. Figure 3-10 illustrates a typical precast concrete deck panel (a) and the steel embed along one girder line (b) that is required for panel end connections.



(a) Typical precast concrete deck panel for panel end connections



(b) Steel embed assembly for panel end connections

Figure 3-10: Precast Concrete Deck Panel and Steel Embed Assembly for Panel End Connections

Due to the distance between panel ends, which is typically three metres, the amount of shear stress transferred at each location would be rather large when compared to the other concepts. This may influence the design of web stiffeners required in the plate girder. Geometric tolerance in the longitudinal direction could present a challenge for this connection since it would be necessary for the bearing plates to be tight to one another. Geometric tolerance in the transverse direction could be accommodated by providing slotted holes at the point of connection. Since tolerance in the longitudinal direction is critical, the following fabrication sequence is proposed.

The first step would be to weld the gusseted bearing plates to the top flange of the girder while using the steel angle embeds as spacers. This step should be completed prior to fabrication of the plate girder with the top flange plate level. Once the gusseted bearing plates are welded in place, the steel embeds can be unbolted and removed then sent to the precast fabricator so that the deck panels may be cast. By setting the camber in the plate girder so that the bridge is level after placing the deck panels, alignment of the embeds with the steel angles should be realized during installation. Figure 3-11 illustrates the proposed installation sequence for the deck panels.

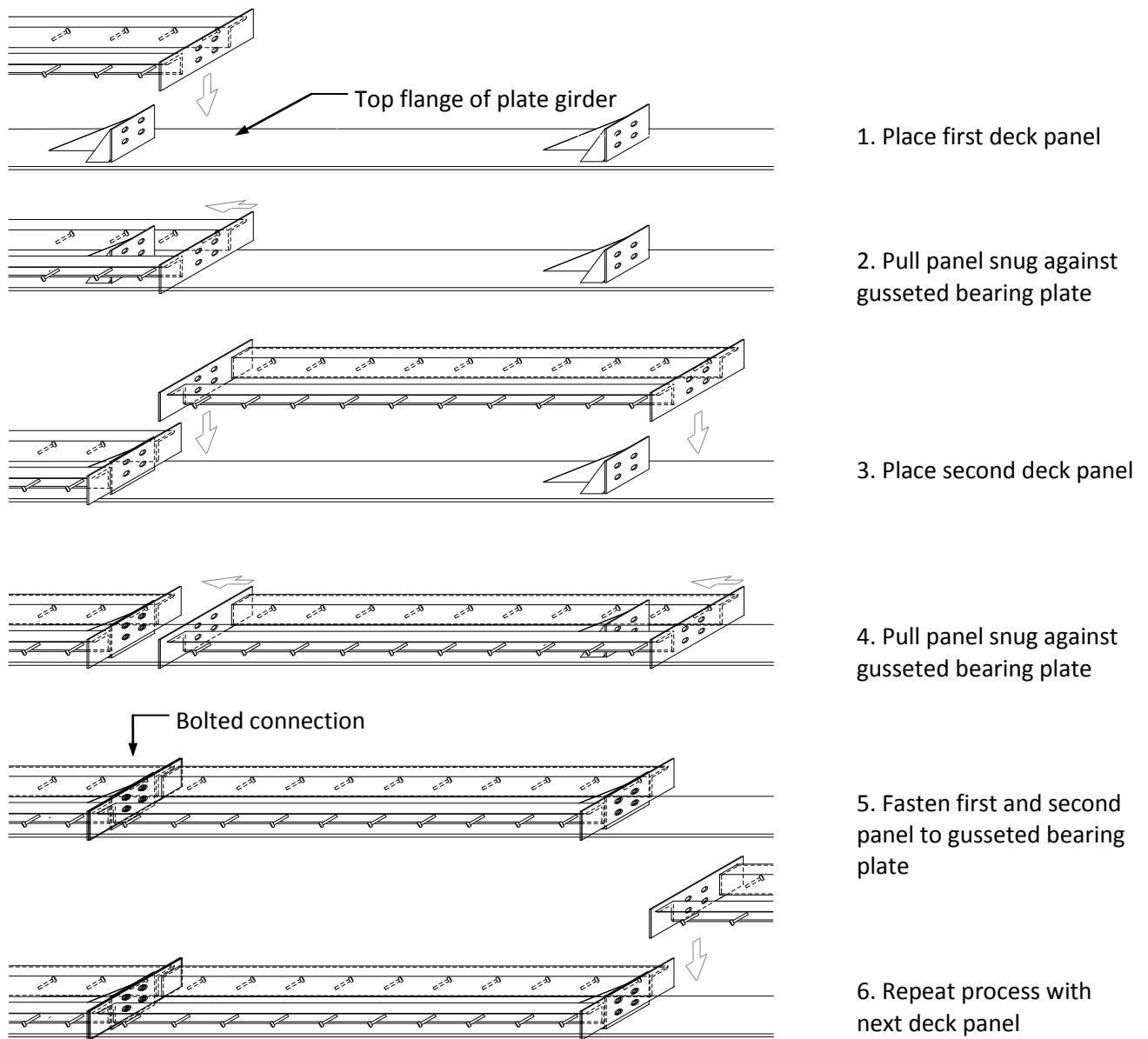


Figure 3-11: Installation Sequence using Panel End Connections

4 MULTI-CRITERIA ASSESSMENT

Chapter 4 begins by introducing the design and assessment criteria used to evaluate each of the connection concepts, followed by a detailed review of each concept. This chapter concludes with the presentation of ratings for each criterion, a sensitivity analysis, and a recommendation for the development of a specific concept.

4.1 Design Load and Bridge Geometry

One of the potential markets for a portable composite bridge is the forest industry. In this industry, it is common for logging trucks to haul exclusively on forest roads and therefore transport heavier loads than those that are legal on public highways. The British Columbia Forest Service (BCFS) has defined four design truck loads based on their gross vehicle weights (GVW). The heaviest truck is classified as a BCFS L165 and has a GVW of 1,468 kN, which is more than two times the standard Canadian CL-625 design truck load (GVW = 625 kN).

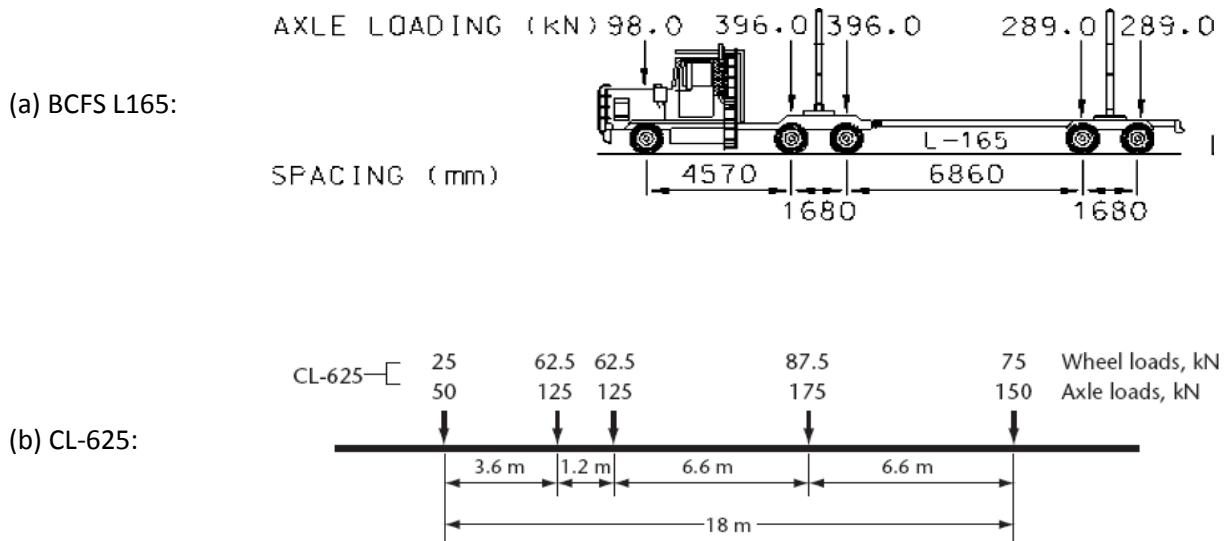
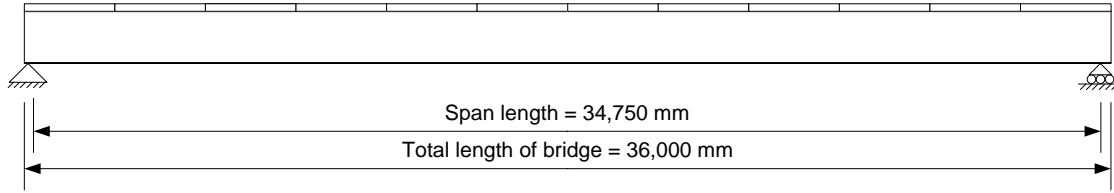


Figure 4-1: BCFS L165 Logging Truck compared to a CL-625 Design Truck

In addition to a 235% increase in vehicle weight, the length of a BCFS L165 truck is 3.21 metres shorter than the CL-625 design truck. This means that the design loads used for bridges in the logging industry can be significantly larger than those realized on public highways.

A common clear span for composite forestry bridges ranges from 24 to 36 m. To evaluate the shear connection concepts presented in Chapter 3, a BCFS L165 design truck has been chosen with a two girder single lane, simple span 36 m composite bridge (see Figure 4-2).



(a) General Arrangement – Single Span



(b) Cross Section

Figure 4-2: General Arrangement and Cross Section of Design Bridge

Since the maximum moment would be located extremely close to mid-span it is assumed for this analysis that half of the total span can be used to develop the composite resistance. Using factored resistances, it is also assumed that the plastic neutral axis of the bridge is located in the girder so that the entire depth of the concrete deck can be developed in a section analysis. Alternatively, if the composite neutral axis was located within the concrete deck, the section of concrete below the neutral axis would be neglected. For a simple span composite bridge it is therefore preferred to have the composite plastic neutral axis in the steel plate girder. In Chapter 6 a design example and specific bridge cross-section is presented in which the plastic neutral axis, based on factored resistances, is located in the steel plate girder.

According to clause 10.11.8.3 of the Canadian Highway Bridge Design Code CAN/CSA S6-06 [2006]; if the plastic neutral axis of a composite member is located in the steel section, then the factored force which must be transferred by shear connectors between points of maximum and zero moments at the ultimate limit state is:

$$P = 0.85\phi_c f'_c b_e t_c + \phi_r A_r f_y \quad [4-1]$$

Where ϕ_c is the resistance factor for concrete, f'_c is the compressive strength of the concrete, b_e is the effective width of the concrete deck, t_c is the depth of the concrete deck, ϕ_r is the resistance factor for reinforcing steel, A_r is the total area of reinforcing steel, and f_y is the yield strength of the reinforcing steel.

The British Columbia Ministry of Forest [1999] specifies a standard precast concrete deck for forestry bridges; details for this deck are presented in Appendix A. This drawing provides structural details for a precast concrete deck that is designed for a two girder composite bridge with a BCFS L 165 truck load. Solving for P in Equation 4-1 (see calculation in Appendix B) indicates that the factored force needed to be transferred by the shear connection is 15,237 kN per girder. Since this force can be developed over an 18 m length, the uniform shear flow is 847 kN/m. A uniform shear flow assumption is valid when a plastic stress distribution can be assumed, as in systems with a ductile shear connection. For non-ductile connections, an elastic stress distribution will be present at the ultimate limit state and the magnitude of the shear flow will vary along the length of the bridge.

4.2 Assessment Method

Each of the ten connection concepts examined herein have been evaluated based on three primary categories: performance, function, and economy. Table 4-1 provides a brief description for each criterion used to perform the multi-criteria assessment.

Table 4-1: Description of Connection Assessment Criteria

Performance	Strength	Ability to transfer the longitudinal shear stress required to develop a full composite section
	Ductility	Ability to form a ductile response at the ultimate limit state
	Fatigue	Vulnerability to strength loss due to cyclic loading
Function	Durability	Ability to withstand adverse effects due to: environmental influences, transportation of bridge components, installation, and removal
	Sensitivity	Vulnerability of the connection's performance due to foreseen difficulties to be expected during bridge installation, removal, and transportation
Economy	Construction	Based on a relationship between the estimated cost, specific to each connection concept, to fabricate and install a portable composite bridge and a control cost
	Re-use	Based on a relationship between the estimated cost, specific to each connection concept, to remove and reinstall a portable composite bridge and a control cost

Each concept was evaluated independently of one another using all seven criteria. Scores for each criterion range between 0 and 10, with the higher scores representing optimal performance or minimal cost. The rating for strength is based on calculations that are presented in Appendix B and summarized in sub-sections 4.3.1 through 4.3.10. Due to the impossibility of providing a detailed assessment at this conceptual phase, the scores assigned to ductility, fatigue, durability, and sensitivity have been limited to one of three choices: 0, 5, or 10. Limiting the scores for these categories to three choices allowed justifiable ratings based on the conceptual details for each connection and avoided an unsupported level of accuracy that would have accompanied a finer point scale. Finally, each of the seven categories is assigned an importance factor, expressed as a percentage, and a specific overall rating is assigned to each concept based on a weighted average of all the criteria.

4.2.1 Performance

Each of the connections has been analyzed for strength based on the demands associated with the design bridge (36 m span rated for an L165 Logging Truck). Based on the results of each analysis, members and components specific to each concept have been detailed with results summarized in the Section 4.3. The findings indicate that each of the concepts can transfer the longitudinal shear stress required to develop a full composite section; therefore, each concept was given a rating of 10 for strength. These findings were based on applying a uniform stress distribution along the concrete/steel interface. In the case that the connection is non-ductile, this assumption of uniform shear distribution may not be valid. Since an independent assessment criterion exists for ductility, assuming a uniform stress distribution for assessing strength avoids a double penalty for concepts that lack ductility.

Having a ductile shear connection in a composite bridge is advantageous because it promotes a uniform distribution of shear stress along the length of the bridge. This reduces the demand at shear connections within regions of peak longitudinal shear stress. For example, in a simple span composite bridge, the peak longitudinal shear stress along the concrete to steel interface is concentrated near the supports. If the shear connection lacks ductility, redistribution of the longitudinal shear stress may not be possible and designing the connection for a uniform shear distribution could result in overloading, and possibly failing, shear connections in regions of peak shear stress. If non-ductile shear connections are employed, the connection should be detailed so that its resistance along the length of the bridge matches the demand profile imposed by longitudinal shear stress. With this understanding, connection concepts that utilize shear studs are considered to be ductile and rated with a score of 10 while bolted connections that involve through bolting, without the use of impression casting, lack ductility and were

rated with the a score of zero. The two connection concepts that combine impression casting with through bolting are expected to have some degree of ductility and are rated with a score of 5. The final criterion considered under the performance category was fatigue.

All bridges are subject to cyclic loads and structural fatigue of bridge members and connections must be considered in the design. The impact of fatigue on structural connections is a function of the connection type, number of load cycles, and the absolute difference between the maximum and minimum stress experienced by the element or connection over the duration of a complete load cycle. Members that are fatigue sensitive must be designed, or checked, for fatigue limit states in addition to other structural and service requirements. Welded connections are typically more sensitive to fatigue than bolted connections. In CAN/CSA S6-06 [2006] structural connections are grouped into detail categories, Clause 10.17.2.4, to simplify member design for load-induced fatigue. CSA S6-06 classifies shear stud connections as a 'Detail Category C' with a constant amplitude threshold stress range of 69 MPa while bolted connections (between steel members) are classified as a 'Detail Category B' with a constant amplitude threshold of 110 MPa. Based on these 'Detail Category' assignments, connection concepts that incorporate shear studs are considered to be moderately susceptible to structural fatigue and are assigned a fatigue rating of 5 while bolted connection concepts clearly present a superior resistance to fatigue and are assigned fatigue rating of 10. For the two concepts that require impression casting with the steel tabs on the girder, the detail category (as defined by CSA S6-06) is influenced significantly by the specific details of the connection; however, it is expected that these connection types would be moderately affected by structural fatigue and so they have been assigned a rating of 5.

4.2.2 Function

Bridges are often subject to environmental conditions that cause structural deterioration. In marine environments and in cold climates where freezing conditions occur and de-icing salts are employed, the durability of a bridge is a critical item that needs to be considered during design. For a modular portable bridge system durability of its structural components during fabrication, transportation, installation, and removal of the bridge must also be addressed. The connections proposed for this portable composite bridge have been reviewed and details that present a high risk for pre-mature deterioration of the structure have been identified. Concepts that facilitate a continuous concrete deck and do not have protrusions or impressions on the soffit of the precast panels are expected to be most durable and assigned a durability rating of 10. Connections with either protrusions, discontinuity of the precast panel deck surface, or requiring impression casting were considered vulnerable to damage during

transport and or deterioration during service and were given durability ratings of 5. Concepts were assigned a durability rating of zero if they incorporate more than one of the details that constituted a rating of 5. In addition to durability, a criterion called sensitivity has been included in the function category.

Sensitivity has been defined in Table 4-1 as the vulnerability of the connection’s performance due to foreseen difficulties that could be expected during bridge installation, removal, and transportation. This criterion is not to be confused with constructability of the bridge, which has been accounted for in the economic rating. For example, concepts requiring construction practices that present a reasonably high expectation for error that result in substantial loss of composite strength were assigned a sensitivity rating of zero. A connection concept that fits this description, and was given a sensitivity rating of zero, is the ‘Discrete Embed Bolted to Flange’. Further discussion regarding this rating is presented in Section 4.3.8. When the occurrence of these foreseeable construction challenges can be minimized by ensuring adequate quality control measures, or when the consequence of the foreseeable construction challenge does not result in a substantial loss of composite strength, a rating of 5 is given for sensitivity. If the construction practices required for a particular concept do not vary significantly from current bridge building practices a rating of 10 is assigned.

4.2.3 Economy

The economy rating for each concept was determined by comparing the estimated *total cost* to fabricate and construct a portable composite bridge incorporating each connection respectively to a component of the *total cost* referred to as the *control cost*. The control cost was assumed to be the component of the total cost for a modular composite bridge that remains constant regardless of the type of connection between the precast deck panels and the steel plate girders. The total cost was determined by summing the control cost and a varying component of the total bridge cost, which accounts for; modifications to the standard precast concrete deck panels to facilitate a removable bridge deck, modifications to the steel plate girders to accommodate a removable bridge deck, equipment required to install the deck panels, and field labour required to install the deck panels. A ratio of the total cost divided by the control cost was then used as a denominator in Equation 4-2 to produce an economy rating for each concept using a 10 point scale.

$$\text{Economy Rating} = \frac{10}{\frac{\text{total cost}}{\text{control cost}}} \quad [4-2]$$

The economic rating formula presented in Equation 4-2 was chosen because it provides a fair comparison between concepts by accounting for the total cost of the bridge. If the economic rating was based entirely on the cost that is specific to the connection between the deck panels and steel girders then significant, and unfair, spreads between ratings would occur. Consider the following example. The total cost for a bridge with connection type 'A' is \$350,000 of which \$50,000 are costs directly associated with the connection while the total cost for a bridge with connection type 'B' is \$400,000 of which \$100,000 are costs directly associated with the connection. If the total cost of the bridge is not considered then the economic rating assigned to connection type 'A' may be twice the rating assigned to connection type 'B' when there was only a 14% increase in total cost between the two bridges. Other advantages of the formula in Equation 2 are that ratings will always remain within the bounds 0-10 and that additional concepts can be added to the study at a later date without influencing the economic rating previously assigned to existing concepts. Estimates for the total cost for each concept have been performed and are presented in Appendix C with the results summarized in Section 4.3.

The control cost for initial construction and bridge re-use were determined with the assistance of Surespan Construction Ltd., a bridge building construction company located in North Vancouver, Canada. An estimated cost to fabricate and install a 36 metre modular composite bridge designed for an L165 design truck load is \$300,000 in 2010 Canadian dollars. For this bridge, Surespan finds that it typically takes two 12 hour work days to install the precast concrete deck panels using a four man bridge building crew. The cost of these two days amounts to \$20,682 as follows; 96 hours at \$100/hr for field labour, 24 hours at \$307.83/hr for a 110 conventional boom crane, 24 hours at \$140.65/hr for a 30 ton hydraulic excavator, and 24 hours at \$13.28/hr for a 185 cfm compressor. Subtracting this cost of \$20,682 from \$300,000 results in a control cost of \$279,318 which is used to rate the construction component of economy. To rate the re-use component of economy, the control cost includes the estimated costs associated with the common activities required to remove and re-install a portable composite bridge, which utilizes any one of the connection concepts respectively. This control cost is extremely difficult to predict accurately since there are many factors that can influence its magnitude. To facilitate this assessment, a control cost for the common tasks associated with removing and relocating a 36 metre portable composite bridge is roughly estimated to be \$200,000.

Life cycle cost is not accounted for in the economy ratings, as the life expectancy of the bridge is primarily affected by its durability which has been assigned an independent rating. Table 4-2 presents the unit costs used to compare the economy of each concept.

Table 4-2: Unit Costs for Economic Analysis*

<i>Description</i>	<i>Unit</i>	<i>Cost</i>
field labour	person hour	\$ 100.00
shop labour	person hour	\$ 85.00
structural weathering steel including fabrication	pound	\$ 1.50
drill hole in girder, max bolt 1" dia., max plate thickness 1"	each location	\$ 7.00
1" dia. x 3" long A325 galvanized bolt with washer	each	\$ 3.50
galvanized rebar coupler for 1" bolt / 25M bar	each	\$ 6.50
175mm x 350mm 25M rebar with one end threaded	each	\$ 7.00
7/8" dia. x 5" long shear stud installed	each	\$ 5.00
7/8" or 1" dia. x 3" long A325 bolt w/ washer, nut (weathering)	each	\$ 2.50
7/8" dia. x 10" long A325 bolt w/ washer, nut (weathering)	each	\$ 4.00
3/4" dia. x 9 1/2" long Hilti Kwik-Bolt™	each	\$ 20.00
bag of grout	0.45 cu ft	\$ 20.00
local shipment of structural steel	load	\$ 800.00
110 ton conventional boom crawler crane without operator	hour	\$ 307.83
30 ton hydraulic excavator without operator	hour	\$ 140.65
185 cfm compressor	hour	\$ 13.28

** unit costs are estimates, based on 2010 Canadian dollars, provided by Surespan Construction Ltd.*

The unit cost of labour includes overhead, benefits, small tools, shop allowance, and a living out allowance. The cost of structural steel will vary depending on the simplicity of fabrication; however, significant variation from an average cost of \$1.50 per pound is not expected. Equipment costs are taken directly from the 2009/2010 edition of the Equipment Rental Rates Guide issued by the B.C. Road Builders & Heavy Construction Association [2008]. This guide is typically referred to as 'The Blue Book' and is used by the British Columbia Ministry of Transportation for determining equipment rates for public projects.

4.3 Concept Evaluation

All ten concepts are evaluated and rated with a score between 1 and 10 for each of the seven assessment criteria. The results of calculations and cost estimates presented in Appendix B and Appendix C respectively are summarized in each of the following sections.

4.3.1 Threaded Concrete Insert

A preliminary structural analysis of this connection has been performed using the CAN/CSA S6-06 [2006] in combination with the Concrete Design Handbook CSA A23.3-04 [2006]. Clause 8.9.5 of S6-06 is used to determine the interface shear transfer between the precast concrete deck and the top plate of the steel girder. The Canadian Highway Bridge Design code does not quantify the coefficient of friction between concrete and steel; therefore, a friction coefficient of 0.60 was used as recommended in Clause 11.5.2 (d) of A23.3-04. The proposed connection consists of attaching threaded splices to 25M bars so that two female threaded connections are located in the deck incrementally along the length of each girder facilitating a bolted connection. Design calculations, presented in Appendix B, show that 2-25M bars coupled with 1" diameter A325 bolts spaced at 200mm on center provide the required interface shear transfer; however, a uniform spacing of the bolts may not be suited to this type of connection.

Based on these calculations it is expected that this connection could provide the strength required to develop a full composite section; however, since this slip critical connection is expected to be non-ductile the system response would need to be analyzed in order to determine an appropriate interface shear distribution and connection spacing. Since the connection does not utilize welded members it is expected to provide exceptional resistance to fatigue. This explains why the ratings under the structure category are; strength – 10, ductility – 0, and fatigue – 10.

Continuity of the bridge over each point of connection would protect the concrete deck and steel girders from excessive exposure to water enabling a relatively durable structure. During fabrication of the precast deck panels, it should be expected to have a small number of the threaded connections move during placement of the concrete. If the entire insert moves, correction would be required in order to facilitate the bolted connection in the field; alternatively, if the insert remains in its correct position but is not plumb during casting of the panel then an undesired flexural stress may be introduced to bolts which may cause bolts to fail during impacting. This explains why the ratings under the structure category are; durability – 10 and sensitivity – 5.

The cost analysis for each concept is presented in Appendix C and referenced according to the section in which they appear in the text. The additional cost associated with fabrication and initial installation for a connection using a threaded concrete insert is estimated to be \$30,102 while the expected cost to remove and re-install the deck for this bridge type is \$21,478. Using Equation 4-2, the threaded concrete insert connection concept received ratings of 9.0 and 9.0 respectively for the economies of construction and re-use.

4.3.2 Post Installed Connection

With the exception of a different anchorage type, the structural system presented with this concept is the same as that in the previous section. One particular post-installed anchor designed for heavy duty applications produced by Hilti is called a Kwik Bolt™. Adhesive anchors, such as the Hilti Hit HY150™ series, or equivalent, provide similar resistances to a Kwik Bolt™ but are more expensive to supply and install. As calculated in Appendix B, two 3/4" diameter by 9 1/2" long Kwik Bolts™ at 150mm on center are required per girder to provide the required interface shear resistance.

Since the structural system presented with this concept is the same as the threaded concrete insert the same ratings have been assigned to the three category under the performance rating; strength – 10, ductility – 0, and fatigue – 10.

As with the previous concept, continuity of the bridge over each point of connection would protect the concrete deck and steel girders from excessive exposure to water enabling a relatively durable structure. A mid-point rating of 5 was assigned for durability because once the bridge deck is removed from the girders the protruding anchors will be vulnerable to damage due to unexpected impacts during deck handling. Despite efforts by the precast supplier to keep re-bar clear of the anchorage locations, it should be expected that occasional interference with re-bar will be realized. When this happens, relocating the hole is not a simple solution; therefore, the sensitivity rating has been given a mid-point rating of 5.

As summarized in Appendix C, the additional cost associated with fabrication and initial installation for a connection using a post installed anchor is estimated to be \$66,924 while the expected cost to re-move and re-install the deck for this bridge type is \$18,985. Using Equation 4-2, the post installed anchor concept received ratings of 8.1 and 9.1 respectively for the economies of construction and re-use.

4.3.3 Impression Cast Deck with Concrete Insert

With this concept, once friction between the deck panels and plate girders is overcome, the impressions on the soffit of the concrete will engage the steel tabs on the top flange of the girder. At an ultimate limit state, the potential failure mode is presented in Figure 4-3.

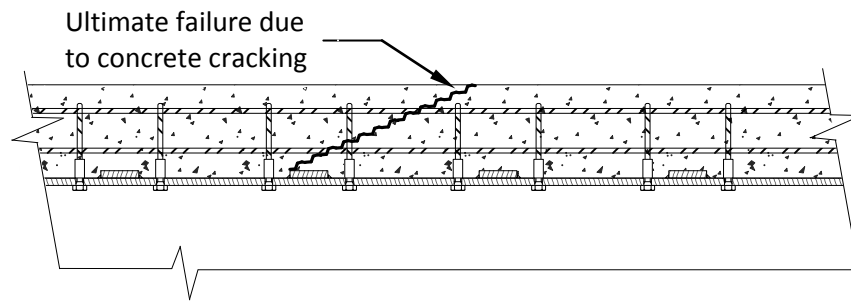


Figure 4-3: Failure Mode of an Impression Cast Deck at the Ultimate Limit State

Clause 8.9.5.1 of CAN/CSA S6-06 [2006] was used to evaluate the amount of interface shear transferred along this potential failure plane. For failure to occur, the cohesion must first be overcome so that a continuous crack is formed. Once this crack is formed, vertical separation of the two elements will be prevented by the bolted connection which extends through the crack. This results in the development of mechanical interlock between aggregates along the failure plane. For this type of failure, Clause 8.9.5.2.1 of S6-06 suggests cohesion of 1.00 MPa and a friction coefficient of 1.4. Design calculations, presented in Appendix B, show that 2-25M bars coupled with 1" diameter A325 bolts spaced at 500 mm o/c provide the clamping force required to develop the interface shear transfer. Spacing of the steel tabs is expected to be 500 mm o/c.

Based on these calculations it is expected that this connection could provide the strength required to develop a full composite section. Since the steel impressions will resistance longitudinal slip it is expected that this connection will have a marginal amount of ductility. Since structural welds are required, this connection will be affected by fatigue. Ratings under the performance category are; strength – 10, ductility – 5, and fatigue – 5.

As with the previous two concepts, continuity of the bridge over each point of connection would protect the concrete deck and steel girders from excessive exposure to water enabling a relatively durable structure. In addition to the risk of misaligned concrete inserts this concept also depends on having a snug fit between the steel girder and concrete deck. If the corner of any impression on the soffit of the concrete deck is chipped, and the spalled aggregate gets crushed between the precast deck and the steel girder the structural performance of the connection would be compromised. This explains why the ratings under the function category are; durability – 5 and sensitivity – 0.

As summarized in Appendix C, the additional cost associated with fabrication and initial installation for a connection using an impression cast deck with concrete inserts is estimated to be \$24,174 while the expected cost to re-move and re-install the deck for this bridge type is \$19,966. Using Equation 4-2, an impression cast deck with concrete inserts received ratings of 9.2 and 9.1 respectively for the economies of construction and re-use.

4.3.4 Through Bolt with Steel to Steel Contact

According to the provisions of S6-06, the factored slip resistance for a 1" diameter A325 bolt in a single shear slip critical connection is 99.8 kN based on a mean slip coefficient of 0.50 and a class B coating of the steel surfaces. If a steel to steel bolted connection between the precast concrete and the plate girder is chosen, 308 bolts per girder would be required for a full composite section. A detailed calculation with code references is provided in Appendix B.

Based on these calculations it is expected that this connection could provide the strength required to develop a full composite section; however, since this slip critical connection is expected to be non-ductile the system response would need to be analyzed in order to determine an appropriate interface shear distribution and connection spacing. Since the connection does not utilize welded members it is expected to provide exceptional resistance to fatigue. This explains why the ratings under the performance category are; strength – 10, ductility – 0, and fatigue – 10.

Unlike the previous three concepts, this connection requires cover plates over each connection to provide continuity of the bridge deck. A mid-point rating of 5 was assigned for durability because an opportunity for water to collect in the steel pockets will exist. The sensitivity rating has also been given a mid-point rating of 5. Despite efforts to keep the soffits of the precast panels clean it should be expected that on occasion the slip critical connection between the steel embeds and the girder will be compromised due to the presence of mud or dirt on the soffit of the precast panels.

As summarized in Appendix C, the additional cost associated with fabrication and initial installation for a connection using through bolts with steel to steel contact is estimated to be \$26,334 while the expected cost to re-move and re-install the deck for this bridge type is \$20,578. Using Equation 4-2, through bolts with steel to steel contact received ratings of 9.1 and 9.1 respectively for the economies of construction and re-use.

4.3.5 Through Bolts with Concrete to Steel Contact

The structural mechanics of this connection are the same as the concept presented earlier in section 4.3.1. Since the design strength of the bolts is not limited by the strength of the reinforcing steel, the connection spacing for this concept can be increased in comparison to the spacing associated with the threaded concrete inserts without reducing the amount of clamping force introduced along the shear interface. For each girder, 240 – 22 mm diameter A325 bolts are recommended.

Based on these calculations it is expected that this connection could provide the strength required to develop a full composite section; however, since this slip critical connection is expected to be non-ductile the system response would need to be analyzed in order to determine an appropriate interface shear distribution and connection spacing. Since the connection does not utilize welded members it is expected to provide exceptional resistance to fatigue. Performance ratings are as follows; strength – 10, ductility – 0, and fatigue – 10.

Similar to the previous concept, this connection requires some form of cover for the bolts, such as a cold packed asphalt pavement, to provide continuity of the bridge deck. A mid-point rating of 5 was assigned for durability because an opportunity for water to penetrate into the bolt holes will exist. The sensitivity rating has also been given a mid-point rating of 5. Despite efforts to keep the soffits of the precast panels clean it should be expected that on occasion the connection between the soffit of the deck and the top flange of the girder will be compromised due to the presence of mud or dirt.

As summarized in Appendix C, the additional cost associated with fabrication and initial installation for a connection using through bolts with concrete to steel contact is estimated to be \$18,102 while the expected additional cost to re-move and re-install the deck for this bridge type is \$32,943. Using Equation 4-2, through bolts with concrete to steel contact received ratings of 9.4 and 8.6 respectively for the economies of construction and re-use.

4.3.6 Impression Cast with Through Bolts

While similar to the connection presented in Section 4.3.3, the strength of the bolts would not be limited by the relatively low yield strength of the reinforcing steel. Calculations, presented in Appendix B, suggest that pairs of 22 mm diameter A325 bolts spaced at 500 mm o/c along the length of each girder would enable a full composite connection. Since pre-tensioning these bolts is not required for this connection, special care should be taken during bolt installation to ensure that full torque is not

introduced. If full torque is introduced, then elongation of the bolt will be realized and the bolts may not be able to be re-used. Spacing of the steel tabs is expected to be 500 mm o/c.

Based on these calculations it is expected that this connection could provide the strength required to develop a full composite section. Since the structural performance of this connection is the same as that for the previous impression cast system, the same ratings under the structure category are assigned as follows; strength – 10, ductility – 5, and fatigue – 5. This concept was given ratings of zero for both criteria in the function category. In addition to an opportunity for the soffits of the precast panels to chip or spall near the recessed regions on the soffit, there is also an opportunity for water to penetrate into the bolt holes.

As summarized in Appendix C, the additional cost associated with fabrication and initial installation for a connection using an impression cast deck with through bolts is estimated to be \$21,450 while the expected additional cost to re-move and re-install the deck for this bridge type is \$32,175. Using Equation 4-2, an impression cast deck with through bolts received ratings of 9.3 and 8.6 respectively for the economies of construction and re-use.

4.3.7 Continuous Embed with Ductile Shear Studs

With this connection concept, the load from the concrete deck would be transferred through the shear studs into the embedded steel plate. Since the shear studs are ductile it is expected that a relatively uniform shear flow will be present between the steel embed plate and the top flange of the girder. The bolted connection will then enable a slip critical connection. Based on calculations presented in Appendix B, pairs of 25 mm diameter bolts will be required at 200 mm o/c while pairs of 22 mm diameter shear studs will be required at 300 mm o/c. Additional shear transfer between the precast deck and the steel embed may be realized due to the nuts from the bolts that protrude into the concrete deck. If this additional shear transfer occurs, the demands on the shear studs may be reduced; however, the ductility of the connection between the embed and precast panel may be influenced which would affect the spacing of the bolts and shear studs.

Based on these calculations it is expected that this connection could provide the strength required to develop a full composite section. By introducing shear studs, ductility would be realized but the connection of the studs to the steel embed plate would be subject to fatigue. Ratings under the performance category are; strength – 10, ductility – 10, and fatigue – 5.

Durability was given a rating of 10 because continuity of the bridge deck is achieved and after removing the deck there is nothing protruding from the precast panels. Sensitivity was given a mid-point rating of 5 because if the occasional bolt or nut strips during impacting, which should be expected, it would be difficult to remove the bolt and nearly impossible to replace the nut.

As summarized in Appendix C, the additional cost associated with fabrication and initial installation for a connection using a continuous embed with ductile shear studs is estimated to be \$23,751 while the expected additional cost to re-move and re-install the deck for this bridge type is \$20,758. Using Equation 4-2, a continuous embed with ductile shear studs received ratings of 9.2 and 9.1 respectively for the economies of construction and re-use.

4.3.8 Discrete Embed Bolted to Flange

If embeds are spaced at 1000mm o/c, each embed would require a minimum of 7 – 7/8" diameter shear studs. To enable a sufficient amount of weld, the dimensions of the steel tab which welds to the top flange would be 300 mm wide by 50 mm long and 19 mm thick. The outer dimensions of the steel embed are expected to be approximately 500 mm wide and 250 mm long. Width and length correspond to the transverse and longitudinal directions of the bridge respectively. The bearing stress for the epoxy used to fill the void between the steel embed and the steel tab would be upwards of 150 MPa.

Based on these calculations it is expected that this connection could provide the strength required to develop a full composite section. By introducing shear studs, ductility would be realized but the connection of the studs to the steel embed plate would be subject to fatigue. Ratings under the performance category are; strength – 10, ductility – 10, and fatigue – 5.

Durability was given a rating of 10 because continuity of the bridge deck is achieved and after removing the deck there is nothing protruding from the precast panels. Sensitivity was given a rating of zero because the strength of the connection is entirely dependent on the injection of an epoxy into a void which is not visible. Ensuring that the void has been completely filled would be a challenge.

As summarized in Appendix C, the additional cost associated with fabrication and initial installation for a connection using discrete embeds bolted to the girder top flange is estimated to be \$51,488 while the expected additional cost to re-move and re-install the deck for this bridge type is \$62,767. Using Equation 4-2, discrete embeds bolted to the girder top flange received ratings of 8.4 and 7.6 respectively for the economies of construction and re-use.

4.3.9 Discrete Embed Bolted to Web

This bolted connection facilitates double shear; therefore, the resistance per bolt in this connection would be twice the resistance of bolts used with the concepts 4.3.4 and 4.3.7. If these discrete embeds were spaced at 1000 mm o/c each connection would require 7 – 22 mm diameter shear studs, 6 – 22 mm diameter A325 bolts, and a connection length of 350 mm.

Based on these calculations it is expected that this connection could provide the strength required to develop a full composite section. By introducing shear studs, ductility would be realized but the connection of the studs would be subject to fatigue. Ratings under the performance category are; strength – 10, ductility – 10, and fatigue – 5.

The durability of this connection would be compromised once the panels were removed from the structure because the steel tabs protruding from the soffit of the deck would be vulnerable to damage. As mentioned with previous concepts this connection would be sensitive to mud or dirt getting in between the two steel plates which connect the deck panels to the girder. Durability and sensitivity were both given mid-point ratings of 5.

As summarized in Appendix C, the additional cost associated with fabrication and initial installation for a connection using discrete embeds bolted to the girder web is estimated to be \$35,839 while the expected additional cost to re-move and re-install the deck for this bridge type is \$20,038. Using Equation 4-2, discrete embeds bolted to the girder web received ratings of 8.9 and 9.1 respectively for the economies of construction and re-use.

4.3.10 Panel End Connection

With this connection, shear studs transfer load from the concrete to steel angles which are embedded entirely in the precast concrete deck running parallel to the girders. The steel angles, which run the full length each precast deck panel, then distribute this force to steel bearing plates located at either end of the deck panel. Gusseted connection plates are located between each of the deck panels to transfer this load to the top flange of the steel plate girder.

Based on calculations presented in Appendix B, shear studs would be required at 300 mm on center fastened to L127 x 127 x 13 steel angles. The thickness of steel plate would be 13 mm and the total amount of longitudinal and transverse weld at each connection point would be 1,300 mm and 600 mm respectively. This would be provided with 8 mm welds on each side of the; 500 mm long center gusset, 150 mm long side gussets, and 300 mm wide bearing plate.

Based on these calculations it is expected that this connection could provide the strength required to develop a full composite section. Since the load is transferred from the concrete deck to the steel girders with welded steel gussets the connection would present some level of ductility but would be subject to fatigue. Ratings under the performance category are; strength – 10, ductility – 5, and fatigue – 5. Durability was given a mid-point rating of 5 because of the opportunity for water to collect in the voids used to connect the panels to the girders. Since this connection transfers load by bearing and not friction it is expected to be the least sensitive connection and is rated with a 10.

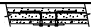

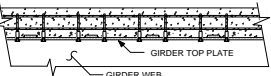


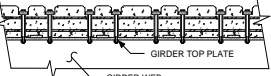



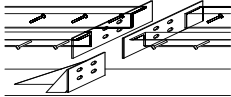
As summarized in Appendix C, the additional cost associated with fabrication and initial installation for a connection using panel end connections is estimated to be \$29,910 while the expected additional cost to re-move and re-install the deck for this bridge type is \$19,198. Using Equation 4-2, panel end connections received ratings of 9.0 and 9.1 respectively for the economies of construction and re-use.

4.4 Concept Evaluation Results

For each concept the ratings assigned for the seven assessment criteria are summarized in Table 4-3. To combine the seven ratings for each concept the following weights have been assigned; strength – 15%, ductility – 10%, fatigue – 5%, durability – 20%, sensitivity -20%, construction -15%, and re-use -15%. The heaviest weights were given to durability and sensitivity as follows: since a life cycle cost analysis is outside the scope of this research, durability is the assessment criteria that accounts for the expected life of the structure; sensitivity was also weighted at 20% because some of the connection concepts require construction techniques that are uncommon to current practices which may negatively impact the performance of the bridge. Strength and the two economic criteria were weighted at 15% because they are essential to the marketability of the bridge. Connections that lack ductility may result in tight connection spacing near locations of peak longitudinal shear stress resulting in complex detailing and a weight of 10% was considered a reasonable assignment for ductility. Fatigue was given the lowest weight because a portable composite bridge will likely not be subjected to a large number of load cycles.

A weighted sum of the seven criteria provides a single score for each of the ten connection concepts. These weights could justifiably be considered biased depending on the interests or background of a particular reader; therefore, a sensitivity analysis was performed and its results are summarized in the following section. In addition to summarizing the individual ratings associated with each assessment criteria, the right hand column in Table 4-3 presents the scores for each concept based on the given weights.

Table 4-3: Assessment of shear connection concepts

	Weight:	Structure			Function		Economics		Score
		Strength 15%	Ductility 10%	Fatigue 5%	Durability 20%	Sensitivity 20%	Construction 15%	Re-Use 15%	
Threaded Concrete Insert		10	0	10	10	5	9.0	9.0	7.7
Post Installed Connection		10	0	10	5	5	8.1	9.1	6.6
Impression Cast with Concrete Insert		10	5	5	5	0	9.2	9.1	6.0
Through Bolt with Steel to Steel Contact		10	0	10	5	5	9.1	9.1	6.7
Through Bolt with Concrete to Steel Contact		10	0	10	5	5	9.4	8.6	6.7
Impression Cast with Through Bolts		10	5	5	0	0	9.3	8.6	4.9
Continuous Embed bolted to Flange		10	10	5	10	5	9.2	9.1	8.5
Discrete Embed Bolted to Flange		10	10	5	10	0	8.4	7.6	7.2
Discrete Embed Bolted to Web		10	10	5	5	5	8.9	9.1	7.4
Panel End Connection		10	10	5	5	10	9.0	9.1	8.5

Based on these results there are two concepts that share the top rating (8.5); the first is the continuous embed with ductile shear connections while the second concept is the panel end connection. To determine the effect of varying the relative weights used to combine the scores from each of the seven criteria, a sensitivity analysis was performed as discussed in the next section.

4.5 Sensitivity Analysis

To determine the sensitivity of this assessment to the weights chosen for each criteria, four additional assessments were performed in which these weights were varied. For this sensitivity study, the assessment from Section 4.4 was labelled Assessment 1. Each of the alternate assessments are described below with reference to Assessment 1.

Assessment 2 has five percentage points taken from 'Construction' and 'Re-use' to increase the weights for 'Durability' and 'Strength' to 20 and 25% respectively. This assessment may suit someone who states that the strength and life expectancy of the portable bridge are critical to its success.

Assessment 3 has 10 percentage points taken from 'Durability' and 'Sensitivity' to increase the weights for 'Construction' and 'Re-use'. This assessment may target a potential owner who is confident that their bridge building contractor is capable of avoiding potential damage during installation, removal, and transportation of the portable bridge.

Assessment 4 has relatively weak weights assigned to the 'Economic' criteria to favour 'Structure' and 'Function'. This division may suit a potential public owner who has very high standards for both short and long term performance of the bridge. It may also be well suited for the purchase of a portable bridge in a period when interest rates are low enabling a long term pay back period.

Assessment 5 is heavily weighted for 'Construction' and 'Re-use'. This weighting may be appeal to a potential owner that requires a quick return on their investment for a portable composite bridge and is confident that the 'Structure' and 'Function' criteria will not influence the short term performance or reliability of their bridge.

To complete the sensitivity analysis, an additional five assessments were performed resulting in a total number of 10 assessments. The final assessments used the same weights as assessments one through five with the differing factor being the method used to evaluate the economic rating for 'Construction' and 'Re-use'. Rather than considering the total cost of the bridge, the economic rating in assessments six through ten was determined using costs specific to the connection of the deck panels to the steel plate girders. A detailed explanation of the method follows.

The investigated alternate method to rate the economy was based entirely on costs associated with each concept that are specific to the fabrication, installation, and removal of the precast concrete deck panels and neglected the total project costs associated with supplying or relocating a portable

composite bridge. Equation 4-2 was still applied; however, the control cost was replaced with an expected cost to fabricate standard precast concrete deck panels that, for the purpose of this assessment, could be fastened to the design bridge in one 12 hour work day utilizing a crew of four men, a 110 ton conventional crane, a 30 ton hydraulic excavator, and a 185 cfm compressor. This control cost for construction was chosen as an estimated lower limit of the cost which could be associated with the fabrication and installation of a precast concrete deck for a modular bridge. This construction control cost is estimated to be \$26,541 as follows; 12 precast concrete deck panels at \$1,350/panel, 48 hours at \$100/hr for field labour, 12 hours at \$307.83/hr for a 110 conventional boom crane, 12 hours at \$140.65/hr for a 30 ton hydraulic excavator, and 12 hours at \$13.28/hr for a 185 cfm compressor. The specific cost of construction is the combination of the cost for a standard precast concrete deck, \$16,200, and the estimated construction costs presented in Appendix C.

For the re-use rating, the control cost was evaluated using an estimated lower limit for the resources required to remove and re-install the deck panels. To ensure a lower bound estimate of the control cost it was assumed that there would be no consumables required to remove and re-install the bridge deck. A control cost for re-use is estimated to be \$17,235 as follows; 80 hours at \$100/hr for field labour, 20 hours at \$307.83/hr for a 110 conventional boom crane, 20 hours at \$140.65/hr for a 30 ton hydraulic excavator, and 20 hours at \$13.28/hr for a 185 cfm compressor. This specific cost for re-use was taken directly from the estimates presented in Appendix C.

The following table lists the various combinations of weights used to complete the sensitivity analysis and highlights the two connection concepts which received the highest ranking with each assessment.

Table 4-4: Sensitivity Analysis

	Structure			Function		Economics		Results		
	Strength	Ductility	Fatigue	Durability	Sensitivity	Construction	Re-use	Preferred Concept	Second Place	
Assessment 1	15%	10%	5%	20%	20%	15%	15%	Continuous Embed*	Panel End*	*tied
Assessment 2	20%	10%	5%	25%	20%	10%	10%	Continuous Embed	Panel End	
Assessment 3	15%	10%	5%	10%	10%	25%	25%	Continuous Embed*	Panel End*	*tied
Assessment 4	20%	10%	10%	25%	25%	5%	5%	Continuous Embed*	Panel End*	*tied
Assessment 5	10%	5%	5%	5%	5%	35%	35%	Continuous Embed*	Panel End*	*tied
Assessment 6	15%	10%	5%	20%	20%	15%	15%	Continuous Embed*	Panel End*	*tied
Assessment 7	20%	10%	5%	25%	20%	10%	10%	Continuous Embed	Panel End	
Assessment 8	15%	10%	5%	10%	10%	25%	25%	Continuous Embed	Panel End	
Assessment 9	20%	10%	10%	25%	25%	5%	5%	Continuous Embed*	Panel End*	*tied
Assessment 10	10%	5%	5%	5%	5%	35%	35%	Continuous Embed*	Panel End*	*tied

For each of the assessments, the top two preferred concepts remain unchanged. The continuous embed connection received the highest ranking with three of the assessments; however, the panel end connection received equal ratings to produce a tie for the remaining seven assessments. These two concepts have similar ratings for economy and identical ratings for strength, ductility, and fatigue. The differentiating factor between these two connections was that the panel end connection has a stronger rating for ‘Sensitivity’ while the continuous embed concept has a stronger rating for ‘Durability’. Assessments two and seven gave higher weight to ‘Durability’ in comparison to ‘Sensitivity’ which

explains why the continuous embed was the preferred concept for these two assessments. The economic rating for the continuous embed was slightly higher than that of the panel end connection which explains why the continuous embed is the preferred connection in assessment eight.

4.6 Concept Recommended for Further Development

Based on the results of the multi-criteria assessment and the sensitivity analysis presented in this chapter there are two concepts that present similar potential for further development. The highest ranked connection is the “Continuous Embed Bolted to Flange”, which is composed of ductile shear studs welded to a steel plate that is embedded into the soffit of the precast concrete deck panels. This embedded steel plate is then bolted to the top flange of the plate girder to enable a composite connection. Based on this assessment it is concluded that this is the superior connection by a small margin; however, due to the relative simplicity of the structural system associated with a bridge that utilizes this connection, it is expected that an experienced structural engineer could design a bridge using this concept with little added benefit gained through further applied research. For this reason, panel end connections are chosen as the concept to be developed further through analytical modelling. Chapter 5 presents the development of an analytical model for a composite girder with conventional shear studs. A load displacement analysis is performed and the finite element analysis results are validated using physical test results reported by Mans et al. [2001].

5 MODEL DEVELOPMENT

The objective for analytical modelling performed in this research is to determine the effects of replacing ductile shear studs in a composite plate girder with the proposed panel end connection. In particular, the panel end connection stiffness, ductility, and spacing are expected to influence the girders response to service and ultimate loads. In this Chapter an initial model is presented that predicts the ultimate response of a composite girder with shear studs. The effect of replacing shear studs with panel end connections is studied in Chapter 6.

The initial model is included in this Thesis to demonstrate that the finite element model used for this study accurately predicts the ultimate response of a composite girder. To validate this initial model, the geometric and material properties from one of the composite girders tested by Mans et al. [2001] were used, and a non-linear load displacement analysis was performed. The FEA output was compared to the laboratory results reported by Mans and the correlation is discussed. The work presented in this Chapter demonstrates that the FEA used in this study accurately predicts the ultimate response of a composite girder with shear studs.

5.1 Finite Element Model

Finite element analysis provides a powerful computational tool that can accurately predict the physical response of composite girders in service and at the ultimate limit state. The model developed for this study uses elements and interaction properties that are very similar to two studies that were presented in the literature review. The input parameters are presented first, followed by a detailed description of the elements and interaction properties chosen for this model.

5.1.1 Input

The material and geometric inputs for the initial model were set to resemble, as close as possible, the physical properties of a composite girder reported in the laboratory experiment by Mans et al. [2001]. The geometric details for this girder are presented in Figure 5-1.

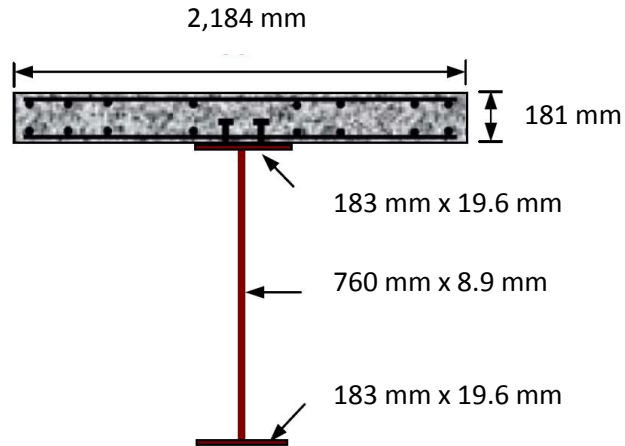


Figure 5-1: Geometric Details for Initial Model [Barth and Wu 2006]

The total length of the girder was 12,497 mm with a clear distance of 12,190 mm between supports. Bearing stiffeners were positioned at the supports and mid-span, and were accompanied by six intermediate stiffeners. The connection between the concrete deck and steel girder required 60 pairs of shear studs. Reinforcing steel in the concrete deck consisted of upper and lower mats of #4 (12.7 mm) bars with longitudinal and transverse bars spaced at 210 mm and 356 mm respectively. Table 5-1 summarizes specific material properties reported by Mans and incorporated in the finite element model.

Table 5-1: Material Properties for Initial Finite Element Model

Component:	Properties:	Comments:
Concrete Deck	$f'_c = 52.5 \text{ MPa}$	Based on cylinder tests by Mans
Reinforcing Steel	$f_y = 415 \text{ MPa}$	Specified by manufacturer
Flange* (upper and lower)	$f_y = 556 \text{ MPa}$ $f_u = 700 \text{ MPa}$	Based on coupon tests by Mans * High Performance Steel
Web*	$f_y = 583 \text{ MPa}$ $f_u = 660 \text{ MPa}$	Based on coupon tests by Mans * High Performance Steel
Stiffeners	$f_y = 345 \text{ MPa}$	Specified by manufacturer

Shear studs used by Mans et al. [2001] were 19 mm in diameter and 114 mm long; however, material properties were not reported. Since the shear studs were a standard product, a common specified ultimate strength of 450 MPa was assumed for shear studs in the current study. Shear studs were

modelled using a slot connection between nodes on the concrete deck and the top flange of the girder. This slot connection, along with its load displacement properties, is described in detail in Section 5.1.2.

The stress-strain relationship for concrete, presented in its general form in Figure 5-2, was modelled with the parabolic function developed by Carreira and Chu [1985]. This stress-strain relationship is the same formulation used by Baskar et al. [2002] and presented in Section 2.3.1 of this thesis. To correspond with experimental values reported by [Mans et al. 2001], the maximum compressive stress, f'_c , and crushing strain, ϵ_u , of the concrete were specified as 52.5 MPa and 0.0036, respectively. The Young's modulus, E_{concrete} , was 28,637 MPa and was determined in accordance with CAN/CSA S6-06 [2006]. The concrete strain corresponding with the maximum compressive strength, ϵ'_c , was defined as 0.002.

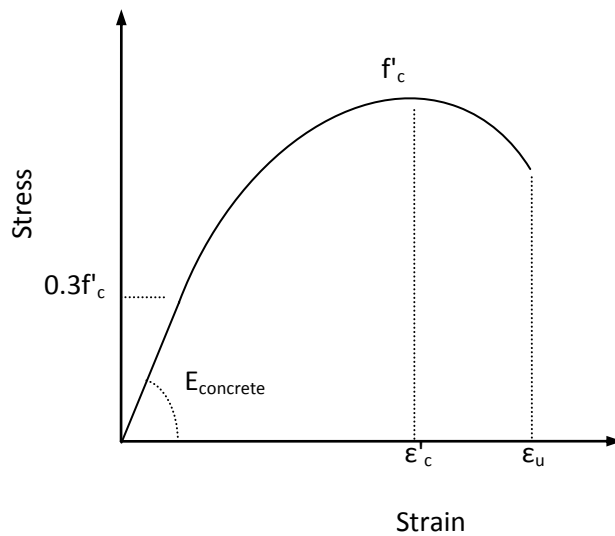


Figure 5-2: Stress Strain Relationship for Concrete

Abaqus (Version 6.7) requires finite data points to define material stress-strain relationships. In this model, 11 linear segments were specified for a discrete representation of the function presented in Figure 5-2.

For structural steel in the webs and flanges of the girder, both yield and ultimate strengths were reported by Mans et al. [2001]; therefore, the effect of strain hardening was included in this model by incorporating a tri-linear stress-strain relationship for steel as presented in Figure 5-3. The following three assumptions were made to define the tri-linear relationship; Young's modulus was taken to be

200 GPa, strain-hardening began after the strain reached 50% of the ultimate strain, and the ultimate strain was equal to 0.1.

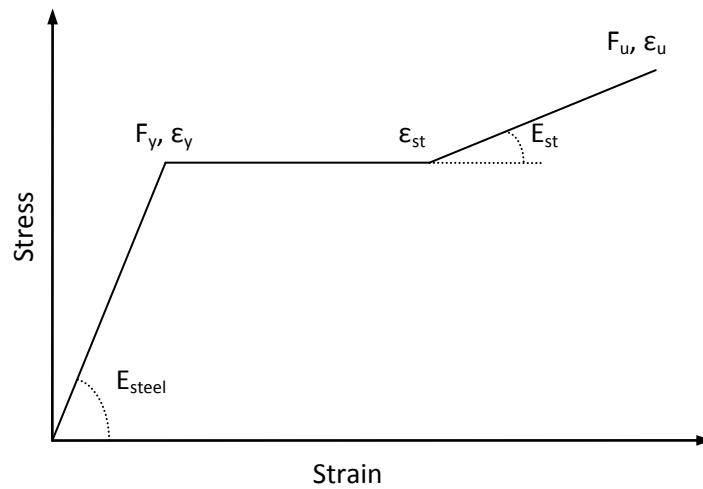


Figure 5-3: Tri-linear Stress Strain Relationship for Structural Steel

The yield, F_y , and ultimate, F_u , strengths were 556 MPa and 700 MPa respectively for the flanges and 583 MPa and 660 MPa respectively for the web.

5.1.2 Element Selection

A composite plate girder consists of the following primary components: a reinforced concrete deck; shear connections between the concrete deck and structural steel; and a plate girder composed of a top flange, bottom flange, web, and stiffeners. With the exception of the shear connections, each of these components was created as individual parts using three dimensional SR4 shell elements.

A Timoshenko beam element may have been suitable for the plate girder during the initial linear-elastic response; however, shell elements were chosen for each of the girders components because they are capable of modelling the non-linear response due to material yielding as well as local buckling failures that can accompany plate structures.

The decision to use shell elements as opposed to brick elements for the concrete deck was influenced by Baskar et al. [2002]. Baskar et al. found that brick elements restricted the rotation, due to bending, of the concrete deck and concluded that thick shell elements could be used to avoid this restriction. The concrete deck was modelled using shell elements with 11 integration points through the thickness of the slab. Multiple integration points through the thickness of the deck allow the model to engage the non-linear stress-strain properties of the concrete. The reinforcing steel in the concrete slab was specified

using the 'Rebar' option in Abaqus. With this option, the location and quantity reinforcing steel is defined and the rebar is automatically incorporated throughout the slab as a one-dimensional strain compatibility element.

During the initial phases of model development, each of the steel plates for the girder was defined as individual parts with specific material assignments. The bottom flange, web, top flange, and stiffeners were then assembled so that their geometric layout was representative of the plate girder. Next, the 'merge' function was used to combine each of these component parts into a new part representing the stiffened plate girder. This function merged the geometry between individual parts to create the new part instance.

Material assignments associated with individual parts remained with their respective components after the merge was complete and the new part was created. The top surface of the plate girder and the bottom surface of the concrete deck were specified so that a contact restraint between the concrete slab and steel plate girder could be defined as explained in Section 5.1.3.

5.1.3 Model Assembly

With the girder pre-assembled, the model consisted of two parts; the reinforced concrete deck and the steel plate girder. The relative position between these two parts was set so that the soffit of the concrete deck was at the same level as the top surface of the plate girder upper flange. With this geometric layout of the assembly complete, two properties were defined to specify the interaction between the concrete slab and steel plate girder as follows: Firstly, a hard contact restraint prevented the slab from passing vertically 'through' the steel girder; secondly, a connection, representative of shear studs, provided shear connectivity and enabled the composite system. The assembled section is presented in Figure 5-4.

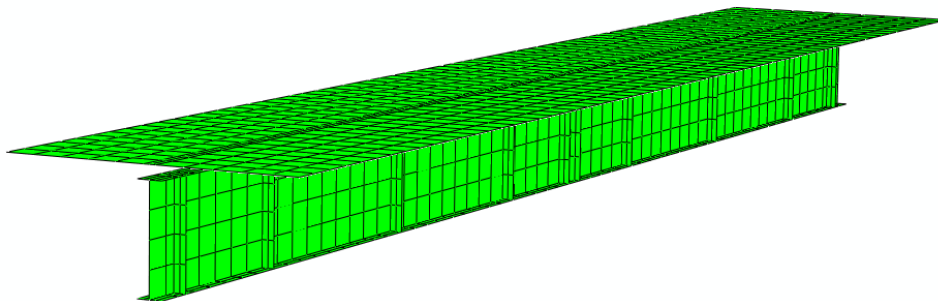


Figure 5-4: Composite Girder Modelled with Shell Elements

The visual representation of the model given in Abaqus is misleading in that it shows only the middle plane of the shell elements. Since the thickness of the concrete deck is not shown, it appears as though the concrete deck is 'floating' above the steel plate girder when in actuality the soffit of the concrete deck is in hard contact with the top of the girder. In this model, a quadrilateral geometric layout was chosen for the shell elements. In Abaqus, any shells that have four sides are classified as Quad elements. In addition to choosing Quad shell elements, the nodes in the model were set to ensure that the specific quadrilateral shape for each element was a rectangle. The approximate size of these elements was set to correspond with the 210 mm shear stud spacing. This ensured that nodes were positioned at the locations of each shear stud. The result of a mesh refinement analysis is presented in the Section 5.2.2.

After the concrete deck and steel plate girder were assembled, as shown in Figure 5-4, the interactions between these two parts were defined. This involved specifying the contact surface between the concrete deck slab and the steel plate girder as well as modelling the shear studs. Without specifying this contact surface, these two parts would be free to pass through one another, unless another interaction constraint prevented this occurrence. In the physical composite system, friction is engaged between the two contact surfaces whenever slip occurs. A friction coefficient can be specified in the model as one of the contact surface definitions. The effect of varying the friction coefficient was investigated and these results are presented in Section 5.2 Model Validation. Next, the composite structural system was developed by introducing the connection between the concrete deck and the steel plate girders.

The composite response between the concrete deck and steel girders was modelled using a slot connection with the load-slip properties of a ductile shear stud. Slot connections between corresponding nodes on the concrete slab and steel plate girder allowed relative longitudinal translations between these nodes while slaving all three rotations as well as translations in the transverse and vertical directions. The load-slip properties for shear studs were defined using the non-linear relationship developed by Hanswille et al. [2007]:

$$P_i = P_{u,0} \left(1 - e^{-1.22\delta_i^{0.59}} \right) \quad [5-1]$$

Where P_i is the load transferred by the shear stud expressed as a function of the static strength of the shear stud, $P_{u,0}$, and the slip, δ_i , in millimetres. The relationship for load-slip behaviour was proposed by Hanswille et al. [2007] during the development of analytical expressions for evaluating fatigue life of

headed shear studs and is based on the load-slip response from 15 static push-out test specimens, as summarized in Figure 5-5.

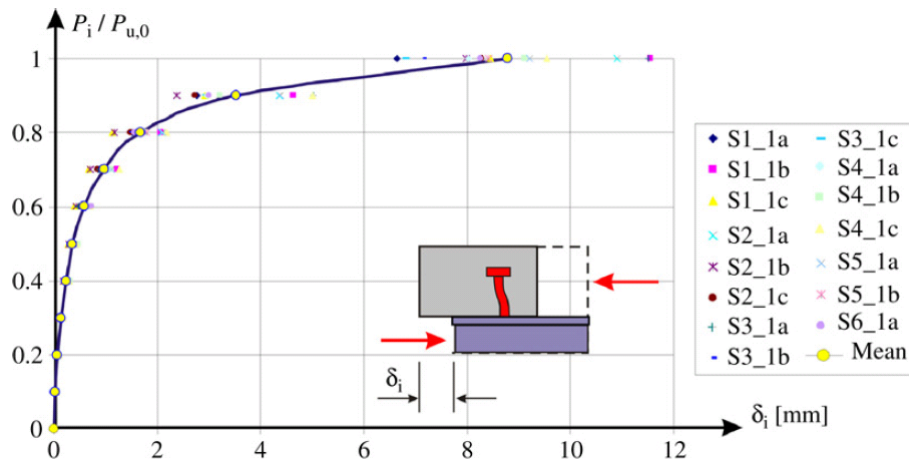


Figure 5-5: Load-Slip Envelope for 15 Static Push-out Tests [Hanswille et al. 2007]

To enable comparison of studs with different ultimate strengths, the load resistance in Figure 5-5 was based on a ratio of load increments relative to the ultimate strength for each stud. The curve represents the mean slip at each of these load increments.

The static tensile strength of the 19 mm diameter shear studs used in this study was found by multiplying the ultimate strength by the cross sectional area of the stud. Figure 5-6 shows the load slip behaviour for these studs defined by the function in Equation 5-1.

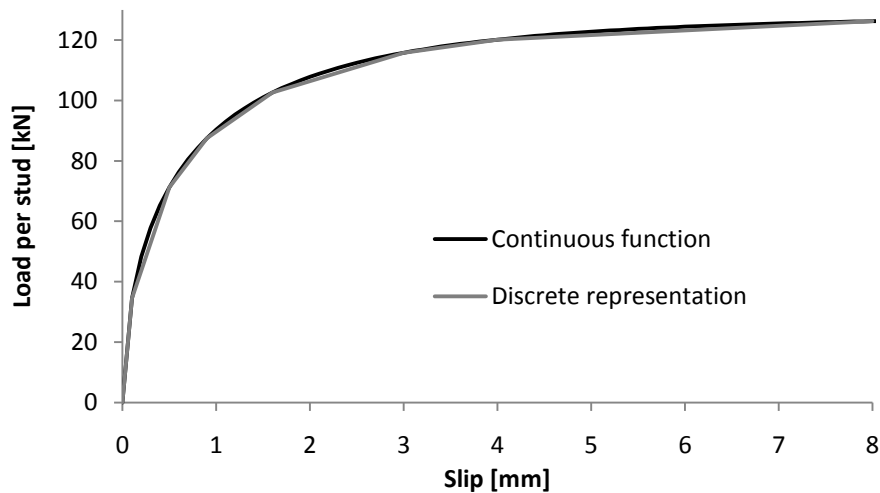


Figure 5-6: Load-Slip Curve for 19mm Diameter Shear Stud

The black line in Figure 5-6 presents the function in Equation 4 while the grey line is the discrete form of this function used to define the connection properties in Abaqus. Seven discrete segments were chosen. The slope of the first segment defined the initial stiffness of the connection. The six remaining segments of the load response curve were defined by specifying the data points at the transition between each segment.

According to Clause 10.11.8.3 of CAN/CSA S6-06 [2006] the resistance of the stud based on a local concrete crushing failure is 174 kN while the ultimate tensile load for the stud is equal to 128 kN. Since the capacity of the connection is governed by the strength of the stud and not crushing of the concrete, this model assumes that a local crushing failure does not occur where the shear stud bears against the concrete in the deck slab.

Finally, the model was completed by specifying boundary conditions and introducing the applied load. Corresponding with the physical test set up used by Mans et al. [2001], the girder was modelled with a pin and roller support at the ends of the span. In the physical test, a stiff spreader beam at the mid-span of the girder was used to apply a single point load to the composite girder. Correspondingly, a surface, equivalent to the width of the spreader beam flange, was defined on the top of the concrete deck and a uniform distributed load was then incrementally applied over this surface area. Within the loaded area, each node was slaved to match the vertical deflection of the node positioned along the centerline of the girder at mid-span. Slaving these nodes prevented transverse bending within the deck during application of the load and simulated the use of a stiff spreader beam.

5.2 Model Validation

To validate this initial finite element model, a mid-span point load was introduced and a load-displacement analysis of the composite plate girder was performed. The analytical load-displacement results were compared to the experimental findings reported by Mans et al. [2001]. This section also presents the results of a sensitivity study which identifies how mesh density, local buckling, and interface friction affect the model.

5.2.1 Finite Element Analysis

The mid-span point load was applied to the composite girder incrementally using the static Riks option. Automatic load increments were chosen that allow Abaqus to apply suitable load increments based on the response of the finite element model. For example, in the initial portion of the analysis when the

model displays a linear response, Abaqus may use relatively large load increments followed by smaller load increments once the load displacement curve begins to transition to its plastic region.

For this finite element analysis, a load greater than the expected ultimate capacity of the system was chosen to ensure that the analysis continued until failure of the composite girder. When a material failure occurs during a finite element analysis, Abaqus aborts the analysis; however, the analysis results associated with each load increment prior to termination of the analysis are recorded and provide the system response up to failure. Figure 5-7 shows the deflected shape and stress distribution within the finite element model after the final load increment was applied.

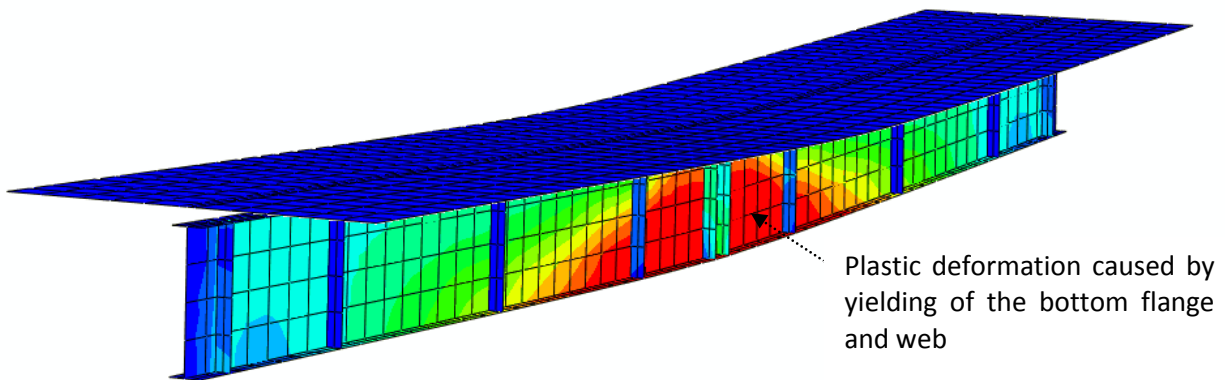


Figure 5-7: Stress Distribution in a Composite Plate Girder at Ultimate Load

The analysis terminated when the strain in the longitudinal direction of the concrete slab reached its specified crushing strain indicating that the top surface of the slab at mid-span of the composite girder had failed due to local crushing of the concrete. This failure predicted with the finite element model agrees with the Mans et al. [2001] report which stated that the ultimate load for the test specimen corresponded with a local crushing failure in the top of the slab in the longitudinal direction at the mid-span of the girder. To determine the ability to predict the linear and non-linear response of the composite girder, a load displacement analysis was performed using the finite element model and the FEA results are compared in Figure 5-8 to the experimental results by Mans et al. [2001].

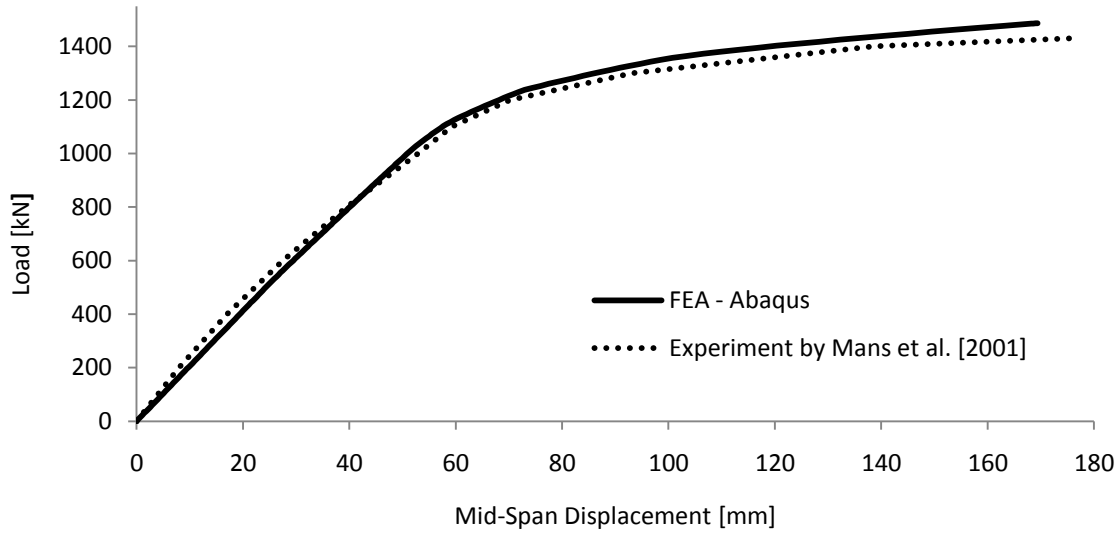


Figure 5-8: Comparison of FEA (Abaqus) and Experimental Load Displacement Results

In the initial phase of the analysis, the composite girder had a linear response until the bottom flange of the girder began to yield. In the finite element analysis the bottom flange of the girder began to yield at a load of 1,005 kN·m while Mans et al. [2001] reported that the bottom flange in the plate girder began to yield at a load of approximately 1,041 kN·m. This confirms that the linear response of the composite girder predicted using the finite element model is representative of the physical system.

A comparison between the ultimate loads and displacements between the analytical and experimental studies is presented in Table 5-2.

Table 5-2: Abaqus Results compared to Experimental Findings by Mans

	Ultimate Load (kN)	Max. Deflection (mm)
Abaqus FEA	1,487	169
Experimental	1,432	177

The ultimate load predicted in the finite element analysis exceeded the ultimate load reported in the experiment by 3.8 percent while the finite element analysis result for mid-span displacement at ultimate was 4.5 percent less than the experimental finding.

This close agreement between the finite element and experimental results indicates that the model developed for this study accurately predicts the non-linear response, up to and including failure, of a composite plate girder.

5.2.2 Mesh Refinement

Choosing an appropriate mesh density is important for ensuring accurate results when performing finite element analysis. In general, a mesh that is coarse produces a model that is stiffer than the physical system, while a fine mesh may be undesired because it is computationally costly. Since nodes are required to correspond with locations of shear studs, a mesh with elements larger than the 210 mm shear stud spacing is not possible. A mesh refinement was performed and the load displacement results are presented in Figure 5-9.

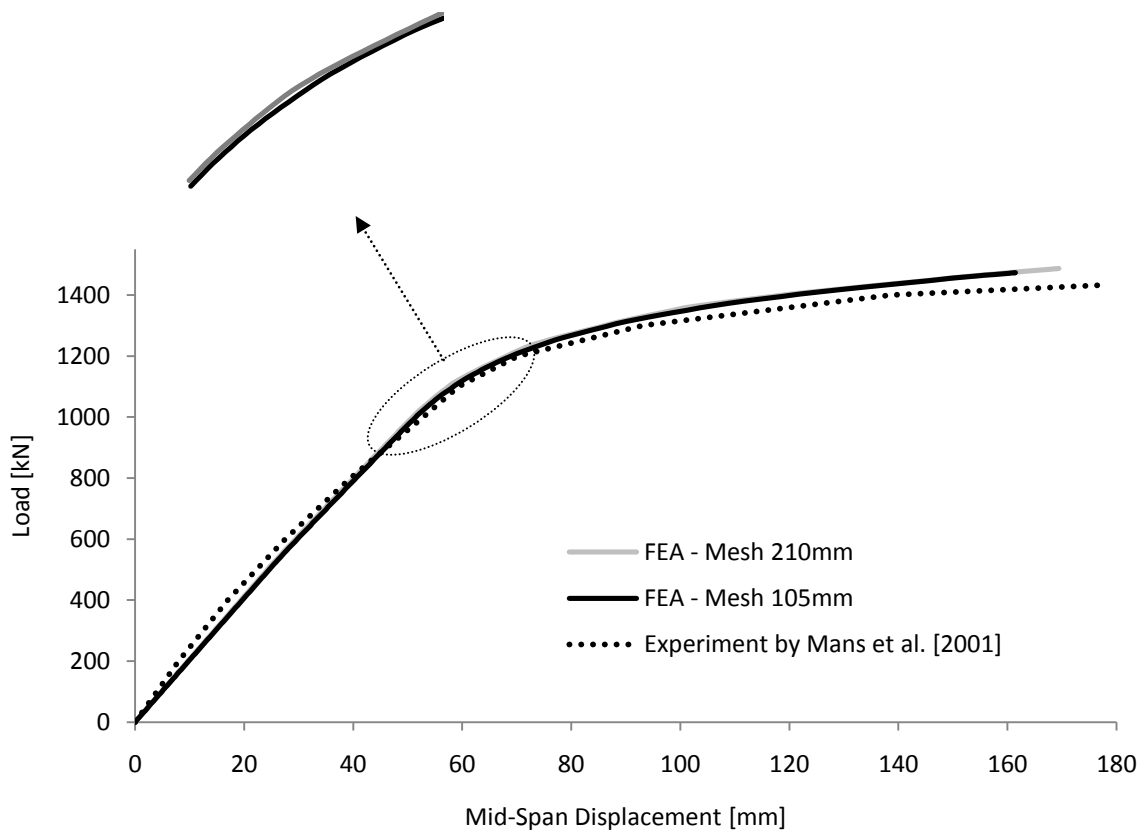


Figure 5-9: Effect of Mesh Density on the Initial Finite Element Model

For this mesh refinement, the size of the original 210mm mesh was reduced so that the approximate element size of each element was 105mm. For ease of the following discussion, the 210 mm and 105 mm mesh is referred to as the coarse and fine mesh respectively.

Figure 5-9 superimposes the results of the fine mesh (black line) on the coarse mesh (grey line). The plots from each mesh present almost identical trends; however, upon close inspection, the response obtained from the coarse mesh is slightly stiffer, particularly near the on set of plastic behaviour, and has a slightly greater ultimate load.

Based on the results of this mesh refinement it is found that the average element size of 210 mm effectively models the full non-linear response of the composite girder. The finer mesh increased analysis run times with negligible benefit.

5.2.3 Web Buckling

Steel plate girders with thin webs that are subject to large shear stresses often experience local buckling of their web. In these situations, local buckling is an expected response and its occurrence enables the development of tension field action which facilitates post-buckling shear capacity. Local buckling is less likely to occur in simple span thin webbed plate girders when the primary stresses are governed by flexure, as in the experiments by Mans et al. [2001]. In finite element models, the effect of local buckling is often considered by introducing an initial imperfection at the element nodes where local buckling is expected to occur. This initial imperfection will trigger local buckling only if the structure is vulnerable to this failure mode; alternatively, if the structure is not sensitive to local buckling this initial imperfection will not affect the system structural response. Baskar et al. [2002] found that local buckling in the webs of plate girders was successfully triggered when an imperfection in a girder web panel was introduced in the form of a sinusoidal function with a maximum value equal to one thousandth of the web panel length. Using this approach, imperfections were introduced in the web of the girder between vertical stiffeners and finite element analyses were performed. Two initial imperfections, as shown in Figure 5-10, were considered.

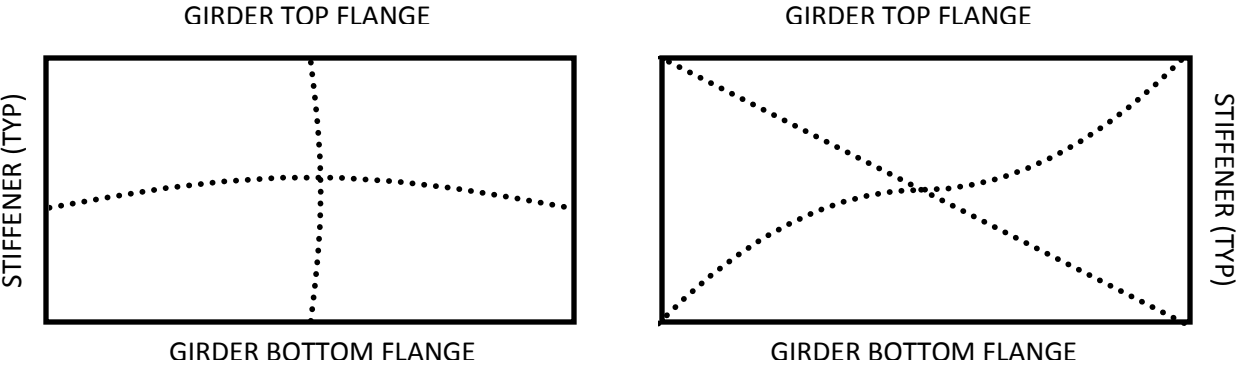


Figure 5-10: Imperfect Shape in Web to Trigger Local Buckling in a Plate Girder

The first shape, as shown in Figure 5-10 (Left), corresponds to the first buckling mode for a plate. With this mode the entire web section had an initial displacement in the same direction with the maximum displacement occurring at the middle of the panel and no displacements around the panel perimeter. First, the vertical mid-section of the panel was defined using a sinusoidal function, then this vertical function was applied to determine the local maximum displacements for each row of nodes. Sinusoidal functions were used at each row to define the complete imperfect shape.

The second shape, as shown in Figure 5-10 (Right), corresponds to the expected mode resulting from local web buckling during the development of tension field action. In this mode, the diagonal represents the tension field where there are no out-of-plane displacements. On either side of the diagonal, the web is expected to buckle in- and out-of-plane. Sinusoidal functions were used with the maximum displacements occurring at mid-height of the web and mid-distance between the stiffeners and the diagonal. To define the complete imperfect shape, the same two-step process described in the previous paragraph was repeated with the following differences; initial sinusoidal functions began at the top left, and bottom right, corner respectively and extended along the mid-distance between the nearest stiffener and the diagonal. These two functions were then used to define the local maximum displacements at each row of nodes. Around the perimeter, and along the diagonal, there were no initial displacements.

Each of these two initial imperfections were specified in the model independent of one another. In total, four analyses were completed as summarized in Table 5-3.

Table 5-3: Finite Element Analysis for Local Buckling

Mode Shape	Maximum Displacement	Observations
First Buckling Mode	Panel length / 1000	Local web buckling did not occur
First Buckling Mode	Panel length / 500	Local web buckling did not occur
Tension Field Mode	Panel length / 1000	Local web buckling did not occur
Tension Field Mode	Panel length / 500	Local web buckling did not occur

Two maximum displacements were considered; the first value, equal to one thousandth of the panel length, corresponded to the value recommended by Baskar et al. [2002], while the second value was twice this magnitude. It was conclusive from the results of all four analyses that local web buckling did not occur. This agrees with the observations and test results reported by Mans et al. [2001].

Based on these findings it is concluded that local web buckling is not expected when the ultimate capacity of the girder is governed by flexure. This conclusion is based on a composite girder with a shear connection facilitated by conventional shear studs. In the next Chapter, the relationship between panel end connections and local buckling is investigated to see if panel end connections have a negative influence the initiation of local buckling.

5.2.4 Interface Friction

The effect of interface friction along the contact surface between the soffit of the concrete deck slab and the top flange of the plate girder was assessed using models with and without friction coefficients specified for this surface. Results from a model with friction coefficient equal to 1.0 are compared in Table 5-4 to the standard analysis results which incorporated a 'frictionless' contact surface.

Table 5-4: Effect of Friction on the Contact Surface between Deck Slab and Plate Girder

Friction Coefficient	Ultimate Load	Mid-span Deflection
0	1,487 kN	169.4 mm
1.0	1,499 kN	167.1 mm

The results of these two analysis showed that friction had a small effect on the strength and stiffness of the composite girder. When the friction coefficient was set to 1.0 the ultimate load increased by 0.8 percent and the mid-span deflection decreased by 1.4 percent. While the influence of friction is small, its effect is not negligible. The models presented in Chapter 6 include friction between the surface of the deck slab and plate girder.

6 FULL-SCALE COMPOSITE BRIDGE GIRDER STUDIES

Based on the outcome of the Multi-Criteria Assessment, the concept chosen for analytical modelling is the panel end connection. The structural system presented by a portable composite bridge that employs a panel end connection is unique in that the discrete connections between the concrete deck and steel plate girders are spaced significantly further apart than shear studs commonly found in composite bridges. Even when shear studs are placed in pockets, the pocket spacing is generally much less than the panel width. To study the implications of this significant change in the structural system, full scale composite bridge girder studies, using finite element analysis, were performed, wherein composite bridges with discrete shear connections were modelled.

To complete these studies, a composite bridge girder with regular shear studs was designed, and modelled using a finite element analysis program. Next, a composite girder with panel end connections was modelled and the results were compared to those from the analysis of the composite girder with shear studs. After discussing and comparing the results, additional model verification studies are presented, which show that the finite element model captures the possible effects of local buckling of the girder plates and lateral torsional buckling of steel girders. A parametric study concludes this section, wherein the sensitivity of the composite system to variations in the shear connector stiffness and spacing is assessed.

Current design codes, such as the Canadian Highway Bridge Design Code CAN/CSA S6-06 [2006], have well established design rules for steel and concrete composite bridges. These design rules have been applied, as summarized in Section 4.3.10, to detail the individual structural components associated with the proposed panel end connection. The reason for developing an analytical model is not to verify these individual structural components, but rather to study how the spacing and stiffness of the panel end connections affect the overall structural system of a composite bridge girder.

6.1 Composite Girder with Shear Studs

A twin girder 36 metre single lane composite bridge designed for a British Columbia Forest Service L165 Logging Truck load was chosen for this study. Since a primary goal in this research is to understand the effect of replacing a conventional studded shear connection with a panel end shear connection in a composite girder, the design was limited to that of the composite girder and did not include the design of other components within the bridge such as cross bracing, plan bracing, girder splices, bearings, and

abutments. The following narrative summarizes the design of the composite girder with conventional shear studs.

6.1.1 General Specifications

The section details associated with the girder designed for this study originated from an L165 33.538 m bridge designed and built by The Surespan Group of Companies. The following details specified for the 33.538 m bridge was carried forward in the 36 m girder design; material specifications, plate thicknesses in the girder, deck geometry, layout for reinforcing steel, bearing locations relative to each end of the girder, and spacing between girders.

The basic design assumptions include: CSA G40.21M Grade 350AT for all plate steel in the girder, CSA A23.1 Exposure Class C1 with a 28 day compressive strength of 35 MPa for the concrete deck slab, CSA G30.18M Grade 400 for reinforcing steel, and a design fatigue life of 500,000 load cycles. The resulting plate girder consisted of a 25 mm bottom flange, 13 mm web, 19 mm top flange, 19 mm bearing stiffeners, and 16 mm intermediate stiffeners. The deck had an average thickness of 250 mm and a total width of 4,876 mm. The deck details and reinforcing steel layout used in this design correspond with those specified for the 33.538 m bridge, which were also the same as the details for the standard British Columbia Ministry of Forest L165 deck panel discussed in Section 4.1 and presented in Appendix A. The bearing locations are specified at an offset of 625 mm inside of each end of the girder, resulting in a clear span of 34.750 m.

6.1.2 Analysis

The L165 load distribution between the two girders was determined in accordance with the standard recommendation of the British Columbia Ministry of Forest as follows: of the total axle load, an unbalanced distribution of 45% and 55% is specified at the tires on each side of the truck respectively; also, the centre of the truck shall have an eccentricity of 450 mm from the centre line of the bridge. Combining these two unbalanced load cases with girders spaced at 3,600 mm on center, the maximum percentage of the total axle load distributed to one girder in this design is 66.2%.

The structural analysis was performed by incrementally moving the design truck along the bridge span. This span was divided into 50 segments and a Visual Basic script was written into an Excel spread sheet to perform this analysis. The routine consisted of placing the front axle of the design truck at the end of the first segment then calculating shear and moment for this particular load case. The truck was then moved along the girder and these calculations were repeated for each truck position. The resulting

shears and moments were recorded during the structural analysis and the following envelopes, shown in Figure 6-1, present the maximum values along the girder span for the unfactored truck load.

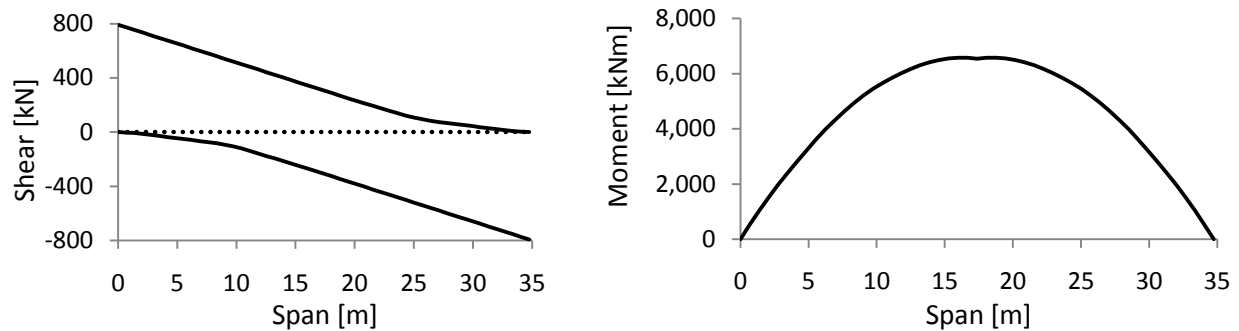


Figure 6-1: Live Shear and Moment Envelopes for an L165 36 m Composite Plate Girder

The maximum unfactored truck load consists of a shear force of 793 kN and a moment of 6,571 kN-m at the support and mid-span respectively. To check the shear connectors for the fatigue limit state, the difference between maximum and minimum shear forces at a specific point along the bridge span due to the passage of the design truck is required. In this study, the shear force of 793 kN presented the greatest difference between maximum and minimum shear at any point along the girder during a single load cycle.

6.1.3 Composite Girder Design

The following approach was taken to select the cross-section geometry for the stiffened plate girder: the flanges were sized as Class 3 members and the depth of the web was chosen to provide a cross section in which the factored tensile resistance of the plate girder exceeded the factored compressive resistance of the reinforced concrete deck. The limit for maximum web depth specified in Clause 10.10.4.2 of CSA S6-06 was observed. Having the tensile resistance of the girder exceed the compressive resistance of the concrete deck ensured that the entire depth of the concrete deck could be utilized in the design.

The plastic neutral axis of the composite girder was 4.7 mm below the top surface of the upper flange. Transverse stiffeners were spaced in accordance with the requirements of Clause 10.10.6.1. It is worth noting that CAN/CSA S6-06 [2006] allows bridge designers to use the full plastic moment capacity of stiffened plate girders (which are typically Class 4 girders) when used in a composite section; however, if the plastic neutral axis is located in the web of the girder, the depth of web that can be utilized in compression is limited by Clause 10.11.6.2.2. The resulting cross-section for this composite girder is presented in Figure 6-2.

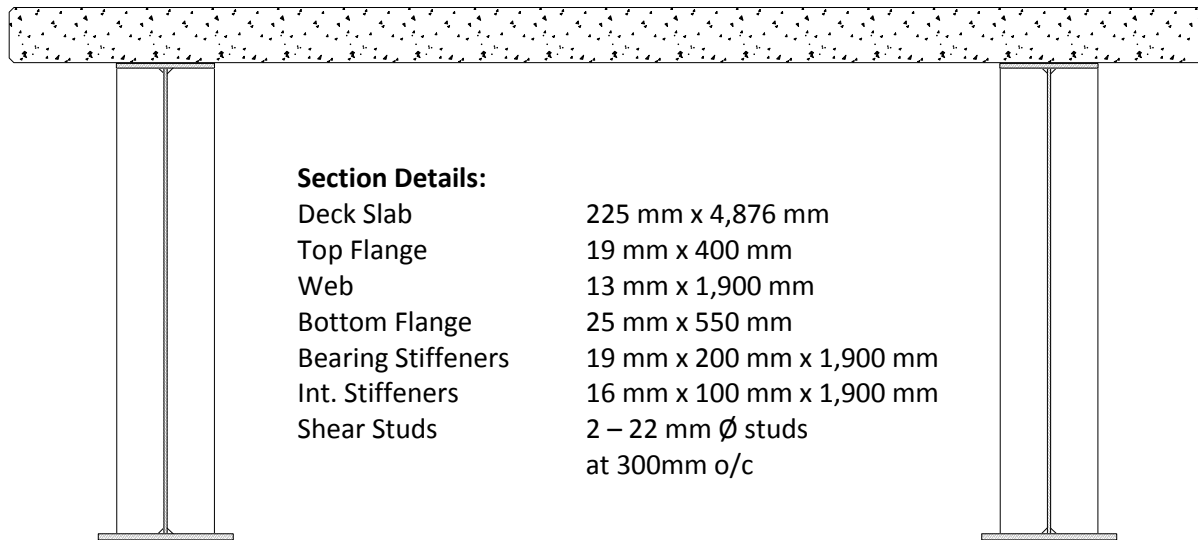


Figure 6-2: Cross-Section for a 36m L165 Composite Bridge Girder

The total number of shear studs required for a full composite section was determined based on strength and checked for fatigue in accordance with Clause 10.11.8.3 and 10.17.2.7 respectively. Material resistance and live load factors, including the dynamic load allowance, were specified in accordance with CAN/CSA S6-06 [2006]. The composite girder was designed for the Ultimate Limit State. The ultimate factored loads included a moment of 17,096 kN·m and a shear force of 2,046 kN. The ratio of the factored loads over the factored resistances was 0.88 for moment and 0.89 for shear. These results indicate that for this design example, shear governs the design by a small margin. The full analysis results are summarized in Appendix D.

6.1.4 FEA – Composite Girders with Shear Studs

A model of the composite girder with conventional shear studs was constructed and analyzed using the finite element analysis program Abaqus [2007]. The composite girder with regular shear studs was modelled to establish a benchmark to measure the performance of the composite girder with panel end connections. The composition of this model for the 36 m girder with regular shear studs was the same as that presented in Chapter 5 with the exception that the material properties and member geometry were defined to match the structure described in this chapter.

A plot of applied moment verses mid-span deflection was chosen for visual presentation of the girder's response. By plotting these parameters the girder's ultimate strength along with its elastic and ductile serviceability properties can be assessed. Since moment is linearly proportional to applied load, either moment or applied load could have been used interchangeably in the plot, as long as the total load

resulted from a single load pattern. Plotting moment was chosen because it enables the opportunity to combine multiple load patterns in one plot. For example, a uniformly distributed dead load combined with a truck load is easily plotted using applied moment but would be difficult to plot if applied load was used in place of applied moment.

Also, since a girder’s strength is often governed by its flexural capacity, plotting applied moment in place of applied load allows for an easy comparison of different load patterns and girder spans. Alternatively, if applied load was plotted, a direct comparison between results would not be possible because the girders ultimate capacity, in terms of total load, associated with each load pattern would be different. For the initial analysis, the position of the design truck was set, as shown in Figure 6-3, so that the largest flexural demand was developed.

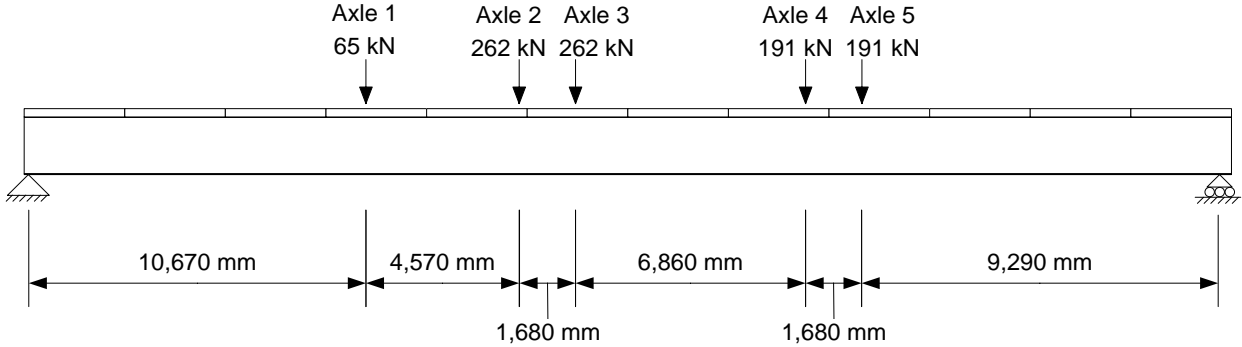


Figure 6-3: Truck Position Resulting in Maximum Moment

The truck position in Figure 6-3 was determined using the “general rules for simple beams carrying moving concentrated loads” as presented in the Handbook of Steel Construction [2007]. The method consists of positioning the truck so that the mid-point between the truck’s centre of gravity and the nearest axle to the centre of gravity is centred at mid-span of the bridge. A detailed explanation of the method can be found in the reference. The maximum moment resulting from the truck position in Figure 6-3 agrees within 0.1 percent of the maximum moment calculated using the incremental positioning approach summarized in Section 6.1.2.

Two steps were used to apply the load to the composite girder in this finite element model. In the first step, the dead load of the steel plate girder and concrete slab, plus 20 percent of this dead load to account for cross bracing, guard rails, and miscellaneous details, was applied. In the second step, the axle loads were introduced gradually in load increments not greater than one percent of the total

specified axle load. The total specified axle load was determined using an Excel solver as follows: the dead load was applied to the girder span, and then the axle loads were increased proportional to one another until the combined moment due to the dead load and axle loads was equal to the unfactored plastic capacity of the composite girder. Table 6-1 presents these ultimate axle loads, which were used as the specified axle loads in the FEA, along with the design axle loads that were used in the analysis presented in Section 6.1.2, and the axle loads which develop the yield capacity of the girder.

Table 6-1: Axle Loads per Girder that Develop the Yield and Plastic Moments

	Design Load	Yield Load	Ultimate Load
Axle 1	65 kN	116 kN	162 kN
Axle 2	262 kN	469 kN	652 kN
Axle 3	262 kN	469 kN	652 kN
Axle 4	191 kN	342 kN	476 kN
Axle 5	191 kN	342 kN	476 kN

To develop the full plastic moment of 19,362 kN·m, an increase of 79% from the original unfactored design axle load was required. Table 6-1 also presents the axle loads that develop the yield capacity of the composite girder based on a transformed section analysis. Yielding of the bottom flange in the plate girder governs the yield moment of the composite girder. The approach used to determine the axle loads that correspond with the yield capacity was the same as that presented in the previous paragraph.

Prior to performing the finite element analysis, a plot of applied moment verses mid-span deflection was developed as a reference for evaluating the FEA output. This plot is presented in Figure 6-4.

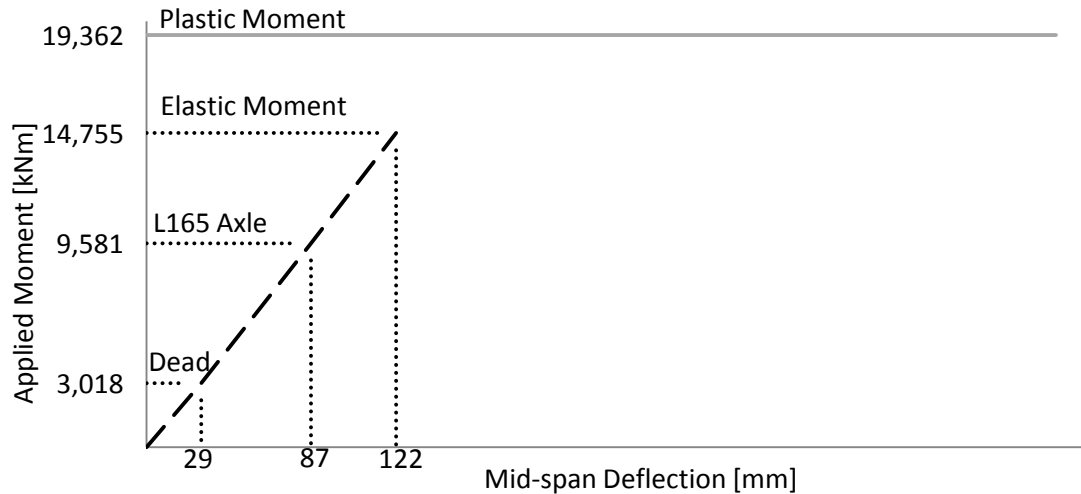


Figure 6-4: Analytical Load Displacement References for Evaluation of FEA Results

The plastic capacity of the girder, 19,362 kN·m, is defined with the solid grey line in Figure 6-4 that extends the full width of the plot and provides an expected capacity of the girder; however, the capacity of the composite girder may exceed 19,362 kN·m if strains in the steel girder are large enough for strain hardening to occur. No prediction is being made regarding the deflection that will be associated with the plastic moment.

The dashed line in Figure 6-4 presents the mid-span deflections associated with the elastic response of the composite girder. These deflections were calculated using the moment of inertia of the transformed section. Although not readily apparent in Figure 6-4, the elastic response of the composite girder is actually bi-linear, with slightly different slopes corresponding to the two load cases: a uniform distributed dead load followed by the incremental application of the axle loads.

The first segment of the dashed line in Figure 6-4 describes the elastic response associated with the uniformly distributed dead load. A mid-span deflection of 29 mm results from the application of the full unfactored dead load. The second segment of the line is determined by calculating the mid-span deflection associated with the axle loads, presented in Table 6-1, scaled to the elastic capacity of the girder. The combined service deflection is equal to 87 mm. Because of the assumed linear-elastic response of the girder, superposition can be used to add the deflections resulting from the dead load and axle loads to predict the total mid-span deflection associated with the elastic capacity of the composite girder. The moment and deflection associated with the design axle loads are also indicated in the plot.

A shortfall of predicting the elastic response of the girder using a transformed section analysis is that the transformed section assumes full interaction between the concrete slab and the steel plate girder. Even though a full shear connection is provided with studs spaced every 250 mm, the shear studs are at discrete locations, which will result in partial interaction between the concrete slab and steel girder. Based on laboratory tests of composite girders, Grant et al. [1977] proposed Equation 6-1 to calculate the effective girder stiffness that accounts for this partial interaction. This equation has also been incorporated in Clause 17.3.1 of CISC [2007].

$$I_e = I_s + 0.85 \cdot (p)^{0.25} \cdot (I_t - I_s) \tag{6-1}$$

Where I_e is the effective moment of inertia ($59,418 \times 10^6 \text{ mm}^4$), I_s is the moment of inertia of the steel beam ($25,679 \times 10^2 \text{ mm}^4$), I_t is the transformed moment of inertia of the composite beam ($65,372 \times 10^2 \text{ mm}^4$), and p is the fraction of full shear connection. Since a full shear connection is provided in this composite bridge girder, p is equal to 1.0. The fraction of shear connection is included so that the stiffness of partial shear connections, which are often used in steel building construction, can be determined. When a full shear connection is provided, the effective moment of inertia is equal to the moment of inertia of the steel beam plus 85 percent of the difference between the moment of inertia of the full transformed section and that of the independent steel beam. By applying this effective moment of inertia, a second line is added to the reference plot (see Figure 6-5).

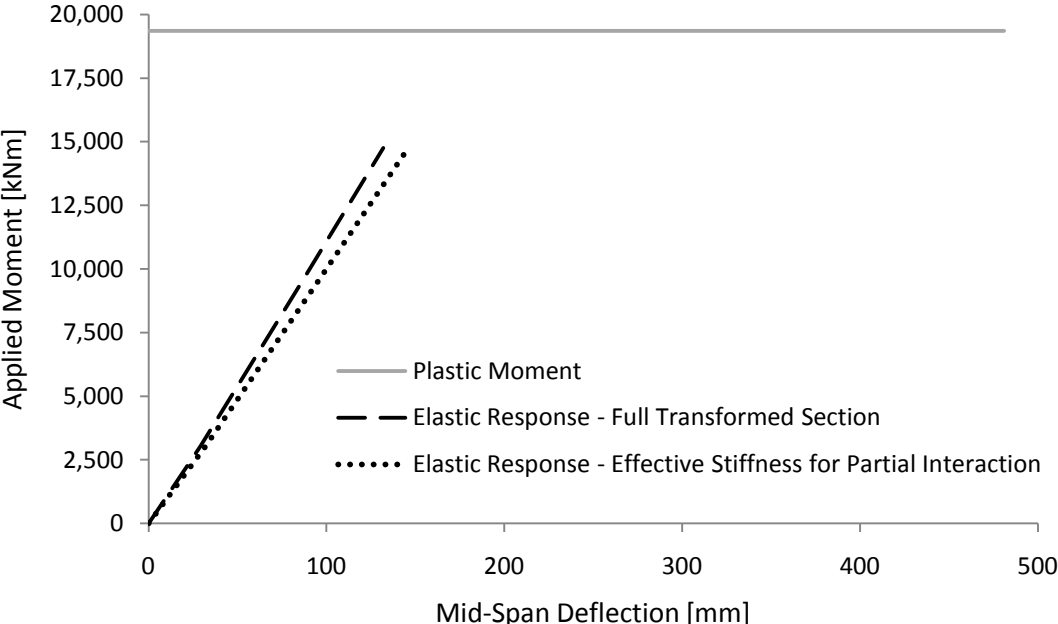


Figure 6-5: Effect of Partial Interaction on Girder Stiffness

The dotted line, representing the deflection based on the effective moment of inertia, predicts slightly larger deflections when compared to those predicted using the full transformed section. The plots in Figure 6-5 will provide a reference for evaluating the analysis output of the finite element model.

With the reference plots established, a finite element analysis was performed using the Abaqus model of the 36 metre composite girder with regular shear studs. As mentioned previously, the unfactored dead load was applied first, followed by the axle loads. The mid-span deflections obtained from the FEA output are presented in Figure 6-6 as a function of the total applied moment.

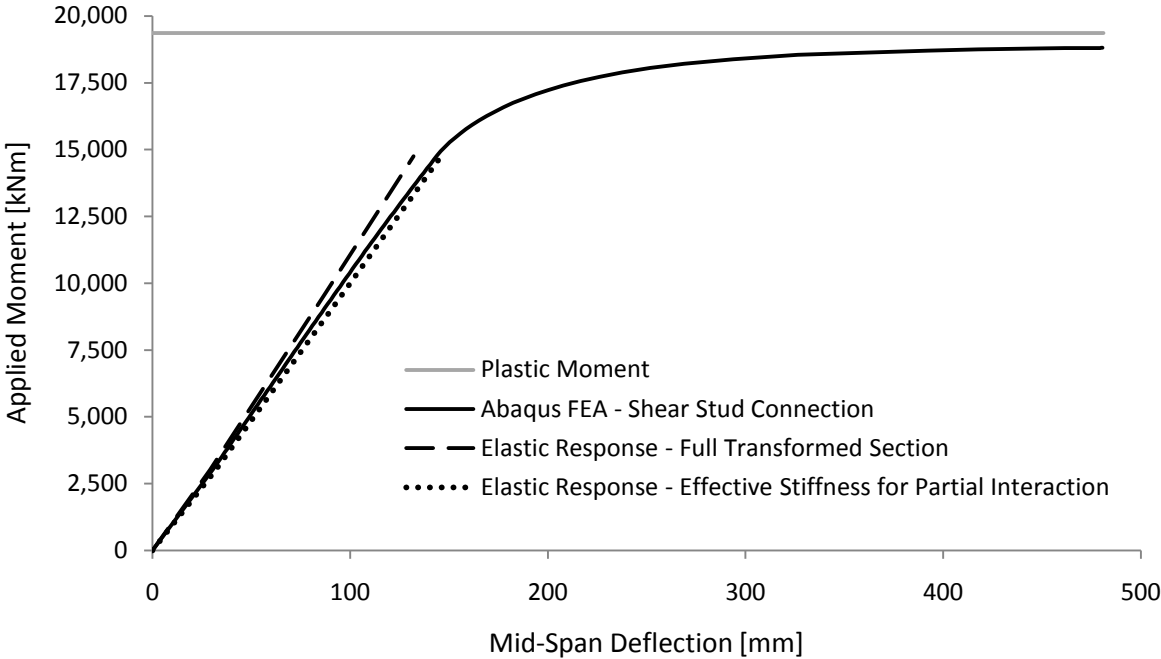


Figure 6-6: Applied Moment and Mid-span Displacement – UDL and L165 Axle Load

The solid black line indicates the mid-span deflections and moments taken from the finite element analysis output. The finite element analysis terminated when the ultimate strain for concrete was reached, indicating a crushing failure in the concrete deck slab. Termination occurred at an applied moment of 18,793 kN·m, corresponding with a mid-span deflection of 468 mm. The following three stages of the load displacement results are discussed in detail: the initial response corresponding to the uniformly distributed dead load, the response up to the predicted elastic capacity of the composite girder, and the post-yield response resulting in plastic deformations and ultimate failure of the girder.

The mid-span deflection resulting from application of the total uniformly distributed dead load (completion of step one) was 30 mm based on the finite element analysis. The mid-span deflection

determined with the finite element analysis agrees, within four percent, with the mid-span deflection predicted using 'hand calculations'. This general agreement observed between these two results was expected because at the end of this step the maximum stress in both the concrete (3.3 MPa) and the steel (69.7 MPa) were below their linear-elastic limits of 10.5 MPa ($0.3 \cdot f'_c$) and 350 MPa (f_y) respectively. The linear elastic limit of 10.5 MPa ($0.3 \cdot f'_c$) corresponds with the concrete model (refer to Figure 5-2) by Carreira and Chu [1985].

In the next step of the finite element analysis the axle load is applied, incrementally, to the composite girder. Up to an applied moment of 8,575 kN·m the load-deflection response of the girder is linear followed by a subtle non-linearity which continues until the bottom flange begins to yield. The initiation of this subtle non-linearity corresponds with strains in the concrete which are sufficient to result in concrete stresses that exceed 10.5 MPa ($0.3 \cdot f'_c$). Based on the concrete material definition, the stiffness of the concrete decreases after the stress exceeds $0.3 \cdot f'_c$, which explains the non-linearity observed in this section of the response. At an applied moment of 14,786 kN·m, yielding in the bottom flange of the plate girder is observed and a significant non-linearity in the load response curve of the composite system is realized due to plastic deformation in the girder.

After yielding began in the plate girder there is a sudden, and substantial, increase in deflection as the plastic deformation progresses throughout the girder. In the final increments of the analysis a perfectly plastic response is approached, but not fully realized. The finite element analysis terminates when the strain in the concrete reached its specified crushing strain (0.0035). The maximum strain in the plate girder (0.0208), observed in the bottom flange, is not large enough to initiate strain-hardening of the steel. The ultimate capacity predicted by finite element analysis, 18,793 kN·m, is 97.1 percent of the 19,362 kN·m predicted by a plastic composite section analysis. While this agreement is good, the small discrepancy could be due to the difference between the actual stress distribution versus the generalized rectangular stress block used to predict the compressive resistance of the concrete deck slab in the plastic section analysis.

These finite element analysis results support the findings from the previous Chapter and demonstrate that the complete non-linear response of a composite plate girder with conventional shear studs is accurately modelled using finite element analysis. The remaining sections of this chapter present the findings associated with replacing the headed shear studs with panel end connections. For this comparison, the analysis results for the 36 metre composite girder with conventional shear studs, as

presented in Figure 6-6, is accepted as the benchmark for evaluating the performance of composite girders with panel end connections.

6.2 Composite Girders with Panel End Connections

Based on the result of the multi-criteria assessment of the connection alternatives for a portable composite bridge, panel end connections were recommended as the preferred alternative for additional study. This Section includes: a detailed design narrative of the proposed panel end connection; a description of the process used to estimate the connector's load-displacement properties; a fatigue check of the gusset plates for the panel end connections; and a presentation of the finite element model, and analysis results, for a composite girder with panel end connections.

6.2.1 Connection Design Narrative

In Chapters 3 and 4, ten connection alternatives were proposed and a conceptual design was completed for each connection. Based on the results of a multi-criteria assessment, the panel end connection was chosen as a preferred alternative. The conceptual design completed in Section 4.3.10 was subsequently reviewed and some minor changes were incorporated into the connection design to improve the fatigue performance and serviceability of the panel end connection. The structural system associated with the revised panel end connection is presented herein.

The composite girder with panel end connections, shown in Figure 6-7, has four primary components: a stiffened plate girder; gusseted bearing plates; a steel embed assembly; and the precast concrete deck panels. Calculations are included in Appendix E to support the details that are presented below. The concrete deck panel is not shown in Figure 6-7 for clarity of the structural steel embed.

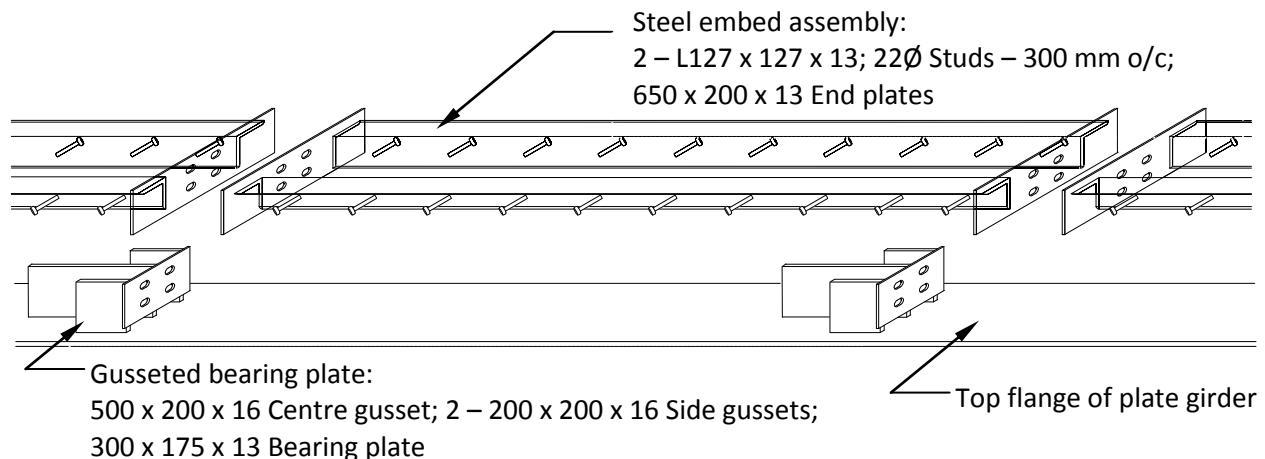


Figure 6-7: Schematic View of a Composite Girder with Panel End Connections

Precast concrete deck panels used for this study were detailed in accordance with the British Columbia Ministry of Forest standard drawing for an L165 deck panel as presented in Appendix A.

The steel embed assembly is provided to engage the concrete deck uniformly along its length in a method that is similar to a regular composite girder. The shear studs on this assembly provide a fully composite system between the concrete deck and the steel angles. Steel plates, welded to the either end of the angles, enable a bolted connection between the steel embed assembly and the gusseted bearing plate.

Bearing plates, supported by gussets that are welded longitudinally to the top flange of the plate girder, provide a point of connection for the precast concrete deck panels. When the fatigue design was performed, it was observed that welded connections that are perpendicular to the top flange of a plate girder are categorized under an extremely poor detail for fatigue (Detail Category E); therefore, the thickness of the steel gusset plates proposed in Section 4.3.10 were increased so that welding the bearing plate to the girder could be avoided.

As mentioned in the previous paragraph, the steel plate girder is connected to the gussets with longitudinal welds. For a detailed narrative of the steel plate girder design, refer back to the composite girder design presented in Section 6.1.3.

6.2.2 Connector Properties

The load displacement response for the panel end shear connection has been idealized as follows; initially, the connector is expected to have a linear elastic response followed by perfectly plastic behaviour once the ultimate shear capacity is developed, as in Figure 6-8 (a). To estimate the ultimate displacement, the entire load is concentrated at the top of the gusset plate, as in Figure 6-8 (b). In reality, the load will not be concentrated as assumed in Figure 6-8. Changes to the placement of the load on the connector will influence the connector stiffness; however, alternate load positions are not considered in this Section because the effect of connector stiffness is presented as a parametric study later in this Chapter.

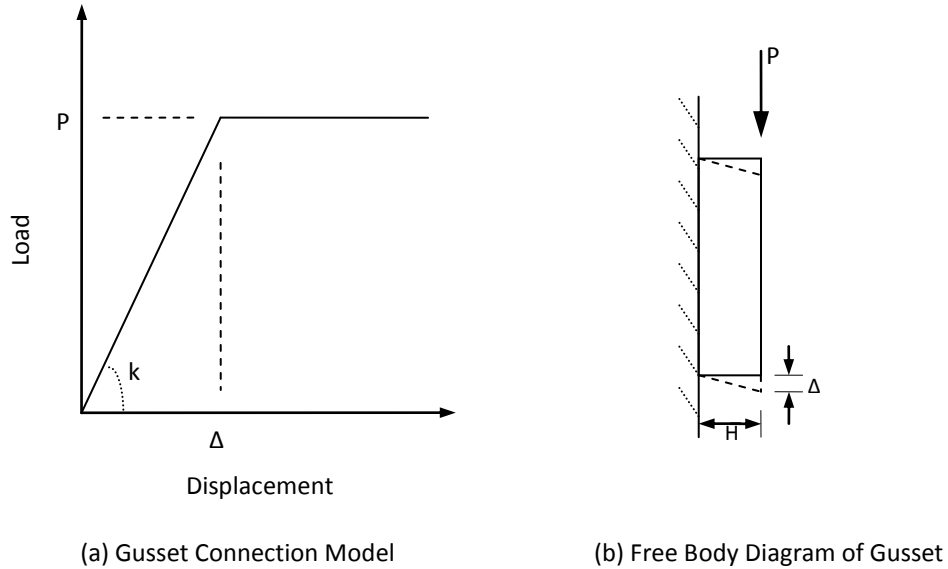


Figure 6-8: Load Displacement Properties for a Panel End Connection

The ultimate capacity of the connection, P , was based on the unfactored shear capacity. The displacement, Δ , was solved using the gusset geometry and shear modulus (77,000 MPa) of the steel. The connection stiffness, k , is the slope of the load-displacement in the elastic range. Two material models were developed to suit the centre gusset plate and two, identical, side gussets respectively. Free body diagrams and calculations for both of these connection models are presents in Appendix E, with the results summarized in Table 6-2.

Table 6-2: Connection Properties for Centre and Side Gusset Plates

	Capacity, P	Deflection, Δ	Stiffness, k
Centre Gusset	1,852,083 N	0.606 mm	3,055,937 N/mm
Side Gusset	740,833 N	0.606 mm	1,222,374 N/mm

Each panel end connection consists of a centre gusset, and two side gussets, for a combined ultimate capacity of 3,333,749 N; however, the finite element model, as described in Section 6.2.4, models each of the gusset plates individually. When each of the gussets are modelled separately, as done in this finite element analysis, the three gussets work together to form a structural system similar to that of three parallel springs by attracting a percentage of the total load in proportion to their individual stiffness. Since each of the gussets has the same yield deflection, as shown in Table 6-2, yielding will take place in each gusset simultaneously.

6.2.3 Fatigue of Gusset Plates in Panel End Connection

The connection of the gusset plates to the top flange of the steel plate girders is a critical component of the composite structural system. Since this connection will be subject to cyclic loading, a fatigue check has been performed, according to CAN/CSA S6-06 [2006], with a conservative modification to Clause 10.17.2.2.

Clause 10.17.2.2 requires that the fatigue stress range in a particular detail is less than its fatigue stress resistance. In this Clause, the fatigue stress range is calculated by finding the maximum stress range due to the passage of a CL 625 design truck, then reducing this stress range with a factor of 0.52 to account for the fact that not all load cycles will be as severe as that induced by the design truck. This reduction factor is considered applicable for use in Highway bridges but would not be suited for use in a specialty bridge application.

In this study, the portable composite bridge is proposed for the resource industry which means that there is a greater expectancy for the daily traffic to consist of heavy trucks as opposed to regular passenger vehicles. Since statistical data regarding axle loads on resource bridges was not considered, a conservative approach was taken where the 0.52 reduction factor was removed, and the full stress range from the design truck was applied. The fatigue stress range was determined from the finite element analysis, which is presented in the following section and consists of a maximum service stress of 81 MPa in the top flange and 69 MPa in the gusset plate connection. These service stresses result from the application of the unfactored truck load with a dynamic load allowance of 0.25.

The fatigue stress range resistance is a function of the expected number of load cycles and the detail category of the connection. As mentioned in Section 6.1.1, the fatigue design for this portable composite bridge is based on 500,000 load cycles. The connection detail, according to CAN/CSA S6-06 [2006], is classified as a Category E and has a nominal fatigue stress resistance of 90 MPa for 500,000 load cycles. For this design, fatigue does not govern because the fatigue stress range resistance of 90 MPa exceeds the calculated design fatigue stress range of 81 MPa. These calculations are presented in Appendix E.

6.2.4 FEA – Composite Girders with Panel End Connections

With the exception of the shear connection, the finite element model for a composite girder with panel end connections is the same as the model presented for a 36 metre composite girder with shear studs. The load was applied in a two step process with the uniformly distributed dead load applied first

followed by the incremental application of axle loads from a British Columbia Ministry of Forest L165 logging truck. For a detailed description of the general components in this model, refer to Sections 5.1 and 6.1.4.

For the finite element model with panel end connections, the precast concrete deck panels were idealized as continuous reinforced concrete slabs. This was considered to be a reasonable simplification because of the single span configuration of the girder. Also, since the focus of this study is to determine the overall response of a composite girder with discrete shear connections, modelling the specific details of the panel end connectors was outside of the scope for this research.

To model the panel end connections, 'slot + align' connectors were employed. A 'slot + align' connector is defined in Abaqus as a connector that allows relative translation in one direction between two nodes while slaving their other two translations, as well as all three rotations. In this model, connectors were spaced every three metres and the relative translation permitted with the 'slot + align' connector corresponded with the longitudinal direction of the girder.

Presented herein are reasons for choosing the 'slot + align' connector: Slaving the rotations was chosen because in a composite girder the curvature of the concrete deck will match that of the plate girder; Forcing vertical translations to be the same at the point of connection between the girder and the concrete deck models an expected response since the truck load is applied to the deck and vertical displacements of the steel plate girder will have to match those in the concrete slab. Since different relative rotations, or vertical displacements, between the concrete deck and steel plate girder is not expected, slaving the rotations and vertical displacements is not expected to have a significant effect on the behaviour of the composite system when compared to an equivalent system in which these four degrees of freedom are not slaved. One reason these constraints were used in the model was to maintain the local coordinate system that defines the orientation in which relative slip between the concrete deck and steel plate girder is permitted.

For the relative transverse translation, a small lateral force on the shear connection could be presented due to the tendency of the steel plate girder to deform by lateral torsional buckling; however, It was found during the study on lateral torsional buckling that the maximum lateral force on this shear connection is equal to 4.0 kN (0.1 percent of the longitudinal force). This lateral force would be easily resisted by the slip critical bolted connection which fastens the precast concrete deck panels to the gusseted bearing plates.

Connector property models, presented in Section 6.2.2, were assigned to the centre and side gusset plates respectively and a finite element analysis was performed. The results of this finite element analysis of a composite girder with panel end connections is presented in the form of an applied moment verses mid-span deflection plot (see Figure 6-9). A plot of applied moment verses mid-span deflection was chosen because it allows for an easy assessment of the service and ultimate response of the composite system. The result from the finite element analysis for composite girders with regular shear studs (Section 6.1.4) is also plotted in Figure 6-9 to set a comparative benchmark.

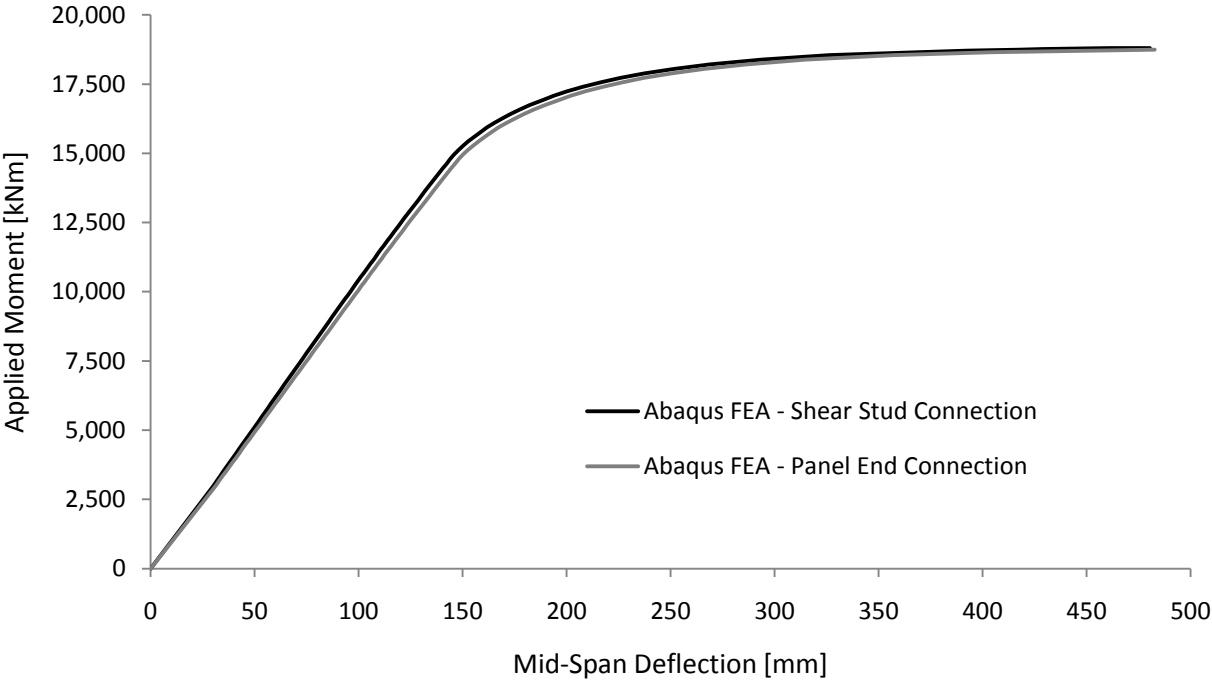


Figure 6-9: Shear Stud Connection Compared to Panel End Connection

The finite element analysis for a composite girder with panel end connections, plotted with the grey line in Figure 6-9, presents the same trend and a very similar response to the analysis of a composite girder with regular shear studs. The analysis (with panel end connections) terminated when the ultimate compressive strain for the concrete was realized at the mid-span. This indicates that a crushing failure in the concrete deck governs the ultimate capacity of the composite girder with panel end connections. Table 6-3 summarizes the service and ultimate limit states associated with each of the two finite element analyses.

Table 6-3: Service and Ultimate Limit States of a Composite Girder

	Unfactored Dead + L165 Axle		Ultimate Limit State	
	Moment	Deflection	Moment	Deflection
Shear Studs	9,581 kN·m	92 mm	18,793 kN·m	468 mm
Panel End Connections	9,581 kN·m	99 mm	18,612 kN·m	492 mm

The service limit state is defined as the moment that results from the application of dead load plus the L165 axle load. The deflections associated with each of the two systems are similar (within 8 percent) to each other; however, it is noted that the deflections in each of the composite systems are rather large. This is because the design L165 logging truck is over two times heavier than a standard Canadian CL 625 truck load. Since deflection limits for bridges not used by pedestrians are not specified in CAN/CSA S6-06, the limit specified in AASHTO LRFD [2002] is used for comparison of the observed mid-span deflections. AASHTO specifies a deflection limit equal to $L/800$, which corresponds with an allowable deflection of 45 mm for a 36 metre span. Even if the dead load component (30 mm) of the mid-span deflection is compensated by camber of the girder, the deflections in each of the two composite systems exceed the limits presented by AASHTO. In conclusion, the deflection limits set by AASHTO are exceeded for this particular bridge design; however, these deflection limits would not be imposed on a rural resource bridge.

At the ultimate limit state, the magnitudes of the moments and deflections associated with the shear stud connection, and the panel end connection, are different by 1.0 and 5.1 percent respectively with the panel end connection assuming the lower moment capacity and greater ultimate deflection. While this difference in ultimate performance between the two connections is small, a similar trend is observed in the parametric study: increased deflections correspond with decreased flexural capacities. An explanation for this relationship, with reference to girder stiffness, will follow in Section 6.4.1.

Based on these results, it is expected that the performance of a composite girder with discrete shear connections, spaced every 3 metres, will be nearly identical to a conventional composite girder with regularly spaced shear studs. This result is supported in Section 6.3 by verifying the finite element model's ability to capture the effects of local flange buckling, lateral torsional buckling, and web buckling and by showing that these effects do not compromise the proposed composite system. A parametric

study is then presented in Section 6.4 to determine the sensitivity of the composite system to the connection stiffness and spacing.

6.3 Model Verification

This section presents three studies that investigate the effects of local flange buckling, lateral torsional buckling, and web buckling on the behaviour of the composite girder with discrete shear connections. There are two objectives in each of the following sub-sections. The first objective is to show that finite element analysis will model the local effects described above. To achieve this objective, the composite plate girder modelled in Section 6.2.4, was modified to enable these local effects to occur. The second objective is to demonstrate that these local effects do not influence the response of the proposed composite girder with panel end connections.

6.3.1 Local Buckling in Compression Flange of Girder

When a composite plate girder is designed to the CAN/CSA S6-06 [2006], local buckling of the compression flange is prevented by Clauses that restrict the width to thickness ratio of the compression flange and the maximum spacing of shear studs. With panel end connections, or other discrete shear connections, the distance between connection points will greatly exceed the allowable spacing permitted in CSA S6-06 for shear studs. The analysis described in this section shows that local buckling does not occur in the top flange of the design girder and also demonstrates that finite element analysis is capable of modelling local buckling. Also, a hand calculation method that can be used to check for local buckling is presented.

To initiate local buckling in the compression flange of the steel plate girder, an initial imperfection was introduced over the three metre distance between shear connections. This imperfection was introduced in the form of a sinusoidal function with maximum amplitude equal to one thousandth of the three metre length (see Figure 6-10).

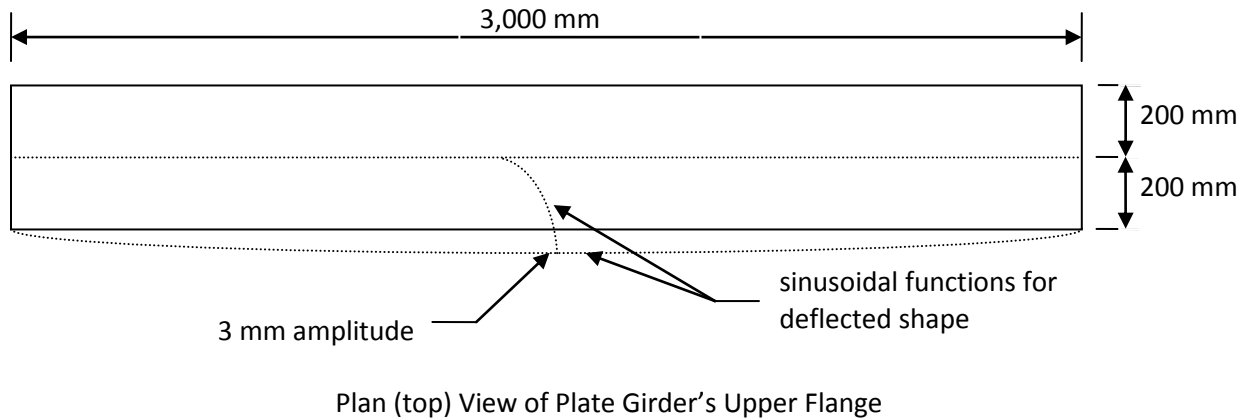


Figure 6-10: Initial Imperfection in the Top Flange of the Plate Girder for Local Buckling

The initial imperfection was introduced on one side of the girder top flange so that the flange was offset from the concrete deck by a maximum displacement of 3 mm at the mid-distance between points of shear connection. With this initial imperfection specified in the model, a finite element analysis was performed using the composite design girder with panel end connections. Local buckling was not observed with the top flange plate thickness (19 mm) of the design girder. This is consistent with the hand calculations presented at the end of this section that indicate local buckling was not expected in the top flange of this plate girder. A further observation worth noting is that the initial imperfection in the top flange of the girder had no effect on the behaviour of the composite system.

To ensure that the finite element analysis will model local buckling, an additional study was performed in which non-composite plate girders with top flanges of 6, 9, 13, and 19 mm thick were subjected to a uniformly distributed load. With the exception of the top flange thickness, the material properties and geometric layout of this non-composite girder was an exact replica of the 36 metre plate girder used in the composite section presented previously in this Chapter. The girder was loaded by applying increments of a uniform distributed load along the top flange of the girder. The full yield strength of the girder's top flange was developed for flange thicknesses of 9, 13, and 19 mm and local buckling was not observed in these simulations; however, when the flange thickness was reduced to 6 mm local buckling was observed (see Figure 6-11).

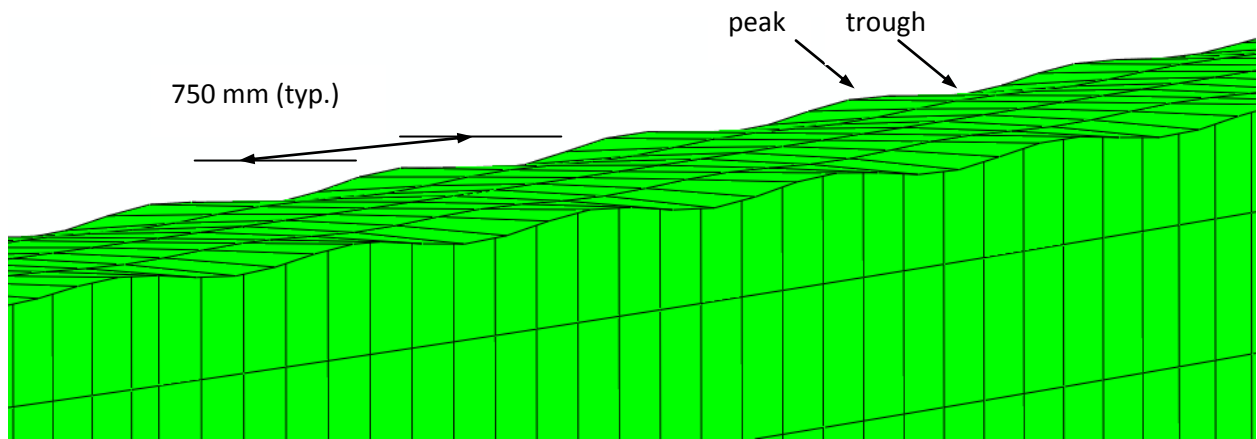


Figure 6-11: Local Buckling in Top Flange of Plate Girder

Local buckling was first identified based on the deflected shape in the top flange of the girder. The following observations regarding the buckled shape are noted: the buckled length, as identified in Figure 6-11, was consistently 750 mm; a trough in the flange on one side of the web corresponds with a trough on the alternate side; the buckled shape is facilitated by a downwards displacement at the trough (as illustrated in Figure 6-12); and upwards displacements at the peaks did not occur. To confirm the visual observation of local buckling, the local displacement between the edge, and the centre, of the top flange was plotted as a function of stress (see Figure 6-12).

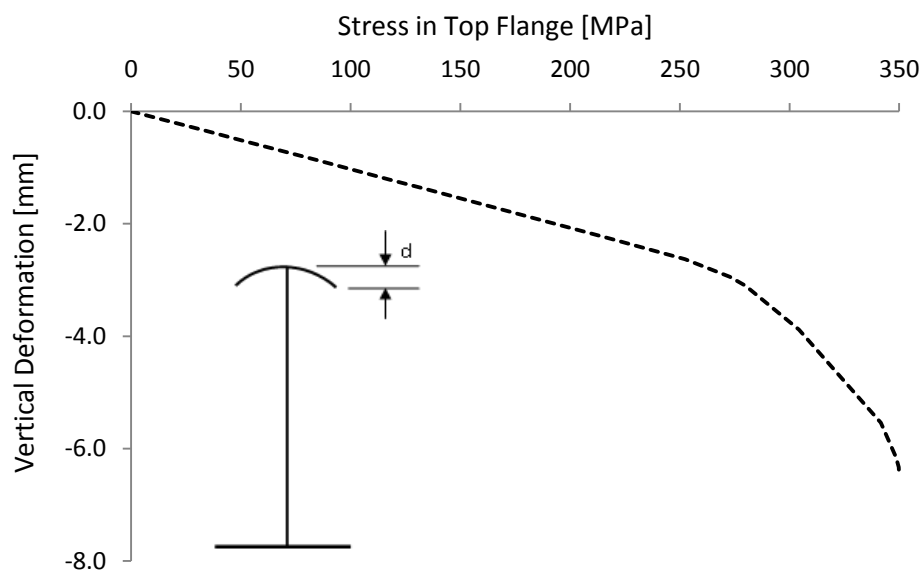


Figure 6-12: Local Displacement to Illustrate Local Buckling in Top Flange of Plate Girder

Initially, there is a small local displacement that is linearly proportional to the stress in the top flange of the girder. When the stress reaches 271 MPa, there is a sudden increase in the local displacement which corresponds with a visual observation of local buckling at this particular load increment.

Finally, a hand calculation method is presented for predicting local buckling in the compression flange of a composite plate girder with discrete shear connections. Stresses that cause local buckling of thin plates that have length to widths ratios greater the 4.0 can be predicted using Equation 6-2 [Roorda, 1988] presented in Figure 6-13.



$$\sigma_{crit} = \frac{k \cdot \pi^2 \cdot E}{12 \cdot (1 - \nu^2)} \cdot \left(\frac{t}{b}\right)^2 \quad [6-2]$$

where:

k =	0.425 (Case 1: Pin); 1.28 (Case 2: Clamp)	Buckling stress coefficient
E =	200,000 MPa	Young's modulus
ν =	0.3	Poisson's ratio
t =	refer to table	Plate thickness of top flange
b =	200 mm	Un-supported width of top flange

Figure 6-13: Critical Stress in a Steel Plate to Cause Local Buckling

Buckling stress coefficients were obtained from [Roorda, 1988], and account for the effect of plate boundary conditions. In thin plates, local buckling occurs when the critical buckling stress, predicted by Equation 6-2, is reached. If the critical buckling stress is higher than the yield strength of the plate, local buckling will not govern the capacity of the plate.

Two cases have been considered, corresponding to two different boundary conditions. In the first case, a pinned connection is assumed where the top flange connects to the web of the girder, while in the second case a clamped connection is assumed indicating that there will be no rotation of the plate along this edge. The real system will be somewhere between these two boundary conditions as the connection will be neither pinned, nor fully fixed. For both cases, the end supports were considered pinned. Table 6-4 compares the critical buckling stresses calculated with Equation 6-2 to those observed in the finite element analysis for four plate thicknesses.

Table 6-4: Critical Buckling Stresses in Top Flange of Non-Composite Plate Girder

Top Flange Thickness	Critical Buckling Stress		Stress [Abaqus FEA]	Response
	Case 1: Pin	Case 2: Clamp		
19.05 mm (3/4")	693 MPa	2,087 MPa	350 MPa	Yielding
15.875 mm (5/8")	484 MPa	1,458 MPa	350 MPa	Yielding
12.7 mm (1/2")	310 MPa	933 MPa	350 MPa	Yielding
6.35 mm (1/4")	77 MPa	232 MPa	271 MPa	Local Buckling

As thinner plates are considered the critical buckling stress decreases. With plate thicknesses of 13, 16, and 19 mm, local buckling did not occur as the top flange reached the material strength and yielded. When the finite element analysis was performed with a 6 mm thick top flange, local buckling was observed, initiating at a stress of 271 MPa. The stress in which local buckling occurred in the finite element analysis exceeded the critical buckling stress predicted using the hand calculation, which suggests that there is a greater resistance to buckling than what was predicted using Equation 6-2, even with the assumption that the flange was fully fixed along its centre where it connects to the web of the girder. To apply Equation 6-2 with better precision, buckling stress coefficients that are specific to the real boundary conditions would be required.

From the studies presented in this section it is concluded that: local buckling will not occur in the design girder; the finite element analysis is capable of modelling local buckling; and the stress in which local buckling occurs can be predicted (conservatively) using a hand calculation method.

6.3.2 Lateral Torsional Buckling

Steel girders that are unsupported along their span are vulnerable to lateral torsional buckling. In composite steel bridge construction, this mode of failure is prevented during erection by bracing two or more girders together, and it is prevented during service by the composite concrete deck slab. Two objectives are met in this section:

- First, it is demonstrated that the finite element model accurately captures the expected lateral torsional buckling response in a non-composite plate girder;
- Second, the occurrence of lateral torsional buckling between points of discrete shear connections is investigated, and the effect of lateral torsional buckling on the ultimate strength of the composite girder with panel end connections is discussed.

To demonstrate that this finite element model is capable of predicting lateral torsional buckling, a study was completed on a non-composite plate girder. Similar to the study for local flange buckling, the material properties and geometric layout of this non-composite girder were an exact replica of the 36 metre plate girder used in the composite section previously presented in this Chapter. Two different models were developed to study lateral torsional buckling; one that employed an eccentric load and another that employed an initial geometric imperfection. Each of these models is described in the following two paragraphs respectively.

In the first model, a small unbalanced load was specified, followed by the incremental application of the axle loads described in Section 6.1.4. The centre of the unbalanced load was offset from the centre of the girder by 150 mm. This initial load accounted for 0.2 percent of the elastic flexural capacity of the girder. Lateral support was provided to the girder by restricting lateral movements at the middle of the top flange (see Figure 6-14).

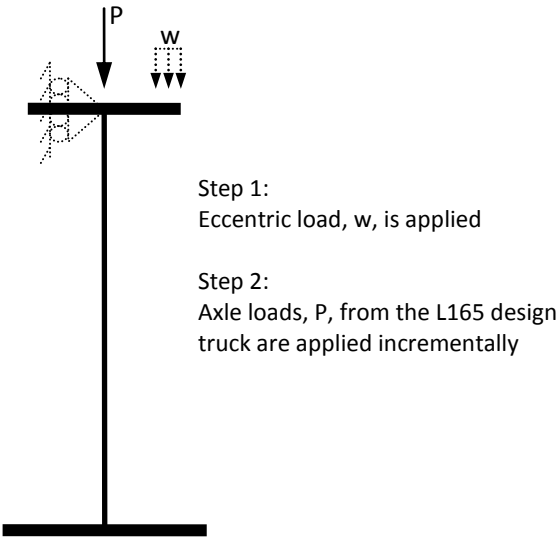


Figure 6-14: Two Step Loading for Modelling Lateral Torsional Buckling

In the second model, the eccentric load was replaced with an initial geometric imperfection. This initial lateral imperfection was specified along the entire length of the girder using a single mode sinusoidal function with the following boundary conditions: Zero lateral displacements at either ends of the girder and a maximum displacement at the girder mid-span equal to one-thousandth of the girder length (36 mm). The magnitude for this initial imperfection in the plate girder corresponds with the allowable deviation from straightness (often referred to as ‘sweep’) permitted by Clause 5.8 of [CSA W59].

In each of the two models, spaces between lateral supports corresponded with each of the roots for the girder length of 36 metres so that equal spaces between supports were provided. In total, ten independent finite element simulations were performed with each of the model and a plot of flexural resistance verses unsupported length was created (see Figure 6-15). The solid grey line and dashed black line present the results from the models using an eccentric load and initial geometric imperfection respectively.

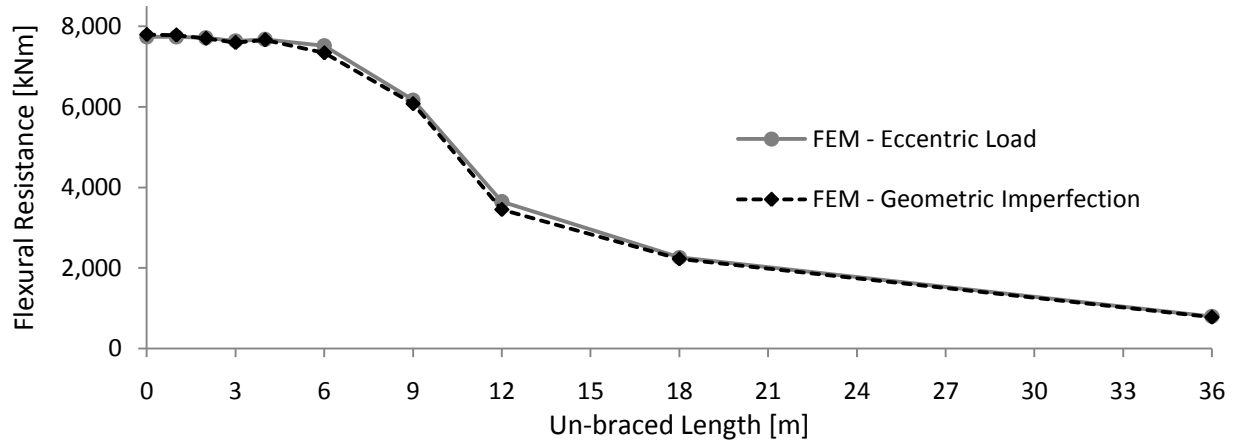


Figure 6-15: Lateral Torsional Buckling – Flexural Resistance Vs. Unsupported Length

The markers on the plot indicate the flexural resistance corresponding with each specific unsupported length. To demonstrate the trend, a linear function is assumed between each data point. The results from each of the two models are very similar and present an expected response; as the un-braced length of the girder increases, lateral torsional buckling begins to govern and there is a sudden, then gradual, decrease in flexural resistance of the girder. A minor decrease (2.1 percent) in capacity was observed between un-braced lengths of 4- and 6 metres followed by a sudden decrease (17.9 percent) between 6- and 9 metres. From these finite element analysis results, it is concluded that 6 metres represents the maximum un-braced length below which lateral torsional buckling does not govern.

The results from these finite element studies for lateral torsional buckling are compared to the calculated values determined using the lateral torsional buckling formula presented by Kulak and Grondin [2006] for a mono-symmetric girder, given by Equation 6-3.

$$M_u = \frac{\omega_2 \cdot \pi}{L_u} \cdot \left\{ \sqrt{E_s \cdot I_y \cdot G_s \cdot J} \cdot \left[B_1 + \sqrt{1 + B_2 + B_1^2} \right] \right\} \quad [6-3]$$

Where M_u is the lateral torsional buckling moment associated with a specific un-braced length, L_u . Each of the other parameters in Equation 6-3 account for material and geometric properties of the girder and are defined in Appendix F along with a worked example. This comparison is presented in Figure 6-16.

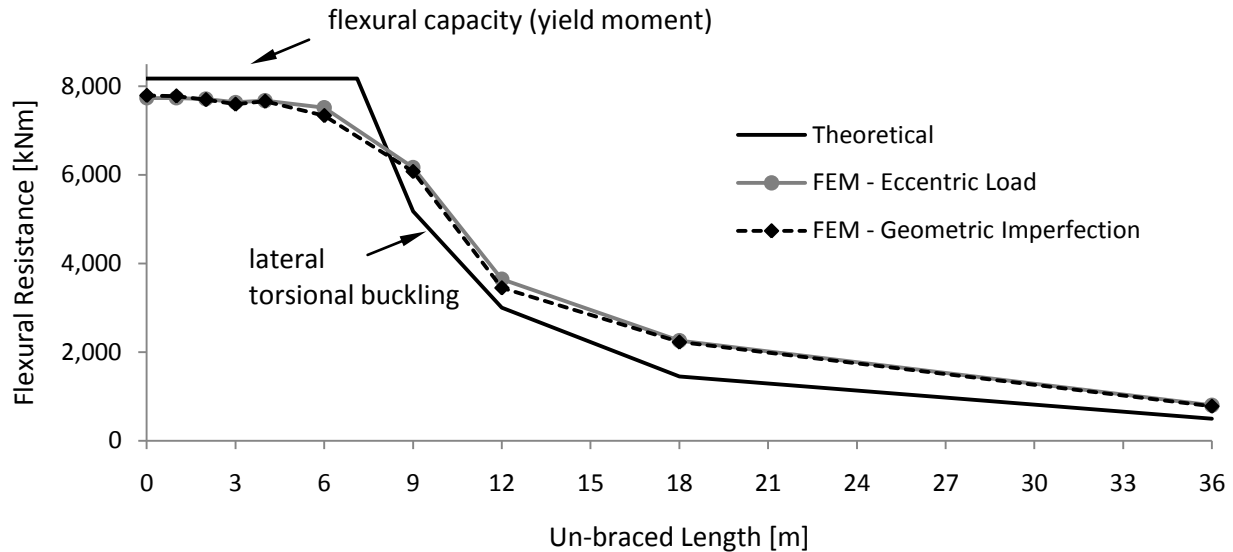


Figure 6-16: Lateral Torsional Buckling – Comparison of FEA and Calculated Results

In Figure 6-16, the theoretical plot of flexural resistance is complimented by an upper bound that is governed by the yield moment of the girder. The theoretical critical un-braced length for lateral torsional buckling is 7,107 mm. This is the length in which the lateral torsional buckling moment equals the yield moment of the girder.

In general, the same relationship between flexural resistance and un-braced length observed using finite element modelling matches the theoretical plot. A detailed study to explain the slight shift between the theoretical and FEM plots was not completed in this study; however, the following three differences between the critical un-braced length calculated using the lateral torsional buckling formula (Equation 6-3) and the critical un-braced length observed by finite element analysis includes:

- The lateral torsional buckling formula assumes that the flexural load in a girder segment results entirely from the application of end moments while in the finite element analysis the loads are applied as point loads to the top flange of the girder; however, since the ω_2 factor in Equation 6-3 is intended to compensate for this effective loading the difference between the results is likely due to one of the following two points. In this example, ω_2 was 1.0 because moments within the laterally un-braced span were larger than the end moments.

- The lateral torsional buckling formula assumes that the load is applied at the shear centre of the girder while in the finite element analysis the loads are applied at the top of the girder. Loads applied to the top of the girder would act to destabilize the structure resulting in lateral torsional buckling occurring in the model at a load less than what is predicted using the formula for a specific un-braced length. This response corresponds with the results in Figure 6-16 for un-braced lengths less than 9 metres.
- The lateral torsional buckling formula assumes that the end conditions for the un-braced section of girder are simply supported in torsion (twisting is prevented but warping of the cross-section is free to take place) while in the finite element model, the end conditions are partially restrained from warping due to continuity of the girder. This partial restraint would result in larger moments required in the model (compared to those predicted by the formula) for the initiation of lateral torsional buckling of a specific un-braced length. This response corresponds with the results in Figure 6-16 for un-braced lengths greater than 9 metres.

A factor that effects lateral torsional buckling in real girders is the presence of residual stresses. This is the reason for the empirical reduction found in Clause 10.10.2.3 of CSA S6-06 and presented below in Equation 6-4.

$$M_r = 1.15 \cdot \phi_s \cdot M_y \cdot \left[1 - \frac{0.28 \cdot M_y}{M_u} \right] \quad [6-4]$$

The maximum un-supported length in which lateral torsional buckling will not occur, based on Equation 6-4, is 4,816 mm. This length is shorter than what is observed by finite element analysis because the effect of residual stresses is not included in the finite element model. The lateral torsional buckling formula presented in Equation 6-3 is better suited for comparison of the finite element analysis results; however, the formula in Equation 6-4 better represents the expected response of a real girder.

These findings show that finite element analysis is capable of modelling lateral torsional buckling in a non-composite plate girder. Based on this conclusion, the effect of lateral torsional buckling within a composite system with discrete shear connections is investigated.

Typically, lateral torsional buckling in a composite plate girder is not considered because the relatively tight spacing of the shear studs and lateral bracing by the slab prevents the lateral torsional response of the girder. Since the shear connection that is being proposed in this thesis is designed to facilitate significantly large spaces between shear connections, there is a possibility for lateral torsional buckling

to occur in the steel plate girder between points of shear connection. The remainder of this section investigates the effect of lateral torsional buckling in the composite system provided by the proposed panel end connections. To distinguish the steel plate girder from the composite system, the section of steel plate girder between points of shear connection will be referred to as the plain girder.

When considering the effect of lateral torsional buckling, a significant observation was made. The plain girder between two composite sections can develop a yield moment that is significantly larger than that of an identical non-composite girder. A cross-section, presented in Figure 6-17, along with the following discussion, illustrates how this occurs.

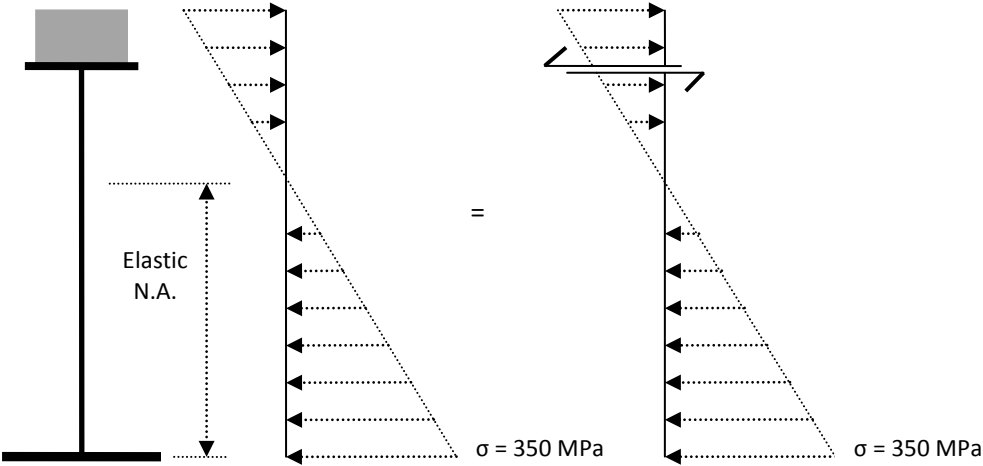


Figure 6-17: Transformed Section Analysis to Determine Moment in Plain Girder

The analysis is completed as follows; a cross-section of the composite girder is taken at a point of shear connection and full interaction between the steel girder and concrete slab is assumed. Using the properties of the transformed section, the elastic neutral axis of the composite girder is calculated. Since the connection between the steel girder and concrete slab transfers only shear stresses, the demand on the shear connection is equal to the force in the concrete slab. The elastic moment in the steel girder is then computed by summing moments resulting from the bending stresses in the steel section and the shear stress resulting from the connection on the top flange of the girder.

Calculations for this analysis are presented in Appendix F, and the resulting yield moment, M_y , in the girder is 13,971 kN·m. The significant observation is that the yield moment of the girder within the composite system (13,971 kN·m) is larger than the yield moment of the same girder in a non-composite system (8,176 kN·m). This is because of a shift of the neutral axis of the non-composite girder to that of

the composite girder. The result is that the critical un-braced length for lateral torsion buckling of the plain girder in the composite system is lower than that expected for the non-composite girder (see Figure 6-18).

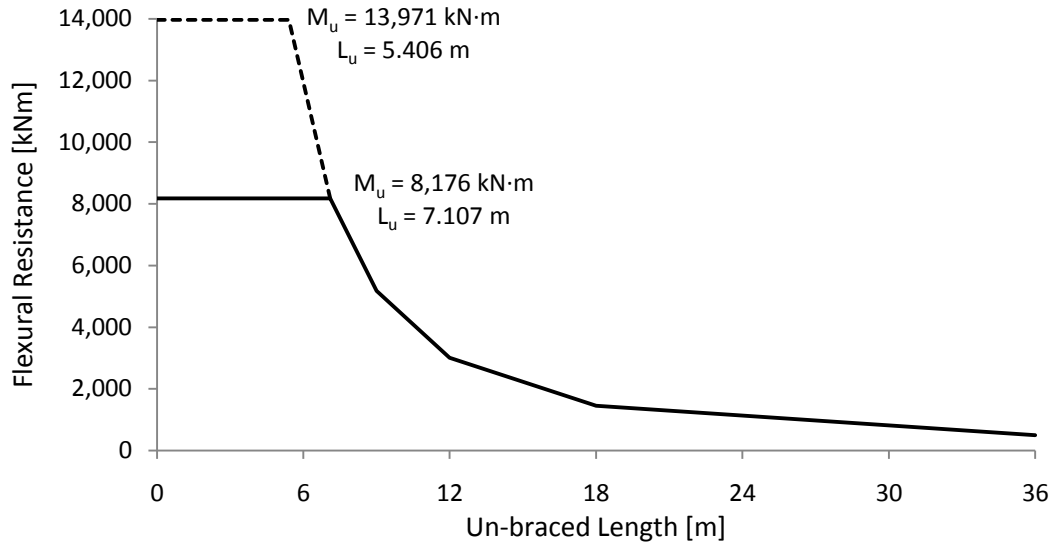


Figure 6-18: Critical Un-Braced Length of a Plate Girder within a Composite System

In the non-composite system, the yield capacity of the girder is 8,176 kN·m, corresponding with an un-braced length of 7.107 metres; however, in the composite system, the yield capacity of the girder increases to 13,971 kN·m, resulting in the critical un-braced length of the plain girder decreasing to 5.406 metres. It is important to keep in mind that the plot in Figure 6-18 is based on Equation 6-3 and does not account for the effect of residual stresses in the girder; therefore, Equation 6-4 was used to account for the effect of residual stress in the plate girder and it was found that the critical un-braced length associated with a moment resistance of 13,971 kN·m is 3.675 metres. For design of this particular composite girder with panel end connections, the critical un-braced length for the plain girder within the composite system is 3.675 metres. Since the shear connections are proposed at 3 metres on centre, lateral torsional buckling will not govern the capacity of this composite system. In addition to this theoretical approach, a finite element analysis was performed to check for lateral torsional buckling in the proposed composite girder with panel end connections spaced at 3 metres.

In this finite element analysis an initial imperfection was introduced along the length of the girder as described in the study for lateral torsional buckling in a non-composite girder and the following two modifications were introduced: the interaction constraint that specified a hard contact surface between the concrete deck and steel plate girder was removed and the axle loads were applied directly to the top

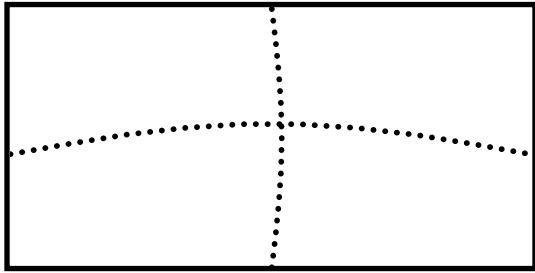
flange of the plate girder. If the hard contact surface was not removed, then it would have acted as a restraint for lateral torsional buckling. While this constraint is beneficial, and is obviously present in the real system, removing the contact restraint was chosen as a conservative approach to check for lateral torsional buckling using finite element analysis. The results of the finite element analysis confirmed that lateral torsional buckling does not occur in the composite system with panel end connections.

Based on this study of lateral torsional buckling, it is concluded: that finite element analysis predicts the expected response of lateral torsional buckling in a plate girder; that girders within a composite system can be subjected to yield moments greater than the same girder in a non-composite system and that this effect acts to reduce the critical un-braced length of the plain girder between two composite sections; and that lateral torsional buckling does not influence the response of a composite girder with the proposed panel end connections spaced at 3,000 mm on centre.

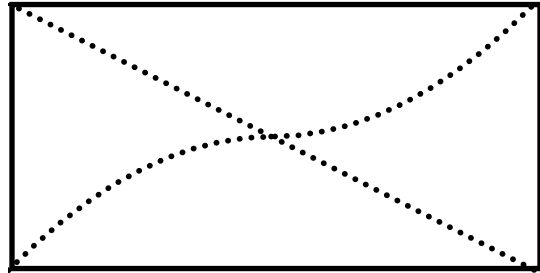
6.3.3 Stiffened Plate Girder Web Buckling

When stiffened plate girders with thin webs are subjected to large shear loads, local buckling occurs in the web and a post buckling response is initiated. With this response, a tension zone is often created within the web panel on a diagonal, and the web buckles in- and out of plane on either side of the diagonal creating double curvature as illustrated in (b) of Figure 6-19. Unlike local buckling in the compression flange and lateral torsional buckling of the plate girder, web buckling is an expected response of a thin webbed plate girder subjected to large shear stresses; therefore, the purpose of the study in this section is to show that the finite element analysis models web buckling and that the ultimate shear capacity of the girder meets, or exceeds, its expected value.

To initiate web buckling two imperfections were chosen for the web panel as shown in Figure 6-19. It has already been stated that the expected buckled shape of the web panel is the double curvature shape; however, performing independent analysis using two different shapes was performed to show that the shape of the initial imperfection does not need to match the final buckled shape.



(a) Single Curvature



(b) Double Curvature

Figure 6-19: Initial Imperfections that Cause Web Buckling in a Plate Girder

Sinusoidal functions with maximum amplitudes equal to one thousandth of the web panel length were used to define the initial imperfections. Refer to Section 5.2.3 for a detailed description of this buckled shape.

Two independent finite element analysis were performed, one using the single curvature imperfection and the other using the double curvature imperfection. To produce a large shear force in the model, the mid-point between the two rear axles of the L165 design truck were positioned at the first intermediate web stiffener. Figure 6-20 shows the post-buckled shape of the web.

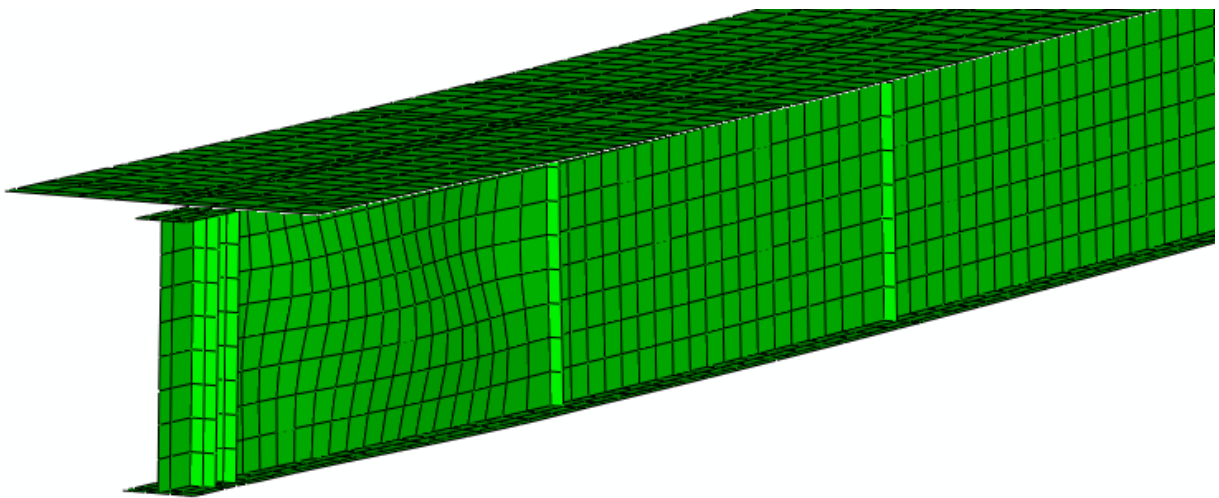


Figure 6-20: Web Buckling for Tension Field Action in a Composite Plate Girder

The results from each analysis were the same, web buckling occurs and its buckled shape presents double curvature. The axle loads used for this finite element analysis resulted in an applied shear of 3,017 kN which is larger than the unfactored shear resistance calculated in accordance with Clause 10.10.5.1 of CAN/CSA S6-06 [2006] of 2,292 kN.

Kulak and Grondin [p.189, 2006] states that thin webbed plate girders that are subject to tension field action have strengths that are significantly greater than those predicted with design formulas. One reason for this is that the tension field action enables the stiffened girder to behave like a Pratt truss and that the shear force transferred by tension field action acts in addition to that supplied by normal beam action. Clause 10.10.5.1 of CAN/CSA S6-06 [2006] states that the shear resistance resulting from tension field action in a girder web end panel should be taken as zero unless a means of anchoring the tension field action is provided. The double stiffener at the bearing location may act as a beam to anchor the tension field action; however, a detailed review for anchorage of tension field action was not within the scope of this research.

It is concluded that the finite element analysis models web buckling and that the shape of the initial imperfection does not need to match the final buckled shape. It was also observed that the post-buckled shear capacity of the girder exceeds the unfactored resistance predicted using CSA S6-06.

6.4 Parametric Study

A parametric study was performed to determine the effect of the stiffness and spacing of discrete shear connectors on the behaviour of composite girders. The finite element analysis completed for panel end connections in Section 6.2.4 was based on the properties of a specific connection designed for application in a portable composite bridge. By completing this parametric study, the sensitivity of the composite girder to its connection properties can be assessed, and the service and ultimate response of a composite bridge can be evaluated for alternate discrete connection designs.

6.4.1 Connection Stiffness

The 36 metre composite bridge girder (refer to Section 6.2), with panel end connections spaced at 3 metres on centre, was employed for this parametric study. Two objectives are met by considering a wide range of connector stiffness: first, the sensitivity of the performance of a composite girder for a portable composite bridge to the connector stiffness is evaluated; and second, a wide range of connector stiffness is considered to enable assessment of alternate discrete shear connector designs.

To perform the connection stiffness parametric study the spacing between connectors remained at a constant spacing of 3 metres and five different connectors were considered.

First, a rigid link was specified at each point of connection by replacing the 'slot + align' connectors, which are used to model finite stiffness shear connections, with 'MPC Beam' connectors. These names refer to the connection types in Abaqus 6.7. Unlike the 'slot + align' connector that facilitates relative translations between two nodes, the 'MPC Beam' connector slaves all translations and rotations between two nodes, providing a rigid link between the desired parts. The model that employed 'MPC Beam' connectors was representative of a composite system with an infinitely stiff shear connection. This infinite stiffness connection was used to set an upper bound for the overall stiffness of the composite girder. The next connector considered was the proposed panel end connection which was analyzed in Section 6.2.4. Finally, three additional finite element analysis results are plotted with connector stiffness ranging from 500,000- to 125,000 N/mm.

The results of each finite element analysis are presented by plotting mid-span deflection against applied moment (See Figure 6-21). By plotting these two parameters, the service, and ultimate limit states corresponding to each connection can be easily compared.

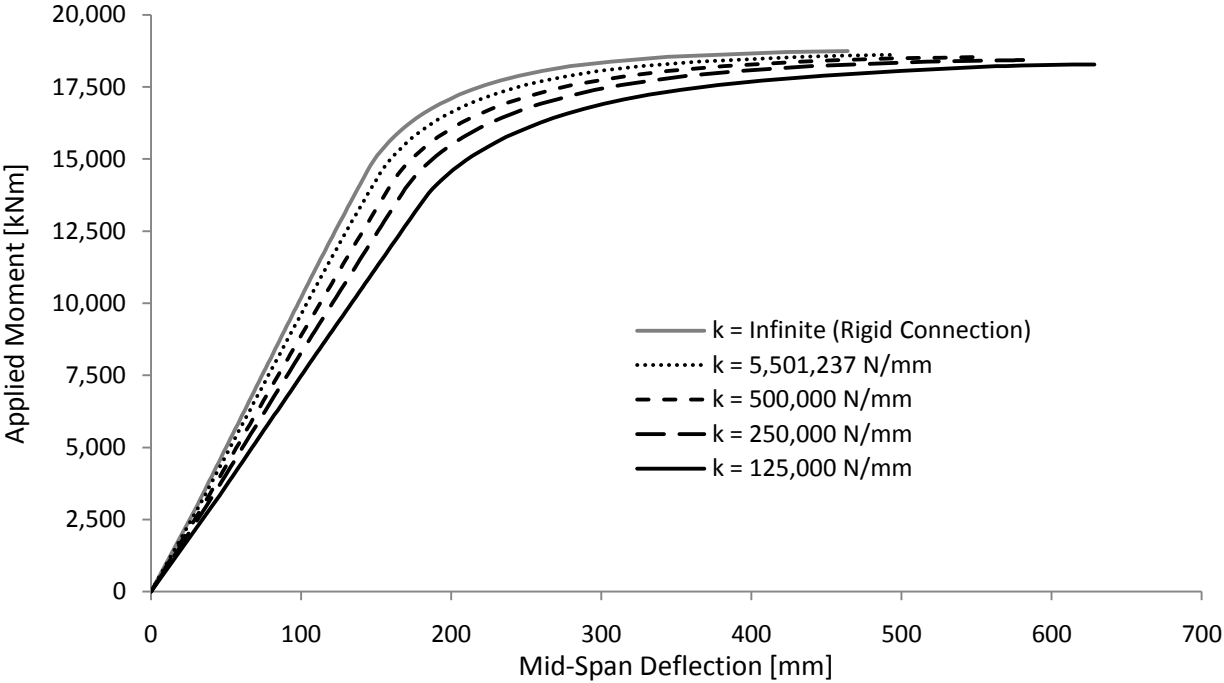


Figure 6-21: Results of Parametric Study for the Effect of Connector Stiffness

In general, the serviceability of the girder is affected by connector stiffness, but there is no significant decrease in the system's ultimate strength. The proposed panel end connection provides nearly the same response as the infinite stiffness connection, as can be observed from the overlay of the dotted black line (panel end connection) on the solid grey line (rigid connection). This illustrates that the panel end connection is sufficiently stiff that it approaches that behaviour of a rigid connection. The following discussions compare, in detail, the composite girder's service and ultimate response corresponding with each connection stiffness.

As expected, the stiffest composite girder corresponds with the rigid connection between the concrete slab and steel plate girder. As the stiffness of the shear connection decreased, the mid-span deflections of the composite system increased and the ultimate capacity decreased. This trend is a result of the following cause and effect: as the stiffness of the connection decreases, the stiffness of the composite girder decreases; as the stiffness of the girder decreases, the deflections increase; as the deflections increase, the strain in the concrete increases; and the increased strain in the concrete results in the development of the concrete's crushing strain. The result of this cause and effect is that the less stiff girder fails at a moment less than the stiff girder due to concrete crushing. Another observation is that with low stiffness connections, greater interface slip between the concrete and steel is necessary to develop the required strength in the connection. Table 6-5 summarizes the moment and mid-span deflection corresponding to the service and ultimate limit states corresponding to each connector.

Table 6-5: Comparison of Effect of Connection Stiffness on Mid-Span Girder Deflections

	Service Limit State		Ultimate Limit State	
	Moment	Deflection	Moment	Deflection
k = Infinite	9,581 kN·m	98 mm	18,601 kN·m	464 mm
k = 5,501,237 N/mm	9,581 kN·m	99 mm	18,612 kN·m	492 mm
k = 500,000 N/mm	9,581 kN·m	103 mm	18,430 kN·m	554 mm
k = 250,000 N/mm	9,581 kN·m	108 mm	18,281 kN·m	581 mm
k = 125,000 N/mm	9,581 kN·m	116 mm	17,961 kN·m	629 mm

The service limit state corresponds with the moment resulting from the dead load plus the L165 axle load. On average, approximately 35 mm of the deflections reported in Table 6-5 result from dead load. It is also noted that the mid-span service deflection associated with the composite girder with shear

studs was 92 mm, only 7 mm less than what is observed with the proposed panel end connection composite system.

All five girders developed a plastic response prior to reaching their ultimate limit state. The ultimate capacity decreased from 18,601 kN·m to 17,961 kN·m (3.4 percent) in the $k = \text{Infinite}$ to $k = 125,000$ N/mm cases while the ultimate deflection increased by 35 percent. The final observation noted is that the stiffness must decrease by a factor of ten, from the stiffness assumed for the panel end connection, before a noticeable difference in the performance of the composite girder is realized.

From this parametric study it is concluded; that the actual stiffness of the panel end connector could decrease from its calculated stiffness by a factor of ten with minimal impact on the performance of the composite girder; that the increase in mid-span service deflection of the composite system with the proposed panel end connection is 7.6 percent (7 mm) larger than a composite girder with shear studs; and that there is a 3.4 percent decrease in strength accompanied by a 35 percent increase in deflections between the composite system composed with the infinitely stiff connection and the $k=125,000$ N/mm connection at the ultimate limit state.

6.4.2 Connection Spacing

This parametric study on connection spacing is independent of effects resulting from flange buckling or lateral torsional buckling. It was already demonstrated in Section 6.3.1 that the stress required for local buckling in the top flange of the girder greatly exceeds the yield strength of the steel, so local buckling of the top flange will not occur; however, in Section 6.3.2 it was demonstrated that lateral torsional buckling could occur in this finite element model when the connection spacing meets, or exceeds, 5.406 metres. Since lateral torsional buckling can be easily prevented by bracing the top flange of the girder, the initial imperfections that trigger lateral torsion buckling have been removed from the models in this parametric study and lateral supports, representative of steel cross-bracing, are provided to the upper and lower flange at each stiffener location.

Four finite element simulations were performed to compare the effect of connectors spaced at 3, 6, 9, and 12 metres. In reality, the connector associated with each connector spacing would have unique properties; however, based on the results of the connection stiffness parametric study, it was concluded that the stiffness of the as-designed connector produces a response nearly identical to that of a rigid connection. So, to study the effects of connector spacing, independent of the connector stiffness, a rigid

link is used to provide the shear connection. The results of these simulations are presented in the form of mid-span girder displacement as a function of applied moment (see Figure 6-22).

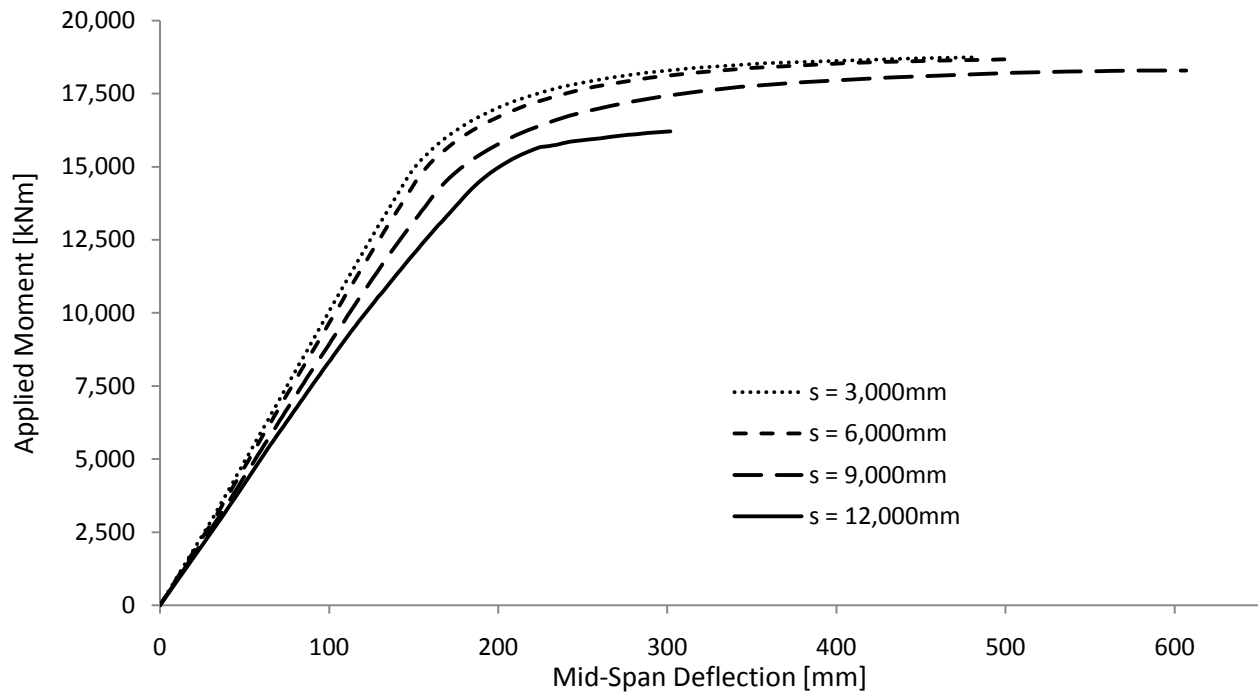


Figure 6-22: Results of Parametric Study for the Effect of Connector Spacing

The general response of the composite system with discrete shear connectors spaced at 3, 6, and 9 metres followed a similar trend to that observed in the connector stiffness parametric study with the difference being that the stiffness of the girder is influenced by the connector spacing, not the connector stiffness. From Figure 6-22, it is observed that as that spacing between shear connections increased, girder deflections increased and the ultimate capacity decreased. This observation indicates that the overall stiffness of the composite girder decreases and the connector spacing increases. The simulation for the 12 metre connection spacing did not follow this trend because local buckling occurred in the web (near the second intermediate stiffener) at a distance of approximately 9 metres from the support. Stiffeners were spaced at approximately 4 metres on centre. This local buckling presented a double curvature deflection similar to that observed for tension field action in Section 6.3.3.

This parametric study on connection spacing was based on the assumption that the discrete shear connection would provide a response similar to that of an infinitely stiff connection, as observed in the proposed panel end shear connection designed for a 3 metre connector spacing. To confirm if this response is similar for other connections spaced further than 3 metres on centre, a simulation of the 9

metre connector spacing was repeated with a finite stiffness shear connection ($k = 5,501,237 \text{ N/mm}$) and it was found that the ultimate capacity was almost identical (within 0.1 percent) of that observed with an infinite stiffness connection.

The results of this study on connector spacing suggests that the difference in performance between a connection spacing of 3 metres, to that of 6 metres, would be minor. A 6 metre discrete shear connection spacing in a composite girder may advantageous in some applications; however, the results of this parametric study does not change the proposed panel end connection spacing of 3 metres for a portable composite bridge. The primary reason for this is that the maximum length of pre-cast concrete deck panels in Western Canada typically do not exceed 3 metres because of legal highway load restrictions. Another difficulty that may accompany a composite girder designed with discrete shear connections that are spaced at 6 metres on center is the detailing required for the connection. Since the demand on the shear connection is proportional to the spacing between connections, the shear force that would need to be transferred with a shear connection spaced at 6 metres would twice what was required of the 3 metre connection spacing.

7 CONCLUSIONS

This research has proposed a shear connection that can be used to facilitate a portable composite bridge consisting of steel plate girders with precast concrete deck panels. The connection is facilitated by bolting a steel embed assembly, that is cast into the deck panels, to gusseted steel bearing plates that are welded to the top flange of the girder during fabrication. Points of shear connection in the proposed composite system correspond to a typical precast panel length of three metres. The research summary provides a brief overview of the key components in this study followed by a concise report of the significant findings and recommendations for future work.

7.1 Research Summary

Initially, ten shear connection concepts were developed and a detailed evaluation of each concept was performed by considering the expected performance, function, and economy of a portable composite bridge that incorporated each connection respectively. The results of these evaluations were applied for a multi-criteria assessment of the ten concepts. Based on the outcome of this assessment, and subsequent sensitivity analysis, a preferred connection concept was chosen.

The next component of this research was a study of the overall structural response of composite girders using finite element analysis. To establish the finite element model, an initial study was performed using the results of a laboratory experiment by Mans et al. [2001]. This initial study was conducted to validate the finite element model. A subsequent study modelled a 36 metre long composite bridge girder with regularly spaced shear studs so that a benchmark for evaluating the performance of a composite girder with the proposed shear connection could be established.

Finally, a composite girder with the proposed shear connection was modelled and its response was evaluated. Local effects considered in the finite element analysis included: buckling of the girder flanges; lateral torsional buckling between points of shear connection; and web buckling. This research concluded with a parametric study in which the response of the composite girder due to various connection stiffness and spacing was considered.

7.2 Significant Findings

The result of the multi-criteria assessment indicated that two shear connection details showed nearly equal potential for enabling a portable composite bridge. The first concept consisted of a bolted connection between the top flange of the plate girder and a steel plate embedded in the soffit of the precast concrete deck panels. The second concept, which became the focus of the subsequent research, consisted of a bolted connection between a steel embed assembly (cast into the deck panels) and gusseted steel bearing plates that are welded to the top flange of the girder. The subsequent finite element analysis work focused on the second concept because it is expected that the first connection could be designed with little added benefit gained through additional applied research.

Several benefits would accompany a composite bridge that employs the proposed shear connection: Precast concrete deck panels can be easily installed, and removed, which enables a portable composite structure; field grout is not required, which will accelerate the installation of deck panels, provide full composite action immediately following construction, and eliminate the need for heating and hording that is otherwise required during sub-zero temperatures. Also, the ability to facilitate rapid bridge installations could make this proposed composite system attractive for permanent structures where accelerated construction is required.

The finite element analyses performed in this study confirmed that finite element models can accurately predict the service and ultimate response of a composite plate girder. In particular, the finite element model of the laboratory experiment by Mans et al. [2001] showed excellent agreement with the reported experimental results. It was also demonstrated that finite element analysis captures local effects including flange buckling, lateral torsional buckling, and web buckling.

Next, a composite girder with the proposed shear connection was modelled and the overall response of the girder was evaluated. A reference to assist with the evaluation of the proposed composite system was provided by modelling a composite girder with a regular shear stud connection. It was found that the proposed shear connection provided a very similar response to the composite girder with regular shear studs as follows: at the ultimate limit state the flexural capacity and deflection agreed within 1.0 and 5.1 percent respectively, while the service deflection of the proposed composite system was 7.6 percent larger than that of the shear stud composite girder. Both girders exhibited the same failure mode which consisted of concrete crushing at the girder mid-span.

Finally, a parametric study was completed to determine the sensitivity of the composite girder to variations in the spacing of the shear connections and the connector stiffness. The results of this study showed that each examined connector stiffness, within one order of magnitude of the proposed connection stiffness, provided equivalent ultimate capacities in the composite system; however, service deflections increased as the connector stiffness decreased. The proposed connection spacing of 3,000 mm, as well as a connection spacing of 6,000 mm, provided a very similar response to a conventional composite system with shear studs spaced every 250 mm.

The two most significant findings include: the proposed shear connection for a portable composite bridge provided a structural response that was nearly equivalent to that provided with conventional shear studs; and a composite bridge with the proposed shear connection was shown to be constructible in terms of shop fabrication and field erection.

7.3 Recommendations

Based on the results of this research, the following recommendations are made to support future developments for a portable composite bridge:

- Complete a detailed market assessment for the proposed portable composite bridge system. This assessment should also explore the possibility of employing the proposed composite bridge system for rapid bridge installation projects.
- Perform a feasibility study of the proposed fabrication method for the steel plate girders and precast concrete deck panels with particular attention to the connection details and the potential influence of fabrication errors on the construction sequence.
- Apply the findings of the market assessment and feasibility study to estimate the life cycle cost of the proposed portable composite bridge.
- Develop a refined finite element model to study the local-behaviour of the proposed shear connection as well as the interaction between the steel embed assemblies and the precast concrete deck panels.
- Test full scale specimens employing the proposed shear connection and compare the experimental findings to the results of the refined finite element analysis.
- Model the contact surfaces between precast concrete deck panels and quantify the effect of geometric imperfections along the contact surfaces of adjacent deck panels.

APPENDIX A: BC MOF DRAWING FOR L165 COMPOSITE DECK PANEL

APPENDIX B: CONNECTION DESIGN CALCULATIONS

Section 4.1 Design Load and Bridge Geometry

Total factored force, P, to be transferred by shear connectors:

$$P = 0.85\varphi_c f'_c b_e t_c + \varphi_r A_r f_y = 15,237 \text{ kN} \quad \text{CSA S6-06 Clause 10.11.8.3 (a)}$$

where:

$$\varphi_c = 0.75 \quad \text{CSA S6-06 Clause 8.4.6}$$

$$f'_c = 35 \text{ MPa} \quad \text{STD - E - 030 -31}$$

$$b_e = 2,438 \text{ mm} \quad \text{STD - E - 030 -31}$$

$$t_c = 225 \text{ mm} \quad \text{STD - E - 030 -31}$$

$$\varphi_r = 0.95 \quad \text{CSA S6-06 Clause 8.4.6}$$

$$A_r = 4,550 \text{ mm}^2 \quad \text{STD - E - 030 -31}$$

$$f_y = 400 \text{ MPa}$$

$$\text{Shear Flow} = \frac{15,237 \text{ kN}}{18\text{m}} = 847 \text{ kN/m per girder}$$

Section 4.3.1 Threaded Concrete Insert

Interface shear resistance, V_r :

$$V_r = \phi_c (c + \mu \sigma) = 1.96 \text{ MPa} \quad \text{CSA S6-06 Clause 8.9.5.1}$$

where:

$$\sigma = \rho_v f_y + \frac{N}{A_{cv}} = 4.348 \text{ MPa}$$

$$\frac{N}{A_{cv}} = 0$$

$$\rho_v = \frac{A_{vf}}{A_{cv}} = 0.01087$$

$$A_{vf} = 5,000 \text{ mm}^2 \text{ per m} \quad \text{2 - 25M bars @ 200 mm o/c}$$

$$A_{cv} = 460 \text{ mm} \times 1000 \text{ mm per m}$$

$$f_y = 400 \text{ MPa}$$

$$c = 0.00 \text{ MPa} \quad \text{CSA A23.3-04 Clause 11.5.2 (d)}$$

$$\mu = 0.60 \quad \text{CSA A23.3-04 Clause 11.5.2 (d)}$$

$$\phi_c = 0.75 \quad \text{CSA S6-06 Clause 8.4.6}$$

Demand:

$$V = 847 \frac{\text{kN}}{\text{m}} \times 1\text{m} \times \frac{1}{460\text{mm} \times 1,000\text{mm}} = 1.84 \text{ MPa}$$

Design Summary:

$$V_r = 1.96 \text{ MPa} \quad > \quad V = 1.84 \text{ MPa}$$

Specify:

2 - 25M bars @ 200mm o/c per girder with 25Ø Burrard Couplers (or equivalent) to fasten 1"Ø A325 bolts to 25M bars

Section 4.3.2 Post Installed Connection

Interface shear resistance, V_r :

$$V_r = \phi_c (c + \pi \sigma) = 1.94 \text{ MPa} \quad \text{CSA S6-06 Clause 8.9.5.1}$$

where:

$$\sigma = \rho_v f_y + \frac{N}{A_{cv}} = 4.31 \text{ MPa}$$

$$\frac{N}{A_{cv}} = 0$$

$$\rho_v = \frac{A_{vf}}{A_{cv}} = 0.0082$$

$$A_{vf} = 3,778 \text{ mm}^2 \text{ per m} \quad 2 - \frac{3}{4}'' \text{Ø Hilti Kwik-Bolts @ 150 mm o/c}$$

$$A_{cv} = 460 \text{ mm} \times 1000 \text{ mm per m}$$

$$f_y = 525 \text{ MPa}$$

$$c = 0.00 \text{ MPa} \quad \text{CSA A23.3-04 Clause 11.5.2 (d)}$$

$$\mu = 0.60 \quad \text{CSA A23.3-04 Clause 11.5.2 (d)}$$

$$\phi_c = 0.75 \quad \text{CSA S6-06 Clause 8.4.6}$$

Demand:

$$V = 847 \frac{\text{kN}}{\text{m}} \times 1\text{m} \times \frac{1}{460\text{mm} \times 1,000\text{mm}} = 1.84 \text{ MPa}$$

Design Summary:

$$V_r = 1.94 \text{ MPa} \quad > \quad V = 1.84 \text{ MPa}$$

Specify:

2 - $\frac{3}{4}''$ Ø Hilti Kwik-Bolts @ 150 mm o/c per girder

Section 4.3.3 Impression Cast Deck with Concrete Insert

Interface shear resistance, V_r :

$$V_r = \phi_c (c + \pi \sigma) = 2.58 \text{ MPa} \quad \text{CSA S6-06 Clause 8.9.5.1}$$

where:

$$\sigma = \rho_v f_y + \frac{N}{A_{cv}} = 1.739 \text{ MPa}$$

$$\frac{N}{A_{cv}} = 0$$

$$\rho_v = \frac{A_{vf}}{A_{cv}} = \frac{2,000\text{mm}^2}{460\text{mm} \times 1000\text{mm}} \quad \text{2-25M bars @ 500mm o/c per metre}$$

$$f_y = 400 \text{ MPa}$$

$$c = 1.00 \text{ MPa} \quad \text{CSA S6-06 Clause 8.9.5.2.1 (c)}$$

$$\mu = 1.4 \quad \text{CSA S6-06 Clause 8.9.5.2.1 (c)}$$

$$\phi_c = 0.75 \quad \text{CSA S6-06 Clause 8.4.6}$$

Resistance of 450mm x 100mm x 19mm steel tab:

weld: CSA S6-06 Clause 10.18.3

$$V_r = 0.67 \phi_w A_m F_u = 1,293 \text{ N/mm} \quad \text{resistance of base metal (top flange of girder)}$$

$$V_r = 0.67 \phi_w A_w X_u (1 + 0.5 \sin \theta) = 1,400 \text{ N/mm} \quad \text{resistance of steel tab when } \theta = 90^\circ$$

$$V_r = 0.67 \phi_w A_w X_u (1 + 0.5 \sin \theta) = 933 \text{ N/mm} \quad \text{resistance of steel tab when } \theta = 0^\circ$$

where:

$$\phi_w = 0.67$$

$$A_m = 6\text{mm}$$

$$A_w = 0.707 \times 6\text{mm}$$

$$F_u = 480 \text{ MPa}$$

$$X_u = 490 \text{ MPa}$$

... *continued*

continued...

$$V_r = (450\text{mm} + 450\text{mm})1,293\text{N/mm} + (100\text{mm} + 100\text{mm})933\text{ N/mm} = 1,350\text{ kN per tab}$$

$$V_r = 1,350 \frac{\text{kN}}{\text{tab}} \times \frac{2\text{tabs}}{\text{m}} = 2,700\text{ kN/m} \quad \text{total shear resistance of steel tab}$$

Stress in Concrete:

$$\text{Bearing Stress} = 847,000 \frac{\text{N}}{\text{m}} \times \frac{\text{m}}{2\text{ tabs}} \times \frac{1}{450\text{mm} \times 19\text{mm}} = 50\text{ MPa}$$

Concrete is tri-axially confined at location of maximum bearing stress; therefore, exceeding the specified cylinder strength of 35 MPa is acceptable

Design Summary:

$$V_r = 2.58\text{ MPa} > V = 1.84\text{ MPa}$$

$$V_r = 2,700\text{ kN/m} > V = 847\text{ kN/m}$$

Specify:

2 -25M bars @ 500 mm o/c per girder with 25Ø Burrard couplers (or equivalent) to fasten 1"Ø A325 bolts to 25M reinforcing bars
450 mm x 100 mm x 19 mm Plate tabs welded to top flange with 6mm weld all-round @ 500 mm o/c

Section 4.3.4 Through Bolt with Steel to Steel Contact

Slip resistance of a bolted connection, V_s :

$$V_s = 0.53c_1k_s m n A_b F_u = 99.8 \text{ kN per each } 1" \text{ } \varnothing \text{ Bolt} \quad \text{CSA S6-06 Clause 10.18.2.3.2}$$

where:

$$c_1 = 0.90 \quad \text{Class B}$$

$$k_s = 0.50 \quad \text{Class B}$$

$$m = 1 \quad \text{Shear surface}$$

$$n = 1 \quad \text{Bolt}$$

$$A_b = 507 \text{ mm}^2 \quad 1" \varnothing \text{ Bolt}$$

$$F_u = 825 \text{ MPa}$$

Note: If steel pipe pockets are spaced at 1 m o/c, then each location must resist 847 kN

$$V_s = 9 \text{ bolts} \times 99.8 \frac{\text{kN}}{\text{bolt}} = 892 \text{ kN} > 847 \text{ kN}$$

Steel Pipe Embed:

CSA S6-06 Clause 10.5.7

$$\text{Resistance} = \varphi_s \sigma_s A_s = 1,026 \text{ kN} > 847 \text{ kN}$$

where:

$$\varphi_s = 0.9$$

$$\sigma_s = 300 \text{ MPa}$$

$$A_s = 200 \text{ mm} \times 9.5 \text{ mm} \times 2 \text{ sides}$$

Steel plate (1/2" thick) welded to bottom of pipe:

6mm weld, assume $\theta = 0^\circ$, $V_r = 933 \text{ kN/mm}$

$$V_r = 305 \text{ mm} \pi 922 \text{ N/mm} = 893 \text{ kN} > 847 \text{ kN}$$

Section 4.3.5 Through Bolts with Concrete to Steel Contact

Interface shear resistance, V_r :

$$V_r = \phi_c (c + \pi\sigma) = 2.09 \text{ MPa} \quad \text{CSA S6-06 Clause 8.9.5.1}$$

where:

$$\sigma = \rho_v f_y + \frac{N}{A_{cv}} = 4.64 \text{ MPa}$$

$$\frac{N}{A_{cv}} = 0$$

$$\rho_v = \frac{A_{vf}}{A_{cv}} = 0.0056$$

$$A_{vf} = 2,585 \text{ mm}^2 \text{ per m} \quad 2 - 7/8" \text{ } \emptyset \text{ A325 bolts @ 300 mm o/c}$$

$$A_{cv} = 460 \text{ mm} \times 1000 \text{ mm per m}$$

$$f_y = 825 \text{ MPa} \quad \text{A325 Bolt}$$

$$c = 0.00 \text{ MPa} \quad \text{CSA A23.3-04 Clause 11.5.2 (d)}$$

$$\mu = 0.60 \quad \text{CSA A23.3-04 Clause 11.5.2 (d)}$$

$$\phi_c = 0.75 \quad \text{CSA S6-06 Clause 8.4.6}$$

Demand:

$$V = 847 \frac{\text{kN}}{\text{m}} \times 1\text{m} \times \frac{1}{460\text{mm} \times 1,000\text{mm}} = 1.84 \text{ MPa}$$

Design Summary:

$$V_r = 2.09 \text{ MPa} \quad > \quad V = 1.84 \text{ MPa}$$

Specify:

2 - 7/8" \emptyset A325 through bolts @ 300 mm o/c per girder

Section 4.3.6. Impression Cast with Through Bolts

Interface shear resistance, V_r :

$$V_r = \phi_c (c + \mu \sigma) = 3.67 \text{ MPa} \quad \text{CSA S6-06 Clause 8.9.5.1}$$

where:

$$\sigma = \rho_v f_y + \frac{N}{A_{cv}} = 2.78 \text{ MPa}$$

$$\frac{N}{A_{cv}} = 0$$

$$\rho_v = \frac{A_{vf}}{A_{cv}} = 0.0034$$

$$A_{vf} = 1,550 \text{ mm}^2 \text{ per m} \quad 2 - 7/8" \text{ } \emptyset \text{ A325 bolts @ 500 mm o/c}$$

$$A_{cv} = 460 \text{ mm} \times 1000 \text{ mm per m}$$

$$f_y = 825 \text{ MPa} \quad \text{A325 Bolt}$$

$$c = 0.00 \text{ MPa} \quad \text{CSA A23.3-04 Clause 11.5.2 (d)}$$

$$\mu = 1.4 \quad \text{CSA A23.3-04 Clause 11.5.2 (d)}$$

$$\phi_c = 0.75 \quad \text{CSA S6-06 Clause 8.4.6}$$

Demand:

$$V = 847 \frac{\text{kN}}{\text{m}} \times 1\text{m} \times \frac{1}{460\text{mm} \times 1,000\text{mm}} = 1.84 \text{ MPa}$$

Design Summary:

$$V_r = 3.67 \text{ MPa} \quad > \quad V = 1.84 \text{ MPa}$$

Specify:

2 - 7/8" \emptyset A325 through bolts @ 500 mm o/c per girder with

450 mm x 100 mm x 19 mm steel plate tabs (6mm weld) at 500 mm o/c

Section 4.3.7 Continuous Embed with Ductile Shear Studs

Slip resistance of a bolted connection, V_s :

$$V_s = 0.53c_1k_s m n A_b F_u = 99.8 \text{ kN per each } 1" \text{ } \emptyset \text{ Bolt} \quad \text{CSA S6-06 Clause 10.18.2.3.2}$$

where:

$$c_1 = 0.90 \quad \text{Class B}$$

$$k_s = 0.50 \quad \text{Class B}$$

$$m = 1 \quad \text{Shear surface}$$

$$n = 1 \quad \text{Bolt}$$

$$A_b = 507 \text{ mm}^2 \quad 1" \emptyset \text{ Bolt}$$

$$F_u = 825 \text{ MPa}$$

$$\text{spacing} = \frac{99.8 \text{ kN}}{847 \text{ kN/m}} \times \frac{2 \text{ bolts}}{\text{per location}} = 0.235 \text{ m} \quad \text{Bolts spaced at } 200 \text{ mm o/c}$$

Resistance of a shear stud:

CSA S6-06 Clause 10.11.8

$$q_r = 0.5 \varphi_{sc} A_{sc} \sqrt{f'_c E_c} \leq \varphi_{sc} F_u A_{sc} = 135 \text{ kN}$$

where:

$$\varphi_{sc} = 0.85$$

CSA S6-06 Clause 10.5.7

$$A_{sc} = 388 \text{ mm}^2$$

7/8" \emptyset Shear Stud

$$f'_c = 35 \text{ MPa}$$

$$E_c = (3,000 \sqrt{f'_c} + 6,900) \left(\frac{\gamma_c}{2,300} \right)^{1.5} = 24,648 \text{ MPa}$$

$$F_u = 410 \text{ MPa}$$

$$\text{spacing} = \frac{135 \text{ kN}}{847 \text{ kN/m}} \times \frac{2 \text{ studs}}{\text{per location}} = 0.318 \text{ m} \quad \text{Studs spaced at } 300 \text{ mm o/c}$$

Steel Plate for Embed:

3,000 mm x 125 mm x 16 mm

Section 4.3.8 Discrete Embed Bolted to Flange

Resistance of a shear stud:

CSA S6-06 Clause 10.11.8

$$q_r = 0.5 \varphi_{sc} A_{sc} \sqrt{f'_c E_c} \leq \varphi_{sc} F_u A_{sc} = 135 \text{ kN}$$

where:

$$\varphi_{sc} = 0.85 \quad \text{CSA S6-06 Clause 10.5.7}$$

$$A_{sc} = 388 \text{ mm}^2 \quad 7/8" \text{ } \emptyset \text{ Shear Stud}$$

$$f'_c = 35 \text{ MPa}$$

$$E_c = (3,000 \sqrt{f'_c} + 6,900) \left(\frac{\gamma_c}{2,300} \right)^{1.5} = 24,648 \text{ MPa}$$

$$F_u = 410 \text{ MPa}$$

$$N = \frac{847 \text{ kN}}{135 \text{ kN/stud}} = 7 \text{ studs per connection}$$

Resistance of weld:

CSA S6-06 Clause 10.18.3

$$V_r = 0.67 \varphi_w A_m F_u = 1,724 \text{ N/mm}$$

resistance of base metal (top flange of girder)

$$V_r = 0.67 \varphi_w A_w X_u (1 + 0.5 \sin \theta) = 1,866 \text{ N/mm}$$

resistance of steel tab when $\theta = 90^\circ$

$$V_r = 0.67 \varphi_w A_w X_u (1 + 0.5 \sin \theta) = 1,244 \text{ N/mm}$$

resistance of steel tab when $\theta = 0^\circ$

where:

$$\varphi_w = 0.67$$

$$A_m = 8 \text{ mm}$$

$$A_w = 0.707 \times 8 \text{ mm}$$

$$F_u = 480 \text{ MPa}$$

$$X_u = 490 \text{ MPa}$$

$$V_r = (300 \text{ mm} + 300 \text{ mm}) 1,724 \text{ N/mm} + (50 \text{ mm} + 50 \text{ mm}) 1,244 \text{ N/mm} = 1,158 \text{ kN}$$

Bearing Stress for Grout:

$$\sigma = \frac{847,000 \text{ N}}{300 \text{ mm} \times 19 \text{ mm}} = 149 \text{ MPa}$$

Section 4.3.9 Discrete Embed Bolted to Web

Resistance of a shear stud:

CSA S6-06 Clause 10.11.8

$$q_r = 0.5 \varphi_{sc} A_{sc} \sqrt{f'_c E_c} \leq \varphi_{sc} F_u A_{sc} = 135 \text{ kN}$$

where:

$$\varphi_{sc} = 0.85 \quad \text{CSA S6-06 Clause 10.5.7}$$

$$A_{sc} = 388 \text{ mm}^2 \quad 7/8" \text{ } \emptyset \text{ Shear Stud}$$

$$f'_c = 35 \text{ MPa}$$

$$E_c = (3,000 \sqrt{f'_c} + 6,900) \left(\frac{\gamma_c}{2,300} \right)^{1.5} = 24,648 \text{ MPa}$$

$$F_u = 410 \text{ MPa}$$

$$N = \frac{847 \text{ kN}}{135 \text{ kN/stud}} = 7 \text{ studs per connection}$$

Resistance of weld:

CSA S6-06 Clause 10.18.3

$$V_r = 0.67 \varphi_w A_w X_u (1 + 0.5 \sin \theta) = 1,244 \text{ N/mm}$$

$$V_r = (350 \text{ mm} + 350 \text{ mm}) 1,244 \text{ N/mm} = 870 \text{ kN} > 847 \text{ kN}$$

Slip resistance of a bolted connection, V_s :

$$V_s = 0.53 c_1 k_s m n A_b F_u = 152 \text{ kN per each } 7/8" \emptyset \text{ Bolt} \quad \text{CSA S6-06 Clause 10.18.2.3.2}$$

where:

$$c_1 = 0.90 \quad \text{Class B}$$

$$k_s = 0.50 \quad \text{Class B}$$

$$m = 2 \quad \text{Shear surfaces}$$

$$n = 1 \quad \text{Bolt}$$

$$A_b = 388 \text{ mm}^2 \quad 7/8" \emptyset \text{ Bolt}$$

$$F_u = 825 \text{ MPa}$$

$$N = \frac{847 \text{ kN}}{152 \text{ kN/bolt}} = 6 \text{ bolts per connection}$$

Section 4.3.10 Panel End Connection

Stud Spacing:

$$q_r = 135 \text{ kN per } 7/8" \text{ } \phi \text{ stud}$$

CSA S6-06 Clause 10.5.7

$$s = \frac{135 \text{ kN}}{\text{stud}} \times 2 \text{ studs} \times \frac{1}{847 \text{ kN/m}} = 0.319 \text{ m}$$

2 - 7/8" ϕ studs at 300mm o/c

Steel Angel:

$$\text{L127 x 127 x 13} \quad \text{Area} = 3,060 \text{ mm}^2$$

$$\text{Resistance of Angle} = \phi_s A_g F_y$$

$$\phi_s = 0.90 \quad \text{Compression}$$

$$\phi_s = 0.95 \quad \text{Tension}$$

$$\text{Resistance of Angle} = 0.9 \times 3,060 \text{ mm}^2 \times 300 \text{ MPa} = 826 \text{ kN}$$

$$\text{Maximum Load per Angle} = \frac{847 \text{ kN}}{\text{m}} \times 1.5 \text{ m} \times \frac{1}{2 \text{ pcs angle}} = 635 \text{ kN} < 826 \text{ kN}$$

Resistance of weld:

CSA S6-06 Clause 10.18.3

$$V_r = 1,724 \text{ N/mm}$$

resistance of steel tab when $\theta = 90^\circ$, $A_m = 8 \text{ mm}$

$$V_r = 1,244 \text{ N/mm}$$

resistance of steel tab when $\theta = 0^\circ$, $A_m = 8 \text{ mm}$

Welded connection of L127 x 127 x 13 to steel plate:

$$V_r = (127 \text{ mm} + 127 \text{ mm} + 114 \text{ mm} + 114 \text{ mm}) 1,724 \frac{\text{N}}{\text{mm}} = 830 \text{ kN}$$

Potential Shear Failure of Bearing Plate:

$$V_r = \phi_s A_g F_y = 1,629 \text{ kN}$$

$$\phi_s = 0.95$$

$$A_g = 12.7 \text{ mm} \times 225 \text{ mm} \times 2 \text{ sides} = 5,715 \text{ mm}^2$$

$$F_y = 300 \text{ MPa}$$

Connection to Top Flange:

$$V_r = (300\text{mm} + 300\text{mm}) 1,724 \frac{\text{N}}{\text{mm}} + (500\text{mm} + 500\text{mm} + 4 \times 150\text{mm}) 1,244 \frac{\text{N}}{\text{mm}} = 3,025 \text{ kN}$$

$$V = 3\text{m} \times 847 \frac{\text{kN}}{\text{m}} = 2,541 \text{ kN}$$

$$V_r = 3,025 \text{ kN} > V = 2,541 \text{ kN}$$

Bolts in Tension:

$$T_r = 0.75\varphi_b n A_b F_u = 1,000 \text{ kN}$$

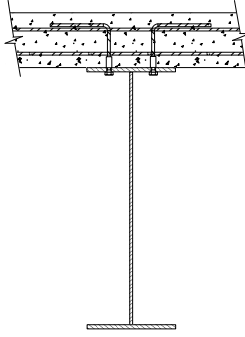
$$\varphi_b = 0.80$$

$$n = 4 \text{ bolts}$$

$$A_b = 506 \text{ mm}^2 \quad 1''\varnothing \text{ A325 Bolts}$$

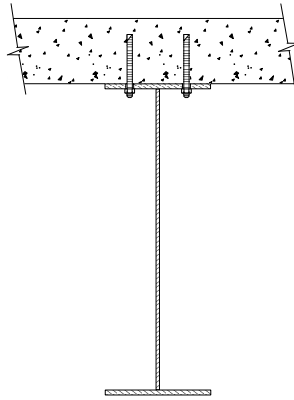
$$F_u = 825 \text{ MPa}$$

APPENDIX C: COST ANALYSIS



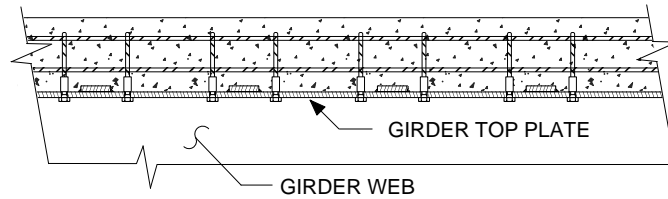
<i>4.3.1 Threaded Concrete Insert - Construction</i>	<i>Qty</i>	<i>Rate</i>	<i>Cost</i>
holes in the top flange	720	\$ 7.00	\$ 5,040
7/8" dia. x 5" long shear stud installed (not required)	480	\$ 5.00	(\$ 2,400)
1" dia. x 3" long A325 galvanized bolt with washer	720	\$ 3.50	\$ 2,520
galvanized rebar coupler for 1" bolt / 25M bar	720	\$ 6.50	\$ 4,680
175mm x 350mm 25M rebar with one end threaded	720	\$ 7.00	\$ 5,040
local shipment of structural steel	1	\$ 800	\$ 800
shop labour – additional 4 hrs per panel x 12 panels	48	\$ 85	\$ 4,080
field labour for deck installation	48	\$ 100	\$ 4,800
110 conventional boom crawler crane without operator	12	\$ 307.83	\$ 3,694
330 hydraulic excavator without operator	12	\$ 140.65	\$ 1,689
Compressor	12	\$ 13.28	\$ 159
		<i>Total</i>	\$ 30,102

<i>4.3.1 Threaded Concrete Insert – Re-use</i>	<i>Qty</i>	<i>Rate</i>	<i>Cost</i>
field labour to remove deck	40	\$ 100	\$ 4,000
field labour for deck re-installation	48	\$ 100	\$ 4,800
1" dia. x 3" long A325 galvanized bolt with washer	720	\$ 3.50	\$ 2,520
110 conventional boom crawler crane without operator	22	\$ 307.83	\$ 6,772
330 hydraulic excavator without operator	22	\$ 140.65	\$ 3,094
Compressor	22	\$ 13.28	\$ 292
		<i>Total</i>	\$ 21,478



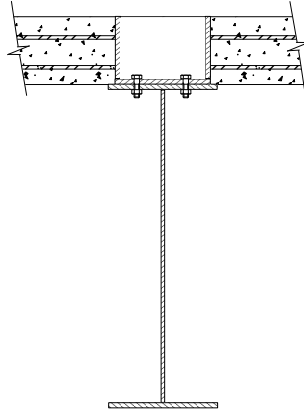
<i>4.3.2 Post Installed Connection – Construction</i>	<i>Qty</i>	<i>Rate</i>	<i>Cost</i>
holes in the top flange	960	\$ 7.00	\$ 6,720
7/8" dia. x 5" long shear stud installed (not required)	480	\$ 5.00	(\$ 2,400)
3/4" dia. x 9 1/2" long Hilti Kwik-Bolt™	960	\$ 20.00	\$ 19,200
shop labour – additional 2 hr per panel x 12 panels	24	\$ 85	\$ 2,040
field labour for deck installation	192	\$ 100	\$ 19,200
110 conventional boom crawler crane without operator	48	\$ 307.83	\$ 14,776
330 hydraulic excavator without operator	48	\$ 140.65	\$ 6,751
Compressor	48	\$ 13.28	\$ 637
		<i>Total</i>	\$ 66,924

<i>4.3.2 Post Installed Connection – Re-use</i>	<i>Qty</i>	<i>Rate</i>	<i>Cost</i>
field labour to remove deck	40	\$ 100	\$ 4,000
field labour for deck re-installation	48	\$ 100	\$ 4,800
110 conventional boom crawler crane without operator	22	\$ 307.83	\$ 6,772
330 hydraulic excavator without operator	22	\$ 140.65	\$ 3,094
Compressor	22	\$ 13.28	\$ 292
		<i>Total</i>	\$ 18,985



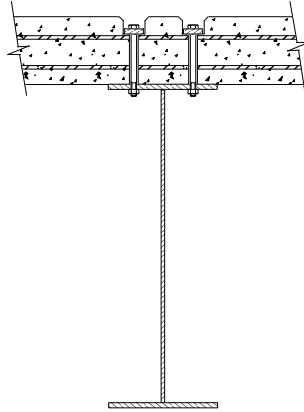
<i>4.3.3 Impression Cast Deck with Concrete Insert - Construction</i>	<i>Qty</i>	<i>Rate</i>	<i>Cost</i>
holes in the top flange	288	\$ 7.00	\$ 2,016
7/8" dia. x 5" long shear stud installed (not required)	480	\$ 5.00	(\$ 2,400)
steel tabs welded to girder top flange – 15 lbs each x 288 locations	4,328	\$ 1.50	\$ 6,480
1" dia. x 3" long A325 galvanized bolt with washer	288	\$ 3.50	\$ 1,008
galvanized rebar coupler for 1" bolt / 25M bar	288	\$ 6.50	\$ 1,872
175mm x 350mm 25M rebar with one end threaded	288	\$ 7.00	\$ 2,016
local shipment of structural steel	1	\$ 800	\$ 800
shop labour – additional 2 hr per panel x 12 panels	24	\$ 85	\$ 2,040
field labour for deck installation	48	\$ 100	\$ 4,800
110 conventional boom crawler crane without operator	12	\$ 307.83	\$ 3,694
330 hydraulic excavator without operator	12	\$ 140.65	\$ 1,689
Compressor	12	\$ 13.28	\$ 159
		<i>Total</i>	\$ 24,174

<i>4.3.3 Impression Cast Deck with Concrete Insert – Re-use</i>	<i>Qty</i>	<i>Rate</i>	<i>Cost</i>
field labour to remove deck	40	\$ 100	\$ 4,000
field labour for deck re-installation	48	\$ 100	\$ 4,800
1" dia. x 3" long A325 galvanized bolt with washer	288	\$ 3.50	\$ 1,008
110 conventional boom crawler crane without operator	22	\$ 307.83	\$ 6,772
330 hydraulic excavator without operator	22	\$ 140.65	\$ 3,094
Compressor	22	\$ 13.28	\$ 292
		<i>Total</i>	\$ 19,966



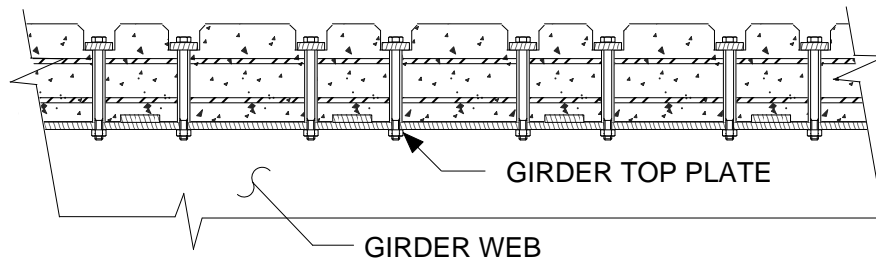
<i>4.3.4 Through Bolt with Steel to Steel Contact - Construction</i>	<i>Qty</i>	<i>Rate</i>	<i>Cost</i>
holes in the top flange	648	\$ 7.00	\$ 4,536
7/8" dia. x 5" long shear stud installed (not required)	480	\$ 5.00	(\$ 2,400)
1" dia. x 3" long A325 bolt w/ washer, nut (weathering)	648	\$ 2.50	\$ 1,620
steel pipe embed with bottom plate and cover – 87 lbs x 72 loc.	6,264	\$ 1.50	\$ 9,396
local shipment of structural steel	1	\$ 800	\$ 800
shop labour – additional 2 hrs per panel x 12 panels	24	\$ 85	\$ 2,040
field labour for deck installation	48	\$ 100	\$ 4,800
110 conventional boom crawler crane without operator	12	\$ 307.83	\$ 3,694
330 hydraulic excavator without operator	12	\$ 140.65	\$ 1,689
Compressor	12	\$ 13.28	\$ 159
		<i>Total</i>	\$ 26,334

<i>4.3.4 Through Bolt with Steel to Steel Contact – Re-use</i>	<i>Qty</i>	<i>Rate</i>	<i>Cost</i>
field labour to remove deck	40	\$ 100	\$ 4,000
field labour for deck re-installation	48	\$ 100	\$ 4,800
1" dia. x 3" long A325 bolt w/ washer, nut (weathering)	648	\$ 2.50	\$ 1,620
110 conventional boom crawler crane without operator	22	\$ 307.83	\$ 6,772
330 hydraulic excavator without operator	22	\$ 140.65	\$ 3,094
Compressor	22	\$ 13.28	\$ 292
		<i>Total</i>	\$ 20,578



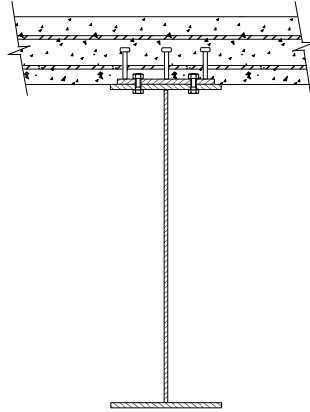
<i>4.3.5 Through Bolts with Concrete to Steel Contact - Construction</i>	<i>Qty</i>	<i>Rate</i>	<i>Cost</i>
holes in the top flange	480	\$ 7.00	\$ 3,360
7/8" dia. x 5" long shear stud installed (not required)	480	\$ 5.00	(\$ 2,400)
7/8" dia. x 10" long A325 bolt w/ washer, nut (weathering)	480	\$ 4.00	\$ 1,920
local shipment of structural steel	1	\$ 800	\$ 800
shop labour – additional 4 hr per panel x 12 panels	48	\$ 85	\$ 4,080
field labour for deck installation	48	\$ 100	\$ 4,800
110 conventional boom crawler crane without operator	12	\$ 307.83	\$ 3,694
330 hydraulic excavator without operator	12	\$ 140.65	\$ 1,689
Compressor	12	\$ 13.28	\$ 159
		<i>Total</i>	\$ 18,102

<i>4.3.5 Through Bolts with Concrete to Steel Contact –Re-use</i>	<i>Qty</i>	<i>Rate</i>	<i>Cost</i>
field labour to remove deck	96	\$ 100	\$ 9,600
field labour for deck re-installation	48	\$ 100	\$ 4,800
7/8" dia. x 10" long A325 bolt w/ washer, nut (weathering)	480	\$ 4.00	\$ 1,920
110 conventional boom crawler crane without operator	36	\$ 307.83	\$ 11,082
330 hydraulic excavator without operator	36	\$ 140.65	\$ 5,063
Compressor	36	\$ 13.28	\$ 478
		<i>Total</i>	\$ 32,943



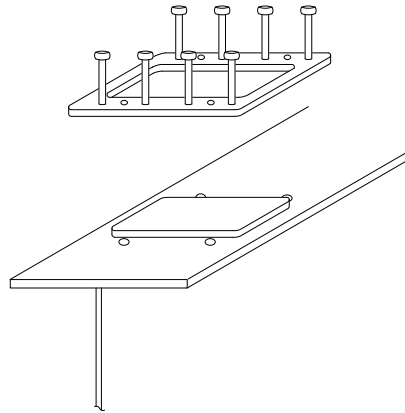
<i>4.3.6 Impression Cast with Through Bolts - Construction</i>	<i>Qty</i>	<i>Rate</i>	<i>Cost</i>
holes in the top flange	288	\$ 7.00	\$ 2,016
7/8" dia. x 5" long shear stud installed (not required)	480	\$ 5.00	(\$ 2,400)
7/8" dia. x 10" long A325 bolt w/ washer, nut (weathering)	288	\$ 4.00	\$ 1,152
steel tabs welded to girder top flange – 15 lbs each x 288 locations	4,328	\$ 1.50	\$ 6,480
local shipment of structural steel	1	\$ 800	\$ 800
shop labour – additional 3 hr per panel x 12 panels	36	\$ 85	\$ 3,060
field labour for deck installation	48	\$ 100	\$ 4,800
110 conventional boom crawler crane without operator	12	\$ 307.83	\$ 3,694
330 hydraulic excavator without operator	12	\$ 140.65	\$ 1,689
Compressor	12	\$ 13.28	\$ 159
		<i>Total</i>	\$ 21,450

<i>4.3.6 Impression Cast with Through Bolts – Re-use</i>	<i>Qty</i>	<i>Rate</i>	<i>Cost</i>
field labour to remove deck	96	\$ 100	\$ 9,600
field labour for deck re-installation	48	\$ 100	\$ 4,800
7/8" dia. x 10" long A325 bolt w/ washer, nut (weathering)	288	\$ 4.00	\$ 1,152
110 conventional boom crawler crane without operator	36	\$ 307.83	\$ 11,082
330 hydraulic excavator without operator	36	\$ 140.65	\$ 5,063
Compressor	36	\$ 13.28	\$ 478
		<i>Total</i>	\$ 32,175



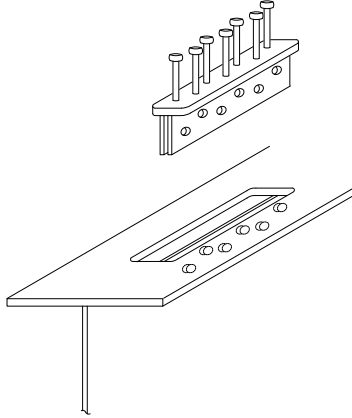
<i>4.3.7 Continuous Embed with Ductile Shear Studs - Construction</i>	<i>Qty</i>	<i>Rate</i>	<i>Cost</i>
holes in the top flange	720	\$ 7.00	\$ 5,040
1" dia. x 3" long A325 bolt w/ washer, nut (weathering)	720	\$ 2.50	\$ 1,800
steel plate for embed	2,486	\$ 1.50	\$ 3,729
local shipment of structural steel	1	\$ 800	\$ 800
shop labour – additional 2 hr per panel x 12 panels	24	\$ 85	\$ 2,040
field labour for deck installation	48	\$ 100	\$ 4,800
110 conventional boom crawler crane without operator	12	\$ 307.83	\$ 3,694
330 hydraulic excavator without operator	12	\$ 140.65	\$ 1,689
Compressor	12	\$ 13.28	\$ 159
		<i>Total</i>	\$ 23,751

<i>4.3.7 Continuous Embed with Ductile Shear Studs – Re-use</i>	<i>Qty</i>	<i>Rate</i>	<i>Cost</i>
field labour to remove deck	40	\$ 100	\$ 4,000
field labour for deck re-installation	48	\$ 100	\$ 4,800
1" dia. x 3" long A325 bolt w/ washer, nut (weathering)	720	\$ 2.50	\$ 1,800
110 conventional boom crawler crane without operator	22	\$ 307.83	\$ 6,772
330 hydraulic excavator without operator	22	\$ 140.65	\$ 3,094
Compressor	22	\$ 13.28	\$ 292
		<i>Total</i>	\$ 20,758



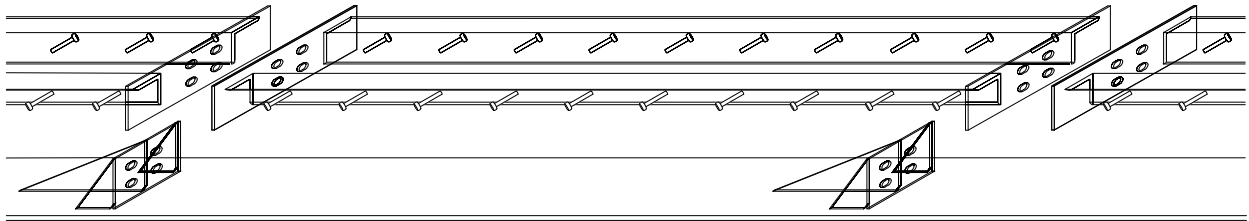
<i>4.3.8 Discrete Embed Bolted to Flange - Construction</i>	<i>Qty</i>	<i>Rate</i>	<i>Cost</i>
holes in the top flange	288	\$ 7.00	\$ 2,016
1" dia. x 3" long A325 bolt w/ washer, nut (weathering)	288	\$ 2.50	\$ 720
steel plate for embeds- 41 lbs each x 72 locations	2,952	\$ 1.50	\$ 4,428
7/8" dia. x 5" long shear stud installed – additional required	24	\$ 5.00	\$ 120
local shipment of structural steel	1	\$ 800	\$ 800
shop labour – additional 2 hr per panel x 12 panels	24	\$ 85	\$ 2,040
field labour for deck installation	192	\$ 100	\$ 19,200
110 conventional boom crawler crane without operator	48	\$ 307.83	\$ 14,776
330 hydraulic excavator without operator	48	\$ 140.65	\$ 6,751
Compressor	48	\$ 13.28	\$ 637
		<i>Total</i>	\$ 51,488

<i>4.3.8 Discrete Embed Bolted to Flange - Re-use</i>	<i>Qty</i>	<i>Rate</i>	<i>Cost</i>
field labour to remove deck	96	\$ 100	\$ 9,600
field labour for deck re-installation	192	\$ 100	\$ 19,200
1" dia. x 3" long A325 bolt w/ washer, nut (weathering)	288	\$ 2.50	\$ 720
110 conventional boom crawler crane without operator	72	\$ 307.83	\$ 22,164
330 hydraulic excavator without operator	72	\$ 140.65	\$ 10,127
Compressor	72	\$ 13.28	\$ 956
		<i>Total</i>	\$ 62,767



<i>4.3.9 Discrete Embed Bolted to Web - Construction</i>	<i>Qty</i>	<i>Rate</i>	<i>Cost</i>
holes in the web	432	\$ 7.00	\$ 3,024
7/8" dia. x 3" long A325 bolt w/ washer, nut (weathering)	432	\$ 2.50	\$ 1,080
additional steel plate for embeds – 24 lbs each x 72 locations	1,728	\$ 1.50	\$ 2,592
additional steel plate for embeds – 30 lbs each x 72 locations	2,160	\$ 1.50	\$ 3,240
cutting holes in top plate of girder – ½ hr each x 72 locations	36	\$ 85	\$ 3,060
7/8" dia. x 5" long shear stud installed – additional required	24	\$ 5.00	\$ 120
shop labour – additional 2 hr per panel x 12 panels	24	\$ 85	\$ 2,040
field labour for deck installation	96	\$ 100	\$ 9,600
110 conventional boom crawler crane without operator	24	\$ 307.83	\$ 7,388
330 hydraulic excavator without operator	24	\$ 140.65	\$ 3,376
Compressor	24	\$ 13.28	\$ 319
		<i>Total</i>	\$ 35,839

<i>4.3.9 Discrete Embed Bolted to Web – Re-use</i>	<i>Qty</i>	<i>Rate</i>	<i>Cost</i>
field labour to remove deck	40	\$ 100	\$ 4,000
field labour for deck re-installation	48	\$ 100	\$ 4,800
7/8" dia. x 3" long A325 bolt w/ washer, nut (weathering)	432	\$ 2.50	\$ 1,080
110 conventional boom crawler crane without operator	22	\$ 307.83	\$ 6,772
330 hydraulic excavator without operator	22	\$ 140.65	\$ 3,094
Compressor	22	\$ 13.28	\$ 292
		<i>Total</i>	\$ 20,038



<i>4.3.10 Panel End Connection – Construction</i>	<i>Qty</i>	<i>Rate</i>	<i>Cost</i>
local shipment of structural steel	1	\$ 800	\$ 800
1" dia. x 3" long A325 bolt w/ washer, nut (weathering)	96	\$ 2.50	\$ 240
steel angle – 626 lbs per panel x 12 panels	7,512	\$ 1.50	\$ 11,268
steel plate for connections – 95 lbs each x 24 locations	2,280	\$ 1.50	\$ 3,420
steel cover plates – 50 lbs each x 24 locations	1,200	\$ 1.5	\$ 1,800
shop labour – additional 2 hr per panel x 12 panels	24	\$ 85	\$ 2,040
field labour for deck installation	48	\$ 100	\$ 4,800
110 conventional boom crawler crane without operator	12	\$ 307.83	\$ 3,694
330 hydraulic excavator without operator	12	\$ 140.65	\$ 1,689
Compressor	12	\$ 13.28	\$ 159
		<i>Total</i>	\$ 29,910

<i>4.3.10 Panel End Connection – Re-use</i>	<i>Qty</i>	<i>Rate</i>	<i>Cost</i>
field labour to remove deck	40	\$ 100	\$ 4,000
field labour for deck re-installation	48	\$ 100	\$ 4,800
1" dia. x 3" long A325 bolt w/ washer, nut (weathering)	96	\$ 2.50	\$ 240
110 conventional boom crawler crane without operator	22	\$ 307.83	\$ 6,772
330 hydraulic excavator without operator	22	\$ 140.65	\$ 3,094
Compressor	22	\$ 13.28	\$ 292
		<i>Total</i>	\$ 19,198

APPENDIX D: 36 M COMPOSITE BRIDGE GIRDER DESIGN SUMMARY

Bridge Name: 36 meter composite

Last updated: July 8, 2010

8:53 AM

Reset all input fields

Span

Distance between support bearings 34.750 m
Total girder length 36.000 m

Design Truck

<input type="button" value="Perform live load analysis"/>	Axle 1	65 kN	Front of design truck ↓ Rear of design truck
	Dist 1	4.570 m	
	Axle 2	262 kN	
	Dist 2	1.680 m	
	Axle 3	262 kN	
	Dist 3	6.860 m	
	Axle 4	191 kN	
	Dist 4	1.680 m	
	Axle 5	191 kN	

Additional dead load per girder 3.33 kN/m

Load Factors

Dead Load	α_D	1.10
Dynamic Load Allowance	DLA	0.25
Live Load	L	1.70

Resistance Factors

Steel - flexure	φ_s	1.00
Concrete	φ_c	1.00
Reinforcing steel	φ_r	1.00
Shear Studs	φ_{sc}	1.00

Material Properties

Structural steel	F_y	350 MPa
	E_s	200,000 MPa
	G_s	77,000 MPa
Concrete	f'_c	35 MPa
	E_c	24,648 MPa
	n	8.11
Reinforcing steel	F_y	400 MPa
Shear studs	F_u	410 MPa

Section Properties

Thickness of concrete	t_c	225 mm	
Effective width of composite concrete deck		2,438 mm	Cl. 5.8.2.1
Top flange thickness	t_t	19.0 mm	
Top flange width	w_{tf}	400 mm	Cl. 10.10.4.1
Web thickness	w	12.7 mm	
Web height	h	1,877.8 mm	≤ 2,138 mm Cl. 10.17.2.5
Bottom flange thickness	t_b	25.4 mm	
Bottom flange width at midspan (max)	w_{bfm}	550 mm	Cl. 10.10.4.1
Bottom flange width (min)	w_{bfs}	550 mm	
Reinforcing steel	A_r	4,500 mm ²	
Maximum distance between stiffeners	a	4,918 mm	≤ 5633 mm Cl. 10.10.6.1

Non-Composite Plate Girder

Elastic N.A.		830 mm	<i>from underside of bottom flange</i>
Moment of Inertia (strong)	I_x	25,679,419,157 mm ⁴	
Moment of Inertia (weak)	I_y	453,814,288 mm ⁴	
St. Venant Torsional Constant	J	5,200,980 mm ⁴	
Section Modulus (Tension)	S_x	30,927,874 mm ³	
Section Modulus (Compression)	S_x	23,518,109 mm ³	
Moment reduction check		169 mm	> 102 mm <i>Cl. 10.10.4.3</i>
Factored Dead Load Moment	M_{FD}	3,141 kNm	
Moment reduction factor		0.99	<i>Cl. 10.10.4.3</i>
Factored Moment Resistance	M_y	8,176 kNm	<i>laterally supported Cl. 10.10.3.2</i>

Transformed Section Analysis

Elastic N.A.		1,550.7 mm	<i>from underside of bottom flange</i>
Moment of Inertia	I_x	65,372,135,031 mm ⁴	
Section Modulus (Tension)	S_x	42,156,255 mm ³	
Maximum Stress in Concrete when Bottom Flange Yields		16.6 MPa	
Un-factored Dead Load Moment	M_D	2,855 kNm	
Un-Factored Elastic Moment Resistance	$M_{r-elastic}$	14,755 kNm	

Composite Section

Compression resultant concrete	C_c	16,319,363 N	
Compression resultant re-bar	C_r	1,800,000 N	
Capacity of reinforced concrete	C_1	18,119,363 N	
Tensile capacity of steel section at midspan	C_2	15,896,321 N	
Location of composite plastic N.A.	====>	<i>Concrete section</i>	
Depth of top flange in compression		0.0 mm	
Location of tensile resultant force		830 mm	<i>from underside of bottom flange</i>
Factored Composite Moment Resistance (Plastic)	M_{rc}	19,362 kNm	<i>Cl. 10.11.5.2.3</i>

Shear Resistance

Height to width ratio of web	h/w	148	
Shear buckling coefficient	k_v	5.92	
Shear buckling stress	F_{cr}	49 MPa	
Tension field component of post-buckling stress	F_t	47 MPa	
ULS shear stress	F_s	96 MPa	
Factored Shear Resistance	V_r	2,292 kN	<i>Cl. 10.10.5.1</i>

Shear Stud Design

Diameter of Shear Stud	\emptyset	22.2 mm	
Number of load cycles	N_c	500,000 cycles	
Factored shear resistance	q_r	159,059 N	<i>Cl. 10.11.8.3</i>
Number of studs required	N	114 studs	<i>Cl. 10.11.8.3</i>
Number of rows	n	2 rows	
Permissible range of interface shear	Z_{sr}	34,517 N	<i>Cl. 10.17.2.7</i>
ULS Spacing (maximum allowable)	s	305 mm	<i>Cl. 10.11.8.3</i>
FLS Spacing (maximum allowable)	s	268 mm	<i>Cl. 10.17.2.7</i>

Results Summary

Maximum Factored Moment	M_f	17,096 kNm
Factored Composite Moment Resistance (Plastic)	M_{rc}	19,362 kNm
Critical M_f/M_r		0.88
Maximum Factored Shear, V_f	V_f	2,046 kN
Factored Shear Resistance	V_r	2,292 kN
Critical V_f/V_r		0.89
Critical $0.727M_f/M_r + 0.455V_f/V_r$		0.67

APPENDIX E: PANEL END CONNECTION CALCULATIONS

Stud Spacing:

$$q_r = 135 \text{ kN per } 7/8" \text{ } \emptyset \text{ stud}$$

CSA S6-06 Clause 10.5.7

$$s = \frac{135 \text{ kN}}{\text{stud}} \times 2 \text{ studs} \times \frac{1}{847 \text{ kN/m}} = 0.319 \text{ m}$$

2 - 7/8" \emptyset studs at 300mm o/c**Steel Angel:**

L127 x 127 x 13

Area = 3,060mm²

$$\text{Resistance of Angle} = \phi_s A_g F_y$$

$$\phi_s = 0.90 \quad \text{Compression}$$

$$\phi_s = 0.95 \quad \text{Tension}$$

$$\text{Resistance of Angle} = 0.9 \times 3,060 \text{ mm}^2 \times 300 \text{ MPa} = 826 \text{ kN}$$

$$\text{Maximum Load per Angle} = \frac{847 \text{ kN}}{\text{m}} \times 1.5 \text{ m} \times \frac{1}{2 \text{ pcs angle}} = 635 \text{ kN} < 826 \text{ kN}$$

Resistance of weld:**CSA S6-06 Clause 10.18.3**

$$V_r = 0.67 \phi_w A_m F_u = 1,724 \text{ N/mm}$$

resistance of base metal

$$V_r = 0.67 \phi_w A_w X_u (1 + 0.5 \sin \theta) = 1,866 \text{ N/mm}$$

resistance when $\theta = 90^\circ$

where:

$$\phi_w = 0.67$$

$$A_m = 8 \text{ mm}$$

$$A_w = 0.707 \times 8 \text{ mm}$$

$$F_u = 480 \text{ MPa}$$

$$X_u = 490 \text{ MPa}$$

Welded connection of L127 x 127 x 13 to steel plate:

$$V_r = (127 \text{ mm} + 127 \text{ mm} + 114 \text{ mm} + 114 \text{ mm}) 1,724 \frac{\text{N}}{\text{mm}} = 830 \text{ kN}$$

Potential Shear Failure of Bearing Plate:

$$V_r = \phi_s A_g F_y = 1,629 \text{ kN}$$

$$\phi_s = 0.95$$

$$A_g = 12.7\text{mm} \times 225\text{mm} \times 2 \text{ sides} = 5,715 \text{ mm}^2$$

$$F_y = 300 \text{ MPa}$$

Connection Gusset Plates to Top Flange:

$$V_r = 0.67 \phi_w A_m F_u = 2,154 \text{ N/mm} \quad \text{resistance of base metal}$$

$$V_r = 0.67 \phi_w A_w X_u (1 + 0.5 \sin \theta) = 1,555 \text{ N/mm} \quad \text{resistance when } \theta = 0^\circ$$

where:

$$\phi_w = 0.67$$

$$A_m = 10\text{mm}$$

$$A_w = 0.707 \times 10\text{mm}$$

$$F_u = 480 \text{ MPa}$$

$$X_u = 490 \text{ MPa}$$

$$V_r = 1,555 \text{ N/mm} \quad \text{resistance of gusset welds, } A_m = 10\text{mm}$$

$$V_r = 4 \cdot (200\text{mm}) \cdot 1,555 \frac{\text{N}}{\text{mm}} + 2 \cdot (500\text{mm}) \cdot 1,555 \frac{\text{N}}{\text{mm}} = 2,799 \text{ kN}$$

$$V = 3\text{m} \times 847 \frac{\text{kN}}{\text{m}} = 2,541 \text{ kN}$$

$$V_r = 2,799 \text{ kN} > V = 2,541 \text{ kN}$$

Bolts in Tension:

$$T_r = 0.75\phi_b n A_b F_u = 1,000 \text{ kN}$$

$$\phi_b = 0.80$$

$$n = 4 \text{ bolts}$$

$$A_b = 506 \text{ mm}^2 \quad 1" \text{Ø A325 Bolts}$$

$$F_u = 825 \text{ MPa}$$

Slip resistance of a bolted connection with slotted holes, V_s :

$$V_s = 0.7 \cdot (0.53c_1 k_s m n A_b F_u) = 69.9 \text{ kN per each } 1" \text{Ø Bolt} \quad \text{CSA S6-06 Clause 10.18.2.3.2}$$

where:

$$c_1 = 0.90 \quad \text{Class B}$$

$$k_s = 0.50 \quad \text{Class B}$$

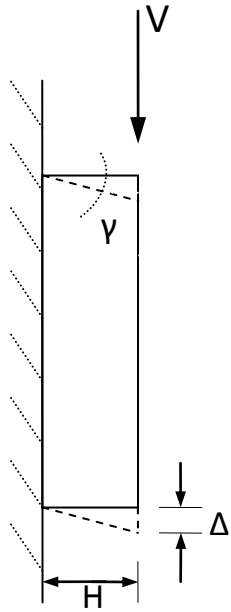
$$m = 1 \quad \text{Shear surface}$$

$$n = 1 \quad \text{Bolt}$$

$$A_b = 507 \text{ mm}^2 \quad 1" \text{Ø Bolt}$$

$$F_u = 825 \text{ MPa}$$

Center Gusset:



Two equations for shear stress:

$$\tau = \frac{V}{A} ; \tau = G \cdot \gamma$$

Rearranging:

$$\gamma = \frac{V}{G \cdot A} = 0.00303 \text{ rads}$$

Applying small angle theory:

$$\tan (0.00303 \text{ rads}) = \frac{\Delta}{H} \cong 0.00303 = \frac{\Delta}{H}$$

Solving for Δ :

$$\Delta = 0.606 \text{ mm}$$

where:

$$V = \frac{2}{3} \times \text{Area} \times F_y = \frac{2}{3} \times 15.875 \text{ mm} \times 500 \text{ mm} \times 350 \text{ MPa} = 1,852,083 \text{ N}$$

$$G = 77,000 \text{ GPa} \quad \text{Shear modulus for steel}$$

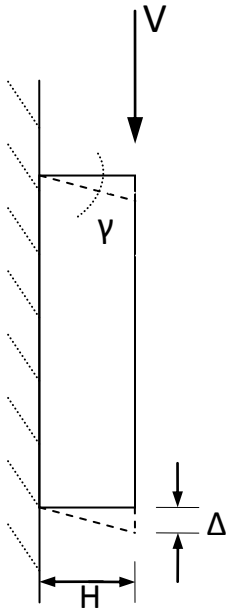
$$A = 15.875 \text{ mm} \times 500 \text{ mm} \quad \text{Area of main gusset plate}$$

$$H = 200 \text{ mm} \quad \text{Height of Gusset}$$

Solving for connector stiffness, k:

$$k = \frac{V}{\Delta} = \frac{1,852,083 \text{ N}}{0.606 \text{ mm}} = 3,055,937 \text{ N/mm}$$

Side Gusset:



Two equations for shear stress:

$$\tau = \frac{V}{A} ; \tau = G \cdot \gamma$$

Rearranging:

$$\gamma = \frac{V}{G \cdot A} = 0.00303 \text{ rads}$$

Applying small angle theory:

$$\tan (0.00303 \text{ rads}) = \frac{\Delta}{H} \cong 0.00303 = \frac{\Delta}{H}$$

Solving for Δ :

$$\Delta = 0.606 \text{ mm}$$

where:

$$V = \frac{2}{3} \times \text{Area} \times F_y = \frac{2}{3} \times 15.875 \text{mm} \times 200 \text{mm} \times 350 \text{MPa} = 740,833 \text{ N}$$

$$G = 77,000 \text{ GPa} \quad \text{Shear modulus for steel}$$

$$A = 15.875 \text{ mm} \times 200 \text{ mm} \quad \text{Area of main gusset plate}$$

$$H = 200 \text{ mm} \quad \text{Height of Gusset}$$

Solving for connector stiffness, k :

$$k = \frac{V}{\Delta} = \frac{740,833 \text{ N}}{0.606 \text{ mm}} = 1,222,374 \text{ N/mm}$$

Fatigue of Gusset Plates in Panel End Connections:

$$0.52 \cdot f_{sr} < F_{sr}$$

CAN/CSA S6-06 Clause 10.17.2.2

$$f_{sr} < F_{sr}$$

Factor of 0.52 removed, as explained in Section 6.2.3

where:

$$f_{sr} = 81 \text{ MPa in the top flange}$$

Fatigue stress range

$$f_{sr} = 69 \text{ MPa in the gusset plate connection}$$

$$F_{sr} = (\gamma/N_c)^{1/3} \geq F_{srt}/2$$

Fatigue Stress resistance

$$\gamma = 361 \times 10^9$$

Fatigue life constant for Detail Category E

$$N_c = 500,000 \text{ cycles}$$

Refer to Section 6.1.1

$$F_{srt} = 31 \text{ MPa}$$

Constant amplitude threshold stress range

therefore:

$$f_{sr} = 81 \text{ MPa} < F_{sr} = 90 \text{ MPa}$$

APPENDIX F: LATERAL TORSIONAL BUCKLING CALCULATIONS

Lateral Torsional Buckling of a Mono-Symmetric Plate Girder:

$$M_u = \frac{\omega_2 \cdot \pi}{L_u} \cdot \left\{ \sqrt{E_s \cdot I_y \cdot G_s \cdot J} \cdot \left[B_1 + \sqrt{1 + B_2 + B_1^2} \right] \right\} = 44,885 \text{ kN}\cdot\text{m}$$

where:

Geometric properties of the plate girder taken from the design example presented in Appendix D.

$\omega_2 = 1.0$ because moment within an un-braced length may be larger than the end moments

$L_u = 3,000 \text{ mm}$ un-braced length

$E_s = 200,000 \text{ MPa}$ Young's modulus of steel

$I_y = 453.8 \times 10^6 \text{ mm}^4$ Moment of inertia of plate girder in weak direction

$G_s = 77,000 \text{ MPa}$ Shear modulus of steel

$$J = \frac{1}{3} \cdot (b_1 \cdot t_1^3 + b_2 \cdot t_2^3 + d \cdot w^3) = 5,200,980 \text{ mm}^4$$

$b_1 = 400 \text{ mm}$

$t_1 = 19 \text{ mm}$

$b_2 = 550 \text{ mm}$

$t_2 = 25.4 \text{ mm}$

$d = 1877.8 \text{ mm}$

$w = 12.7 \text{ mm}$

$$B_1 = \pi \cdot \frac{\beta_x}{2 \cdot L_u} \cdot \sqrt{\frac{E_s \cdot I_y}{G_s \cdot J}} = -7.46$$

$$\beta_x = 0.9 \cdot d_1 \cdot \left[2 \cdot \frac{I_{yc}}{I_y} - 1 \right] \cdot \left[1 - \left(\frac{I_y}{I_x} \right)^2 \right] = -946.3$$

$$I_{yc} = t_1 \cdot b_1 / 12 = 101,333,333 \text{ mm}^4$$

$$d_1 = d + t_1/2 + t_2/2 = 1900 \text{ mm}$$

$$B_2 = \frac{\pi^2 E_s C_w}{L_u^2 G_s J} = 155.6$$

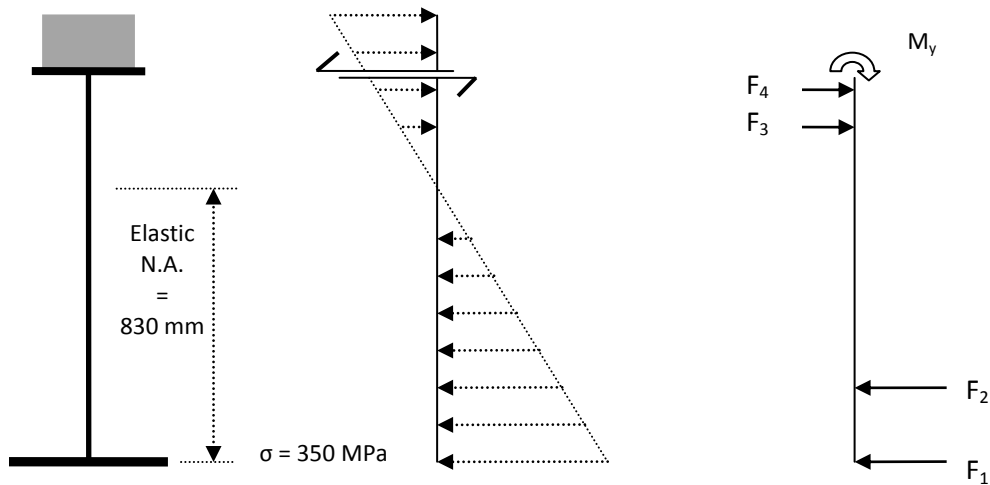
$$C_w = (d')^2 \cdot b_1^3 \cdot t_1 \cdot \frac{\alpha}{12} \frac{\pi^2 E_s C_w}{L_u^2 G_s J} = 2.8407 \times 10^{14} \text{ mm}^6$$

$$d' = 1,900 \text{ mm}$$

$$\alpha = \frac{1}{1 + \left(\frac{b_1}{b_2}\right)^3 \cdot \frac{t_1}{t_2}} = 0.776$$

$$M_u = 44,885 \text{ kN}\cdot\text{m}$$

Transformed Section Analysis to Determine Yield Moment in Plate Girder of a Composite System



Geometric properties of the plate girder taken from the design example presented in Appendix D. Distances for moment calculations correspond with centre of load, measured from the top of the girder's upper flange.

Sum Moment at Top of Girder:

$$M_y = F_1 \cdot d_1 + F_2 \cdot d_2 + F_3 \cdot d_3 + F_4 \cdot d_4 = 13,971 \text{ kN}\cdot\text{m}$$

where:

$$F_1 = (350 \text{ MPa} + 344.3 \text{ MPa}) / 2 \cdot (25.4 \text{ mm} \cdot 550 \text{ mm}) = 4,849,686 \text{ N}$$

$$d_1 = 1,913.7 \text{ mm}$$

$$F_2 = (344.3 \text{ MPa}) / 2 \cdot (12.7 \text{ mm} \cdot 1,525.3 \text{ mm}) = 3,334,771 \text{ N}$$

$$d_2 = 1,413.8 \text{ mm}$$

$$F_3 = (79.6 \text{ MPa}) / 2 \cdot (12.7 \text{ mm} \cdot 352.5 \text{ mm}) = 178,175 \text{ N}$$

$$d_3 = 117.5 \text{ mm}$$

$$F_4 = (79.6 \text{ MPa} + 83.8 \text{ MPa}) / 2 \cdot (19 \text{ mm} \cdot 400 \text{ mm}) = 620,920 \text{ N}$$

$$d_4 = 6.3 \text{ mm}$$

BIBLIOGRAPHY

- ABAQUS (2002). Standard User's Manuals, Version 6.3. Hibbitt, Karlsson and Sorensen, Inc., USA
- ABAQUS (2007). Version 6.7, Dassault Systèmes, USA
- Acrow Bridge. (2010). Vehicular Bridges. Retrieved June 14, 2010, from ACROW Corporation of America <http://www.acrowusa.com/index.php?page=vehicular-bridges>
- Allison, R. W., Johnson, R. P., and May, I. M. (1982). Tension Field Action in Composite Plate Girders. *Proc. Inst. Civ. Eng., Struct. Build., 73, part 2, 255-276*
- AASHTO Load Factor Design (2002). *Standard Specifications for Highway Bridges, Officials, Seventeenth Edition, American Association of State Highway and Transportation, Washington, D.C., 2002*
- Bakht, B. & Jaeger, L.G. (1992). Ultimate Load Test of Slab-on-Girder Bridge. *Journal of Structural Engineering, Vol. 118, No.6, June 1992, pp. 1608-1624*
- Barth, K. E., and Wu, H. (2006). Efficient Non-Linear Finite Element Modelling of Slab on Steel Stringer Bridges. *Finite Elements in Analysis and Design, pp. 1304-1313*
- Baskar, K., Shanmugam, N. E., and Thevendran, V. (2002). Finite-Element Analysis of Steel-Concrete Composite Plate Girder. *Journal of Structural Engineering, September 2002, pp. 1158-1168*
- British Columbia Ministry of Forest. (1999). Resource Tenders and Engineering Branch. *Standard Bridge Drawing 4.9 m x 3.0 m L165 Precast Concrete Deck Panel*
- B.C. Road Builders & Heavy Construction Association. (June 2008). *2008-2009 Equipment Rental Rate Guide "The Blue Book"*. Burnaby, BC: Westhome Graphics
- Canadian Patent No. 2,202,193 (issued April 9, 1997), G. D. Kokonis
- Canadian Standards Association. (2006). CAN/CSA-S6-06 Canadian Highway Bridge Design Code. *Mississauga: Canadian Standards Association*
- Canadian Standards Association. CSA W59 (2003). Welded Steel Construction (Metal Arc Welding). *Mississauga: Canadian Standards Association*

- Carreira, D. J., and Chu, K. H. (1985). Stress-Strain Relationship for Plain Concrete in Compression. *ACI Journal, Proc. 82(11)*, pp. 797-804
- CEB (1970). International Recommendations for the Design and Construction of Concrete Structures, *COMITE EUROPEEN DU BETON – FEDERATION INTERNATIONALE DE LA PRECONTRAINTÉ*
- Cheung, Billy Siu Fung. (2008). Adhesive bonding of concrete-steel composite bridges by polyurethane elastomer. *M.A.Sc. Thesis, University of Toronto*
- CISC (2007). Handbook of Steel Construction, Ninth Edition. CISC Commentary on CAN/CSA-S-16-01 Canadian Institute of Steel Construction
- Concrete Design Handbook. (2006). *CAN/A23.4-04 Design of Concrete Structures. Cement Association of Canada, Ottawa*
- Dauner, H.G. (2005). Neue Verbindungstechnik im Verbundbrückenbau. *ASTRA report no. 583 Bern: Swiss Federal Foods Authority*
- Dywidag-Systems International (2007). Wiltern Parking Structure, Los Angeles, California, USA, *retrieved on July 20, 2010. http://www.dywidag-systems.com/uploads/media/DSI_Markets_wiltern.pdf*
- Grant, A., Fisher, J. W., and Slutter, R. G. (1977). Composite Beams with Formed Steel Deck. *Engineering Journal, AISC, First Quarter*, pp. 24-43
- Hanswille, G., Porsch, M., Ustundag, C. (2006). Resistance of Headed Studs Subjected to Fatigue Loading Part II: Analytical Study. *Journal of Constructional Steel Research 63* pp. 485-493
- Höglund, T., and Nilsson, L. (2006). Aluminum in Bridge Decks and in a New Military Bridge in Sweden. *Structural Engineering International, April 2006*, pp. 348-351
- Kulak, G. L., and Birkemoe, P. C. (1992). Field studies of bolt pretension. *Constructional Steel Design World Developments, Acapulco, Mexico*
- Kulak, G. L., Grondin, G.Y. (2006). Limit States Design in Structural Steel, Eighth Edition, *Canadian Institute of Steel Construction*
- Kwon, G., Engelhardt, M. D., & Klingner, R. E. (2008). Strengthening Existing Non-Composite Steel Girder Bridges by the Use of Post-Installed Shear Connectors. *17th Congress of IABSE, Chicago*

- Thomann, M. (2005). Connexions par adhérence. ICOM report no. 535. Steel structures laboratory ICOM, Ecole polytechnique fédérale de Lausanne
- Thomann, M., and Lebet, J. (2008). A mechanical model for connections by adherence for steel–concrete composite beams. *Engineering Structures*, 30(1), 163-173
- Mabey Bridge. (2010). History of the Bailey Bridge. Retrieved July 20, 2010, from Mabey Bridge Ltd. 2010 <http://www.mabeybridge.co.uk/bailey-bridge-history.asp>
- Mabey Bridge. (2010). Compact Bridging. Retrieved June 14, 2010, from Mabey Bridge Ltd. 2010 <http://www.mabeybridge.co.uk/compact-bridging.asp>
- Mans, P. H., Yakel, A. J., and Azizinamini, A. (2001). Full-Scale Testing of Composite Plate Girders Constructed Using 485-MPa High-Performance Steel, *Journal of Bridge Engineering*, Nov/Dec 2001, pp. 598-604
- Oehlers, D. J., Seracino, R., & Yeo, M. F. (2000). Effect of Friction on Shear Connection in Composite Bridge Beams. *Journal of Bridge Engineering*, May 2000, pp. 91-98
- Rabbat, B., G., and Russell, H.G. (1985). Friction Coefficient of Steel on Concrete or Grout. *Journal of Structural Engineering*, Vol. 111, No. 3, March 1985, pp. 505-515
- Ramsay, C. (2007). Shear resistance of a polyurethane interface in concrete-steel composite beams. *M.A.Sc. Thesis, University of Toronto*
- Roorda, J. (1988). Buckling Behaviour of Thin Walled Columns. *Canadian Journal of Civil Engineering*, Vol. 15, 1988, pp. 107-116
- Seracino, R., & Oehlers, D. J. (2002). Composite Action in Non-Composite Beams. *Advances in Steel Structures*, Vol.1, 471, pp. 471-478
- Si Larbi, A., Ferrier, E., Jurkiewicz, B., & Hamelin, P. (2006). Static Behaviour of Steel Concrete Beam Connected by Bonding. *Engineering Structures*.
- U.S. Patent No. 5,826,290 (issued October 27, 1998), G. D. Kokonis